UNIVERSITA' DEGLI STUDI DI PARMA

Dottorato di ricerca in Medicina Molecolare

Ciclo XXIX

ROLE OF PKCepsilon IN CELL DIVISION AND DIFFERENTIATION: IMPLICATION FOR GENOMIC INSTABILITY AND AUTOIMMUNITY

Settore scientifico disciplinare BIO/16

Coordinatore:

Chiar.mo Prof. LUCIANO POLONELLI

Tutor:

Chiar.ma Prof.ssa GIULIANA GOBBI

Co-Tutor:

Chiar.mo Prof. MARCO VITALE

Dottoranda:

Dott.ssa SILVIA MARTINI

All the data reported in this thesis have been submitted for publication on peer reviewed international scientific journals.

Index

Preface: role of PKCε in cell division and cell differentiation

Protein kinase C epsilon (PKCε) is a serine/threonine kinase involved in many cellular functions, including cell growth, proliferation and differentiation. Due to its unique protective role in ischemic preconditioning, along with its oncogenic potential, PKCε is considered one of the most interesting isoform among the PKCs.

During my PhD, I investigated the involvement of PKCε in two independent but correlated biological processes: cell division and cell differentiation.

Cell division is an extremely regulated process which involves the duplication of the genome of a cell and its segregation into two identical daughter cells. Accurate chromosome segregation during cell division is achieved through the assembly of a bipolar mitotic spindle. It has been demonstrated that PKCε is involved in several cell cycle processes, such as cytokinesis and mitotic catenation resolution during metaphase-anaphase transition. However, a PKCε engagement in earlier (pre)mitotic events was unknown. Here, I describe a novel cell cycle role for PKCε in coordinating centrosome migration and mitotic spindle assembly by regulating cytoplasmic dynein function. Interestingly, PKCε dependency of mitotic spindle organization is related to the properties of transformed cells, supporting PKCε as a potential cancer therapeutic target.

PKCε is also implicated in proliferation of CD4+ T lymphocytes by regulating cell sensitivity to TGF1β, well-known to inhibit proliferation. Particularly, PKCε has been found overexpressed in CD4+ cells from patients with Hashimoto Thyroiditis, an autoimmune disease characterized by abnormal lymphocyte proliferation and activation, suggesting an implication for PKCε in immune-mediated diseases. A novel subset of Interleukin-17 (IL-17) producing CD4+ T cells (Th17) has been recently shown to promote inflammatory responses and to contribute to the pathogenesis of autoimmune diseases such as psoriasis. Mechanisms that underlie human in vitro Th17

differentiation are still unclear. However, it has been demonstrated that Stat3 signalling pathway is essential for Th17 differentiation. In this study, I demonstrate that PKCε is overexpressed in circulating CD4+ T cells from patients with psoriasis and that its expression correlates with the severity of the disease. Furthermore, I show that PKCε is involved in vitro Th17 lymphocytes polarization from CD4+ naïve cells isolated from peripheral blood by regulating STAT3 signalling pathway. Collectively these results, confirming the clinical relevance of PKCε in psoriasis, support the hypothesis that PKCε might be a potential therapeutic target for Th17-mediated disease.

Overall, the data obtained during my PhD add knowledge to the pathological implication of Protein Kinase Cε both in cell division and cell differentiation.

All the data reported in this thesis have been submitted for publication on peer reviewed international scientific journals.

I. PKCε involvement in mitotic spindle organization and early mitotic progression

Introduction

1. Protein Kinase C epsilon (PKCε)

1.1 Protein Kinase C (PKC) family

Mammalian Protein Kinases C (PKC) is a member of the large AGC (protein kinase A, G and C) family which includes phospholipid-dependent serine/threonine kinases (*Murugappan S. et al., 2004*). They play key regulatory roles in many intracellular signal-transducing pathways at the basis of a great variety of cellular processes such as cell cycle progression, apoptosis, migration, motility and differentiation (*Tan S.L. and Parker P.J. 2003; Parker P.J. and Murray-Rust J., 2004; Ivasaka J. et al., 2005*). These enzymes multiplicity, together with variation in cellular and tissue distribution and abundance, might explain why so many signal transduction functions have been attributed to these kinases (*Webb B.L.J. et al., 2000*).

All the members of the PKC family are composed of a N-terminal regulatory domain and a C-terminal catalytic domain. Structural differences within the regulatory domain confer variations in cofactor requirement and way of activation and consequently subdivide the family into three groups: *conventional* isoforms, cPKCs (α**,** βI, βII and γ), *novel* isoforms, nPKCs (δ, ε, θ and η) and the *atypical* ones, aPKCs (ζ and λ (murine)/ι (human)) (*Cameron A.J. and Parker P.J., 2010*) (Figure 1).

The *cPKCs* are activated by the membrane lipid phosphatidylserine (PS) in a calcium dependent manner and by diacylglycerol (DAG), which increases the specificity of the enzyme for PS and also shifts the affinity for calcium into the physiological range. Furthermore, cPKCs are targets of the tumor-promoting phorbol ester (like phorbol 12-myristate 13-acetate, PMA), which activates these enzymes by eliminating the requirement for DAG and decreasing the concentration of Ca^{2+} needed for activation. The *nPKCs* are calcium insensitive, but dependent on DAG or phorbol esters in the presence of PS; the *aPKCs* are activated in the absence of both calcium and DAG.

Finally, the recently discovered protein kinase C-related kinases *PRKs* define a fourth grouping consisting of three members, PRKs 1-3. Like the aPKCs, PRKs are insensitive to Ca^{2++}, DAG and phorbol esters but they bind the activated RhoA GTPase, which leads to a 4-fold activation of the kinase *in vitro* (*Mellor H. and Parker P.J., 1998*).

Members of the protein kinase C family are single polypeptide, composed of an N-terminal regulatory domain (approximately 20-40 kDa), which binds endogenous and exogenous stimulators, linked through the variable V3-hinge region to a C-terminal catalytic domain (approximately 45 kDa), which is responsible for protein phosphorylation (*Nishizuka Y., 1995*). The structure of both domains is composed of a number of conserved regions (C1-C4) alternated by regions of lower homology, so called variable domains, V0-V5 (*Webb B.L.J. e tal.,2000*).

Protein kinase C regulatory regions have been further subdivided into a pseudosubstrate region, conserved regions C1 and C2, and variable regions (*Kikkawa U. et al., 1989; Bell R.M. and Bums D.J., 1991; Dekker L.V. and Parker P.J., 1994*). The regulatory domain serves two key functions: it targets the kinases to the appropriate cellular location and it regulates kinase activity by serving as an autoinhibitory module. The *V1 region* is a pseudosubstrate site, which interacts with the catalytic domain and autoinhibits sterically the kinase function. Binding of cofactors relieves autoinhibition through conformational changes that unmask the active site. The *C1 domain* (C1A and C1B), a sequence of 50-55 aa, is composed of two repeated zinc-finger motifs rich of cysteine and histidine residues and it is involved in binding DAG and phorbol-ester activating compounds (*Castagna M. et al., 1982*). Only cPKCs and nPKCs have a functional and complete C1 domain. The *C2 domain*, consisting in 130aa, is a member of the Ca^{2+}/lipid binding domain superfamily (CaLB) and it serves as a membrane-targeting module that binds anionic phospholipids in a Ca^{2+}-dependent manner. In the novel PKCs, a C2-like region precedes C1 domain in the primary sequence and lacks the functional Asp residue that seems to mediate the calcium binding, making these enzyme DAG-sensitive but Ca^{2+}-indipendent (*Ochoa W.F. et al., 2002*). The atypical PKC group contain only one

zinc-finger with an impaired ligand-binding pocket unable to bind DAG or calcium, but they possess a Phox/Bem1 domain (PB1; protein interaction domain) instead of C2 (*Bynagari-Settipalli Y.S. et al., 2012; Corbalan-Garcia S. et al., 2007*).

Separated by a proteolytically labile hinge, *V3 region*, all the isoforms are characterized by the presence of a catalytic domain that contains the conserved *C3 and C4 regions*, which represented the ATP- the substrate-binding site (*Nishizuka Y., 1995; Fujise A. et al., 1994*). According to over 30 protein kinase structures analysis, they show the same fold: a bilobal structure with an N-terminal lobe that is primarily composed of beta sheet and a C-terminal lobe that is primarily αhelix and the ATP- and substrate-binding site is located in a cleft between the two lobes (*Newton A.C., 2003*).

The C3 region contains the characteristic glycine-rich ATP-binding loop with the consensus GXGXXG sequence (a structural hallmark of protein kinase and nucleotide binding proteins) and an invariant Lys, which structures the enzyme for phosphoryl-transfer from the nucleoside triphosphate to the hydroxyl group of serine and threonine residues of target proteins. The COOH-terminal lobe of the kinase domain is predominantly α-helical and contains the activation loop segment that positions magnesium and peptide substrates for catalysis, followed by the V5 domain at the C-terminus, which contains the turn motif and the hydrophilic motif. A “gatekeeper” residue located in sequence connecting the two lobes of the kinase domain controls access to a pre-existing cavity in the ATP binding pocket (*Steinberg S.F., 2008*).

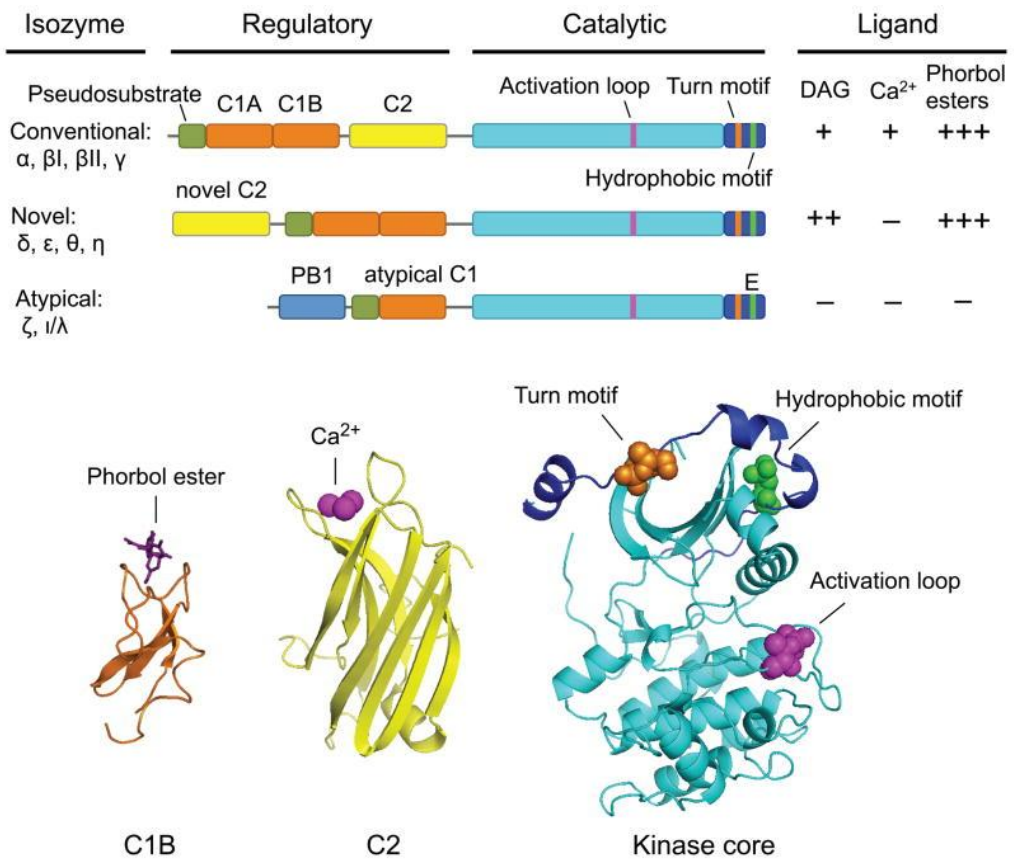

Figure 1. Structure and relative ligand-responsiveness of PKC isozymes. Primary structure of classical, novel and atypical PKCs: autoinhibitory pseudosubstrate segment (green), C1 domains (orange), C2 domain (yellow), kinase core (cyan), and C-terminal tail (dark blue); the activation loop (pink), turn motif (orange), and hydrophobic motif (yellow) phosphorylation sites are indicated. For each subfamily, affinity to DAG, Ca^{2+} and phorbol esters is indicated. Also shown are the crystal structures of the C1B, C2 and kinase domains (Wu-Zhang X.A. et al., 2012)

1.2 Protein Kinase C- epsilon (PKCε) structure and functions

Protein kinase C (PKC)-ε is the first discovered among the novel PKC isoforms and it is expressed in many tissues including neuronal, hormonal, heart, immune, retinal, endothelial and epidermal cells (*Ono Y. et al., 1988*). PKCε shows several structural features in common with other members of the family of nPKCs such as a pseudosubstrate domain, V1, a C2-like phospholipid binding domain, a C1 domain containing two cysteine-rich motifs that bind DAG and others lipid mediators, the catalytic domains C3 and C4, which contain a site rich in purines for binding with ATP, an activation loop and a site for the recognition of the substrate (Figure 2).

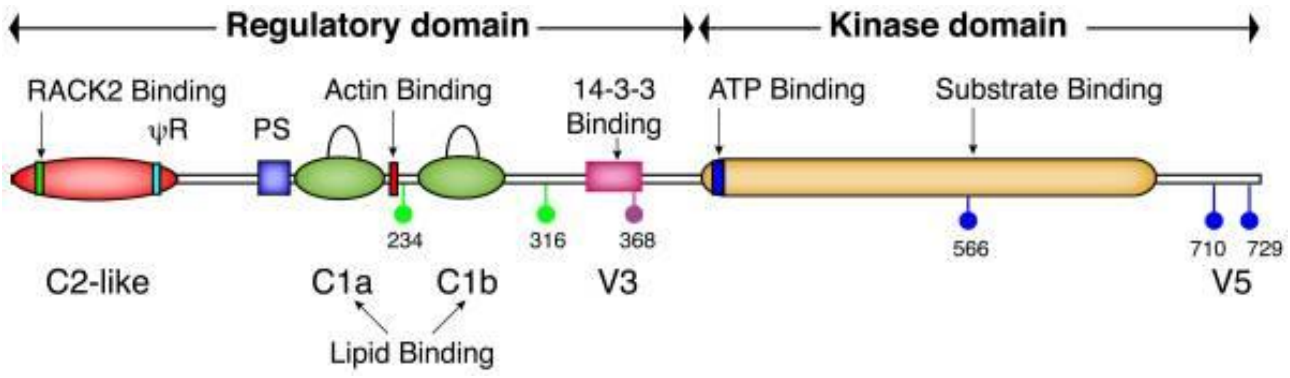

Figure 2: Schematized primary structure of PKCε . The main substrate binding sites are represented. The green and purple dots indicate the potential auto-phosphorylation sites, whereas the blue dots indicate the highly conserved phosphorylation sites. (*Newton A.C. et al., 2011*).

PKCε is unique among the PKC isoforms in containing an F-actin binding site, a hexapeptide (LKKQET) located between domains C1A and C1B at amino acids 223-228. This motif is indispensable for the physical interaction between PKCε and F-actin (*Prekeris R. et al., 1996*). PKCε has also a three amino acids motif, GEE, located in the V3 region, which are essential for selective targeting to cell-cell contacts (*Quittau-Prevostel C. et al., 2004*). Furthermore, in the V3 hinge region there are two particular sequences surrounding Ser 346 and Ser 368, which mediate protein 14-3-3 binding with PKCε (*Saurin A.T. et al., 2008*).

Like other PKC isozymes, PKCε must be primed through phosphorylation to display full enzymatic activity and respond to allosteric regulators: the highly conserved phosphorylated sites are Thr566 in the activation loop, Thr710 in the turn motif and Ser729 in the hydrophobic motif. Phospholipid-dependent kinase 1 (PDK1) phosphorylates the activation loop, whereas the turn and hydrophobic motifs are autophosphorylated in conventional PKCs, and possibly in PKCε (*Cenni V. et al., 2002*), although recent evidence indicates that mammalian target of rapamycin complex 2 may transphosphorylate these sites (*Facchinetti V. et al., 2008*). Three additional sites in PKCε have been identified that can be auto-phosphorylated *in vitro*, which are Ser-234, Ser-316, and Ser-368: however, in intact cells, it appears that these sites are trans-phosphorylated by conventional PKC isozymes (*Durgan J. et al., 2008*).

Mature PKCε is activated by several different second messengers, DAG, PIP3 (phosphatidylinositol 3,4,5-trisphosphate) and fatty acids produced by physiological stimuli such PDGF (platelet-derived growth factor) and bradykinin (*Moriya S. et al., 1996; Graness A., 1998*). Activated PKCε translocates then to different specific subcellular compartements in response to which second messenger is bound to the C1 domain. PKCε translocates to the plasma membrane and or cytoskeleton after DAG and tridecanoic acids activation, whereas it translocates to Golgi-networks in response to arachidonic and linoleic acids (*Shirai Y. et al., 1998*). Also the anchoring protein of PKCε determines its localization. PKCε contains a RACK2 (receptor for activated C-kinase) binding site, located in the C2 region (εV1-2), and the binding with RACK2, a Golgi membrane protein involved in vescicular trafficking, activates Golgi apparatus translocation of mature PKCε (*Dorn G.W. et al., 2002*). In cardiac myocytes RACK2 also localizes PKCε to myofilaments. PKCε binds to RACK1, which is reported to be a selective binding protein for activated PKCβII, with lower affinity than RACK2. In human glioma cells, PKCε is reported to be linked to integrin β1 through interaction with RACK1 thereby mediating increased adhesion and mobility (*Besson A. et al., 2000*).

PKCε regulates various physiological functions including the activation of nervous, endocrine, exocrine, inflammatory, vascular and immune systems (*Akita Y., 2002*) (Figure 3).

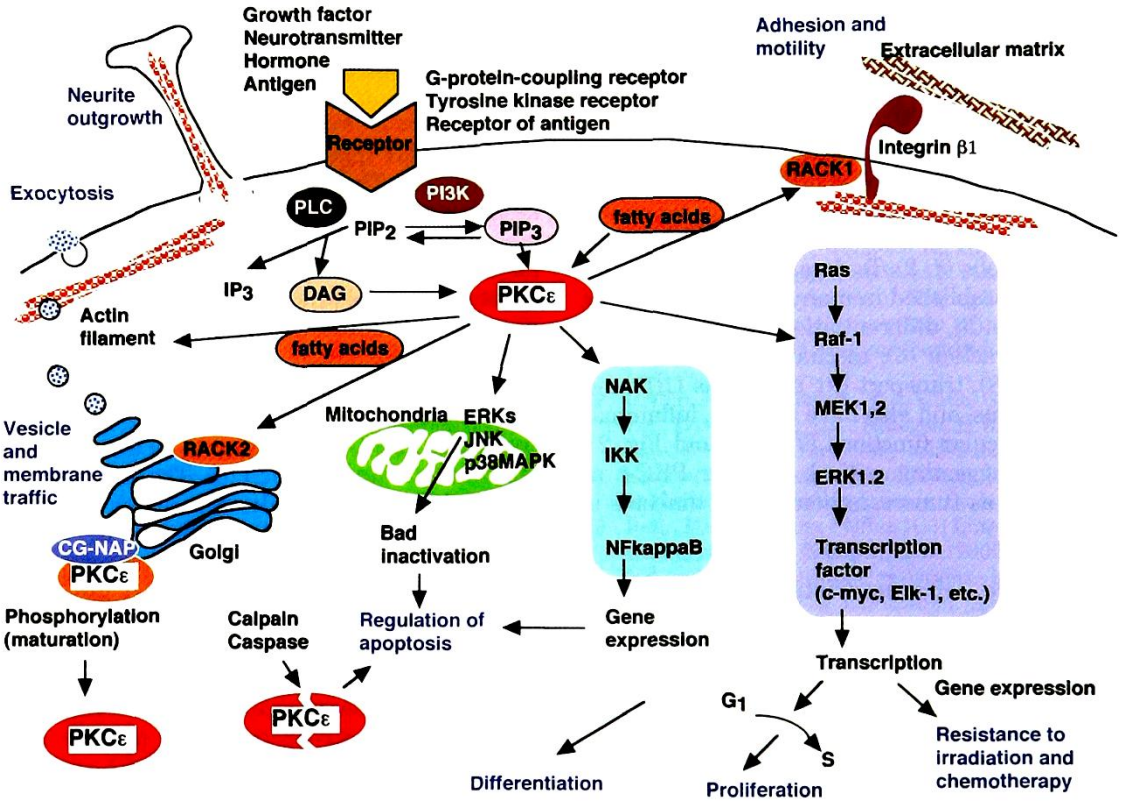

Figure 3: PKCε different pathways. PKCε is known to be involved in several pathways ranging from cytoskeletal remodelling to cell proliferation and differentiation (from *Akita Y., 2002)*

There is the increasing evidence that in the central nervous system, PKCε induces neurite outgrowth during neuronal differentiation through the interaction with actin filaments (*Fagerstorm S. et al., 1998; Hundle B. et al., 1995*). PKCε seems to mediate synaptic function in particular in sensory neurons it has been implicated in the regulation of nociceptor function that participates in various type of pain (*Cesare P. et al., 1999*) as well in neurotransmitter exocytosis through the interaction between actin-binding site and actin filaments (*Prekeris R. et al., 1996*).

It is known that PKCε plays an important role in inflammatory immune systems. This kinase is essential for macrophages activity and IgG-stimulated phagocytosis (*Larsen E.C. et al., 2000*). The role of PKCε in hematopoiesis has been also deeply investigated: this isozyme plays a pivotal role in several process, including erythroid differentiation, myeloid leukemia, megakaryocytopoiesis, platelets maturation and release, thrombosis (*Gobbi G. et al., 2007; Gobbi G. et al., 2013*).

Megakaryocytic cultures from patients affected by primary myelofibrosis (PMF) have higher levels of PKCε expression than healthy controls. Further, inhibition of PKCε function restores PMF megakaryocytes differentiation (Masselli et al., 2015). It has been recently shown that PKCδ and PKCε work as a functional couple with opposite roles in thrombopoiesis and the modulation of their balance strongly impacts platelets production (Carubbi et al., 2016).

PKCε is also studied for its differentiative function in many cell types. It is involved in the differentiation of intestinal cells, in colon epithelium, it has been described a decreasing gradient of PKCε expression from the bottom of the crypts, where intestinal stem cells are resident, to the luminal surface. This expression of PKCε at the base of the crypts, supports the undifferentiated phenotype of intestinal stem cell pool, moreover the down-regulation of PKCε promotes differentiation (*Gobbi G. et al., 2012*).

Moreover, Galli and colleagues have demonstrated that PKCε is involved in cardiomyocyte differentiation regulating early and late cardiac genes expression. PKCε over-expression leads to ERK signaling-dependent down-regulation of the cardiac genes nkx2.5 and GATA4 both *in vivo* and *in vitro,* with negative effects in cardiac differentiation (*Galli D. et al., 2013).* More recently, it has been demonstrated that PKCε is also involved in skeletal muscle differentiation and chondrocytic differentiation in osteoarthritic conditions (DiMarcantonio et al., 2015; Queirolo et al., 2016).

PKCε plays also critical roles in protecting against ischemic damage and enhances post-ischaemic functional recovery, promoting infarct size reduction following ischaemic preconditioning in murine model *(Saurin A.T. et al., 2002)*. The signalling pathways responsible for cardio-protection involve the activation of PI3K upstream and the MERK1/2-ERK1/2 cascade downstream of PKCε with the activation of anti-apoptosis transcriptional factors, but also the interaction of PKCε with MAPKs and ERKs which leads to the phosphorylation and inactivation of pro-apoptotic protein Bad (*Baines C.P. et al., 2002*).

Increased expression of PKCε seems to be involved in the development of diabetes, whereas reduced PKCε activity may contribute to the development of Alzheimer's disease (*Ikeda Y. et al., 2001; Kinouchi T. et al., 1995*).

1.3 PKCε roles in mitosis

During cytokinesis, the contraction of the actomyosin ring drives a process known as furrowing, where the cell membrane is constricted until it can ingress no further due to the presence of a dense bundle of spindle midzone microtubules, which form a specialized electron-dense structure called the "midbody".

In 2008, Saurin et al. found an association between PKCε and 14-3-3-β, during cytokinesis. The 14-3-3 family are proteins that bind to phosphorylated serine and threonine motifs on a target protein. Several studies have been shown that they affect protein localization, stability and/or activity, thereby influencing cell adhesion, cell polarity, cell survival and the cell cycle (Bridges D. and Moorhead G.B., 2005).

Saurin et al. demonstrated that the final stage of abscission is dependent on the PKCε/14-3-3 complex and a deregulation of this complex may lead to tumor formation. The PKCε inhibition with siRNA leads to multinucleation in HeLa cells, which indicates a cytokinesis defect.

Furthermore, they demonstrated that PKCε/14-3-3 complex transiently accumulates at the midbody to control RhoA GTPase function and, consequently, actin depolymerization and exit from mitosis. The absence or inhibition of this functional complex leads to abscission failure in cytokinesis, associated with prolonged RhoA localization at the midbody and elevated RhoA activity (Saurin et al. 2008). These data demonstrate that PKCε activity is required for RhoA exit from this compartment at the end of cytokinesis. To confirm how is important the role of PKCε during the last stages of mitosis, Saurin and colleagues employed then a chemical genetic approach to inhibit PKCε, by over-expressing a gatekeeper mutant of the kinase (M486A), and inhibiting its function with an ATP competitive analogue. In 2009, they observed that in control cells PKCε is uniformly

distributed throughout mitosis, whereas it rapidly accumulates around the actomyosin ring upon inhibition (Figure 9). Furthermore, they observed a prolonged accumulation of RhoA at late stages following furrowing upon PKCε inhibition, and that RhoA localization is controlled by PKCε activity (Saurin A, Brownlow N, and Parker PJ, 2009) (Figure 4).

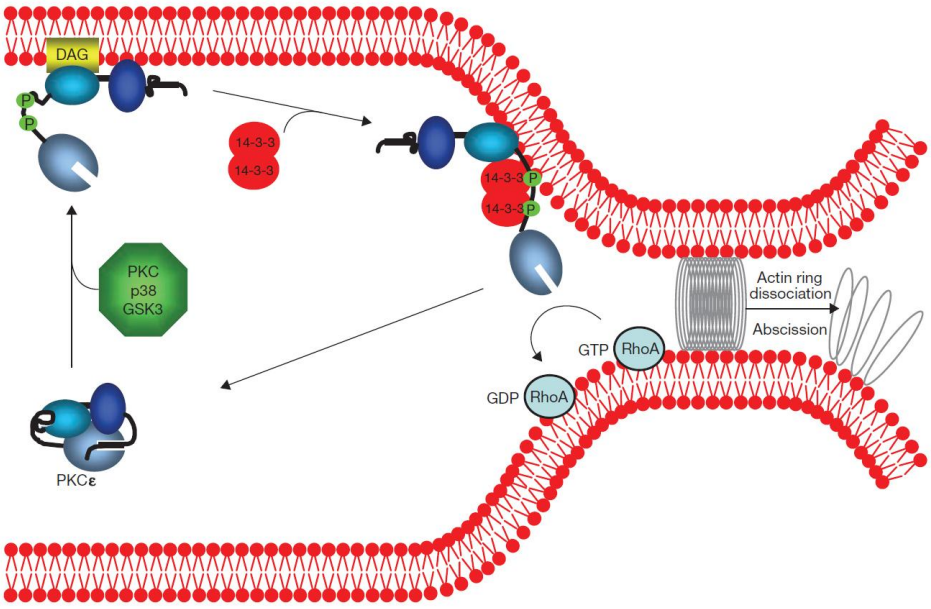

Figure 4. Schematic representation of PKCε/14-3-3 regulation of abscission. Through the upstream phosphorylation by PKC, p38 and GSK3, PKCε is assembled into a complex with 14-3-3. This complex transiently accumulates at the midbody to control RhoA-GTP loading and, consequently, actin depolymerisation and exit from mitosis. When inhibited, PKCε accumulates at the actomyosin ring with RhoA.

It has been recently demonstrated that PKCε regulates also mitotic catenation in metaphase-anaphase transition. DNA catenations physically link sister DNAs and must be resolved in order to allow proper chromosome condensation and segregation. In the model described by Brownlow N et al., PKCε is required to trigger the metaphase delay in response to catenation influencing the silencing of the spindle assembly checkpoint. Interestingly, this appears to occur in a subset of transformed cell lines, which have a weak G2 catenation checkpoint and therefore a higher chance to enter mitosis with detectable DNA catenation. In cells with both an abrogated G2 catenation checkpoint and inhibition or loss of PKCε, cells exit mitosis prematurely with disjunction errors caused by sister chromatid catenation. Furthermore, the same study provides evidence that mitotic exit caused by PKCε inhibition is a dynein-dependent process and shows that the metaphase arrest

stimulated by excess catenation is characterized by stripping of both the RZZ complex and dynein from the kinetochore along with ZW10 (Brownlow N et al, 2014) (Figure 5).

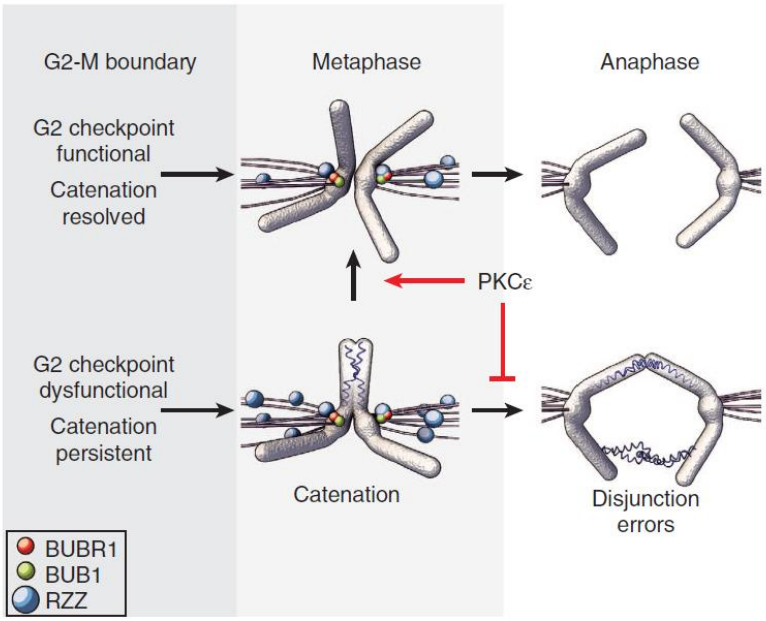

Figure 5. Schematic model of PKCε-dependent metaphase catenation delay. The catenation checkpoint at the G2/M boundary would normally trigger resolution of excess DNA catenation before mitotic entry. If this process fails, as in the case of some transformed cells, there is a failsafe in metaphase, which is dependent on PKCε to both implement a delay and to trigger catenation resolution. This pathway is activated when there is a persistent catenation following the spindle alignment in metaphase. In cells with both an abrogated G2 catenation checkpoint and loss of PKCε, cells exit mitosis prematurely with disjunction errors caused by sister chromatid catenation.

1.4 PKCε and tumorigenisis

PKCs have been linked to cancer progression since the 1980s, when it was discovered that tumour promoting phorbol esters were PKC activators. Extensive research has indeed established the key roles of PKC isoforms in malignant transformation.

Among the several isoforms of serine/threonine kinases, PKCε is one of the best understood for its role as a transforming oncogene: PKCε has been found overexpressed in tumour derived cell-lines and histopathological tumour specimens originating from a variety organs, including: bladder, brain, breast, lung, prostate, head and neck (*Varga A. et al., 2004; Sharif T.R. and Sharif M., 1999; Pan Q. et al., 2005; Bae K.M. et al., 2007; Aziz M.H. et al., 2007; Martinez-Gimeno C. et al., 1995*). It can contribute to malignancy also by enhancing cell proliferation or by inhibiting cell

death (*Basu A. et al., 2007*). Furthermore it seems to be involved in tumour cell invasion and in metastasis formation in several tissues (*Griner E.M. and Kazanietz M.G., 2007*).

Mischak and colleagues discovered that upon PKCε overexpression, NIH 3T3 fibroblasts grew at a faster rate and with increased densities and confluence. (*Mischak H. et al., 1993*).

In vivo, 100% of mice injected with PKCε-overexpressed NIH 3T3 cells developed tumors. Furthermore, PKCε is overexpressed in a panel of HNSCC cell lines (head and neck squamous cell carcinoma) (*Pan Q. et al., 2006*). *In vitro*, HNSCC cell lines with high endogenous PKCε levels are associated with a highly invasive and motile phenotype.

Elevated levels of PKCε have been documented also in lung cancers. In the small cell lung carcinoma cell line (SCLC) NCI-N417, a constitutively active catalytic fragment of PKCε has been reported. Additionally, RNAi-mediated silencing of PKCε in HNSCC and SCLC with high endogenous PKCε levels resulted in a marked reduction in cell invasion and motility and less aggressive phenotype in vitro (*Gorin M.A. and Pan Q., 2009*).

Many details about the pro-tumorigenic signaling pathways modulated by PKCε have been elucidated. For example, PKCε is known to exert its oncogenic effects through modulation of the Ras signaling cascade (*Perletti G.P. et al., 1998*), one of the best characterized signaling pathways in all of cancer biology. Among the many downstream effects, Ras signaling includes increased cell cycling via up-regulation of cyclin D1 (*Soh J.W. and Weinstein I.B., 2003*). Similarly, PKCε carries out its pro-survival effects by activating Akt/PKB through Ser473 phosphorylation (*Wu D. et al., 2004*). PKCε has also been implicated in anti-apoptotic signalling pathways through the modulation of caspases and Bcl-2 family members (*Ding L. et al., 2002; Pardo O.E. et al., 2002*).

PKCε has been demonstrated to mediate IkappaB kinase (IKK) phosphorylation though the activation of NAK, brings to the activation of the transcription factor NF-kappaB, a well-known anti-apoptotic factor (*Tojima Y. et al., 2000*). With the uncontrolled and faster proliferation and the

escape from apoptosis, the deregulation of cellular adhesion and motility are key components of a metastatic phenotype: neoplastic cells are able to invade and disrupt the surrounding tissues and migrate to colonize distal sites. It is proved that the overexpression of PKCε leads to a highly motile and an invasive phenotype. Tachado and coworkers reported that the expression of PKCε promotes polarized cell polarization and *in vitro* cell invasion. (*Tachado S.D. et al., 2002*). Moreover, they found that mice inoculated with NIH 3T3 cells overexpressing PKCε showed tumor invasion of nearby tissues as well as liver metastases. Specific details of how PKCε modulates cell motility are beginning to emerge. PKCε has been also observed to translocate to the cell membrane during the formation of focal adhesions to the extracellular matrix. This process is known as cell *spreading*. In human glioma cells, it is known that activated PKCε binds integrin β1 through interaction with RACK1 and positively regulates integrin-dependent adhesion, spreading and motility (*Besson A. et al., 2002*).

2. Signalling pathways that regulate cell cycle

2.1 The cell cycle: an overview

The cell cycle is the orderly progression of events during which genome, organelles and cytoplasmic components are duplicated and equally distributed to two daughter cells, resulting in cell proliferation. The ability of a cell, to duplicate and divide into two daughter cells, is one of the most fundamental properties that define life *(Poon R.Y.C., 2002)*. The cell cycle consists of four distinct phases: G_1, *S*, G_2 *(interphase)* and *mitosis*. In order to ensure genome integrity through the following generation and a high rate of success over the entire process, each phase must be precisely coordinated and regulated. Errors in cell cycle coordination are associated with many human diseases, in particular inappropriate and uncontrolled proliferation has been identified as one of the hallmarks of cancer *(Hanahan D. and Weinberg R.A., 2000, Hanahan D. and Weinberg R.A., 2011).* In fact, most cancers are in essence caused by a deregulation of the cell cycle, and many

oncogenes and tumor suppressor genes are intrinsic components of the cell cycle or can influence its progression.

After cell division, daughter cells undergo a period of growth, called *G_1 (first gap),* in which cells synthesize most cellular proteins, RNA, membranes components and other macromolecules. G_1 is followed by a phase characterized by DNA synthesis called *S (synthesis)* and then by another period of growth, *G_2 (second gap)* phase. All this events which precede mitosis, are collectively known as interphase. Non-dividing mammalian cells, such as nerve and heart muscle cells, exit the cell cycle at G_1 to enter in *G_0 phase (resting phase)* thus becoming quiescent: they are neither dividing nor preparing to divide and they can also exit the cell cycle during differentiation or senescence.

Mitosis consists into six distinct phases: (1) *prophase*, in which the mitotic spindle begins to assemble in the cytoplasm and chromosomes begin to condense in the nucleus; (2) *prometaphase*, in which the nuclear envelope begins to break down (NEB) and chromosomes attach to the spindle; (3) in *metaphase*, chromosomes are aligned at the metaphase plate; (4) *anaphase A*, in which chromosomes move to the centrosomes, the organelles responsible for mitotic spindle nucleation; (5) the spindle elongates in *anaphase B* and in *telophase (*6) the nuclear envelope reforms around the daughter nuclei. The entire cycle is completed with the physical separation of the two daughter cells in a process known as *cytokinesis.* Two major transitions are required for cell division: one is the G2/M transition and the metaphase/anaphase transition. The first is regulated by the protein kinase cyclin-dependent kinase 1 (CDK1) and its activation is necessary to trigger entry into mitosis. Therefore, CDK1 activation is the key point of many signaling pathways that control the commitment of the cell. These pathways are both positive and negative effects: once cells reach a critical size, CDK1 is activated and mitotic entry occurs, whereas CDK1 activation is delayed in presence of DNA damage. CDK1 activation and mitotic entry triggers the anaphase promoting complex (APC), which regulates metaphase/anaphase transition. The APC allows sister chromatids separation which segregate to opposite poles at anaphase (Figure 6).

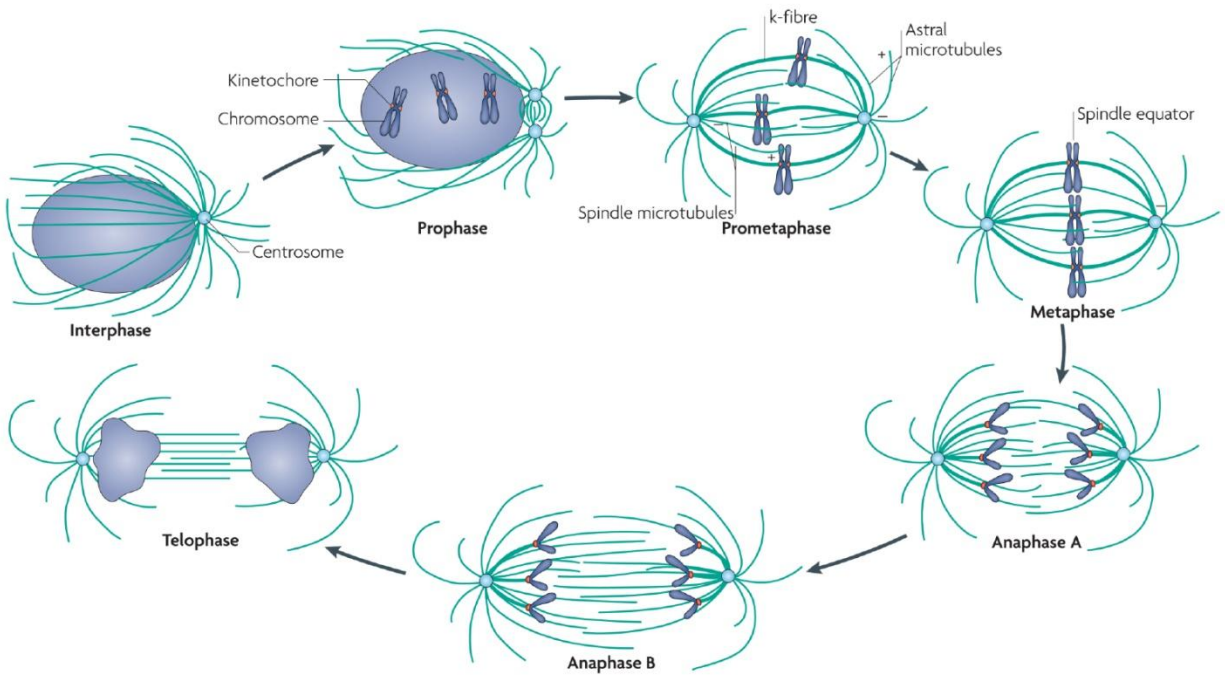

Figure 6. The cell cycle: cell division major events. Mitosis is subdivided into prophase, pro-metaphase, metaphase, anaphase and telophase (from *Walczak et al., 2010*).

2.2 Cyclins/CDKs complexes in cell division control

The complete coordination of biochemical independent processes of the cell cycle and the DNA integrity and fidelity are guaranteed by many checkpoint systems. Above all, chromosomal DNA must be replicated once and only once in each cycle and the two daughter cells must receive an exact copy of parental DNA. Also, a large number of macromolecular components and organelles need to be exactly replicated and equally segregated (*McGowan C. H., 2002*). Cell division major events, such as mitotic entry, chromosome segregation and cytokinesis, are finely regulated by many signalling pathways. Their role is to coordinate potentially independent events and to provide quality control checkpoints that arrest the process when things go wrong. The checkpoint pathways are composed of a sensor component that detects the defective process or error, a transducer that transmits the signal from the sensor and a target that is a regulator of the cell cycle machinery. Checkpoints arrest the progression of the cell cycle, inducing the expression of repair proteins. The

DNA damage checkpoint (G_1/S transition), the DNA replication checkpoint (S/G_2 transition) and the spindle checkpoint (metaphase) have been extensively studied for their involvement in neoplastic transformation (ref). As previously mentioned, an evolutionary conserved engine compose of a family of protein kinases called *cyclin-dependent kinases (CDKs),* is involved in the cell division signaling pathways (Figure 7). CDKs are a family of small Ser/Thr kinases whose periodic activation is driven by forming bipartite complexes with different protein called *cyclins* (*Suryadinata C.R. et al., 2010*). Their activities are highly regulated by protein-protein interaction and phosphorylation. Studies in mammalian cells have demonstrated that cyclin D-CDK4/6 complexes are activated and are essential during G_1 progression (*Matsushime H. et al., 1992, Meyerson M. and Harlow E., 1994*); the transition from G_1 to S is mediated by cyclin E-CDK2 complex (*Ohtsubo M. et al., 1995*) and CDK2 and CDK1 in association with cyclin A have a role during S and G_2 respectively (*Pagano M. et al., 1992*). Progression through mitosis is dependent on cyclin B-CDK1 (*King R.W. et al., 1994*). When active, these complexes function by phosphorylating a multitude of downstream transducers that acts on various components of the cell cycle apparatus.

During early and late G_1 phase, the cyclin D-CDK4/6 complexes act to integrate the extracellular proliferative signals. In early G_1, the product of the retinoblastoma tumour suppressor gene, Rb exists in a hypo-phosphorylated state and so prevents the premature entry into S phase by tightly binding and inhibiting the activity of transcription factors, such as E2F a component of the S-phase-inducing transcription factor (*Harbour J.W. and Dean D.C., 2000*). In addition, pRb inhibits E2Fs by recruiting members of the HDAC (histone deacetylase) family to E2F promoters (*Brehm A. et al., 1998*). HDACs are chromatin remodelling enzymes that inhibits gene expression by blocking the access of transcriptional factors to the promoter. During G_1, cyclin D-CDK4 and cyclin D-CDK6 complexes, expressed in response to mitogen growth signals, inactive pRb through sequential phosphorylation on several serine and threonine residues. Phosphorylation of pRb

destabilizes its interaction with E2F, induces HDACs dissociation and allows de-repression of cyclin E gene and cyclin E activation. As cyclin D levels increase, more cyclin D-CDK4/6 complexes are assembled and more cyclin E is activated. When cyclin E is abundant and conditions are favorable, it interacts with CDK2. Cyclin E-CDK2 complex phosphorylates pRb (*Hinds P.W. et al., 1992*), which is able to completely dissociate from E2F and permit the transcription of genes required for S phase such as cyclin A. Furthermore, cyclin E-CDK2 complex promotes centrosome duplication by phosphorylation of the centrosomal proteins NPM (nucleophosmin)/B23 and CP110 (*Okuda M. et al., 2000; Chen Z. et al., 2002*). Each cell inherits only one centrosome, which consists of a pair of core centrioles surrounded by an amorphous mass of proteins termed PCMs (pericentriolar materials) and centrosome duplication is essential for the formation of functional bipolar mitotic spindle (*Nigg E.A. and Stearns T., 2014*). As cells progress into S phase, cyclin A becomes the primary cyclin associated with CDK2. In order for two copies of the genome to be equally distributed to the daughter cells at M phase, DNA must be precisely replicated in the parental cell during S phase. However, correct S phase progression requires the down-regulation of E2F activity, which is partially accomplished by CDK-mediated phosphorylation. Once DNA has been replicated and cohesion complex has formed the joints between the sister chromatids, the cells enter into pre-mitotic Gap-2 (G_2) phase. G_2 phase is a period of rapid cell growth and protein synthesis during which the cells preparing themselves for mitosis. Even if cyclin A-CDK1 complex is involved in the G_2/M transition it is cyclin B, associated with CDK1, which allows the entry into mitosis. Cyclin A appears in the nucleus upon its synthesis (S phase) and remains nuclear until its degradation in metaphase. In contrast, cyclin B is initially localized in cytoplasm during S phase and G_2 phase, and then translocates to the nucleus at the beginning of mitosis (*Smits V.A.J. and Medema R.H., 2001*).

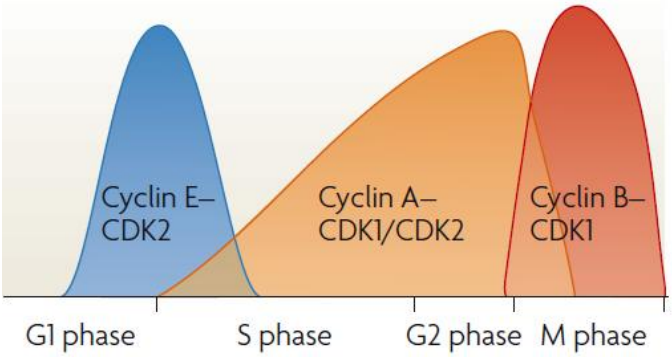

Figure 7. Classical model of cell cycle control. D-type cyclins and CDK4 and CDK6 regulate events in early G1 phase (not shown), cyclin E-CDK2 triggers S phase, cyclin A-CDK2 and cyclin A-CDK1 regulate the completion of S phase, and CDK1-cyclin B is responsible for mitosis. (*Hochegger H et al., 2008*)

2.3 Cell cycle regulation checkpoints

The G_2/M checkpoint delays the mitotic entry in case of DNA damage or incomplete DNA replication. If the G2 checkpoints are not triggered, cells fully activate CDK1 and proceed into mitosis. The G2 phase/mitosis transition involved the reorganization of the nucleus, the condensation of chromosomes and the formation of the mitotic spindle. These events are coordinated by CDK1, which activates a network of other kinases that are involved in G2/M transition, such as Polo-like kinases and Aurora kinases (*Hirota T. et al., 2003; Toyoshima-Morimoto F. et al., 2001*).

Before mitosis, CDK1 is maintained in an inactive state by phosphorylation of CDK1 at Thr14 and Tyr15 residues. Wee1, nuclear protein kinases, is involved in the phosphorylation of Tyr15 residue, whereas Myt1 (myelin transcription factor), a membrane-associated protein kinase, acts on Thr14 residue. As the cell approaches the G2/M transition, in the absence of DNA damage, an elusive signal activates the Cdc25C and cdc25b phosphatase and inhibits Wee1 kinase. Cdc25B and cdc25C activate cyclin B-CDK1 complex by dephosphorylation of Thr14 and Tyr15 residues on CDK1. Studies on fission yeast demonstrated that the opposing activities of Wee1 and Cdc25

underlie the rapid activation of CDK1 at G2/M transition (Nurse, 1975; Russel and Nurse, 1987). This event is regulated by a feedback regulation from CDK1, which can directly phosphorylate Wee1 and Cdc25. CDK1 is also able to activate Polo-like kinase 1 (Plk1), one of the major kinase involved in mitotic progression, which in turn leads to degradation of Wee1 and stimulates Cdc25 phosphatase activity (Kumagai & Dunphy, 1996). This double feedback loop ensures the rapid transition of a low-activity CDK1 state to a high-activity CDK1 state, thus driving the mitotic entry. Cyclin B-CDK1 triggers the phosphorylation of numerous proteins also to promote the profound structural reorganizations that leads the entry of the cells into mitosis. It induces the breakdown of the nuclear envelope and the disassembly of the nuclear lamina (in animal cells), the condensation of chromosomes, and the formation of a mitotic spindle that aligns the condensed chromosomes on the metaphase plate. (*Nigg E.A., 1995; Zacharie W., 1999*).

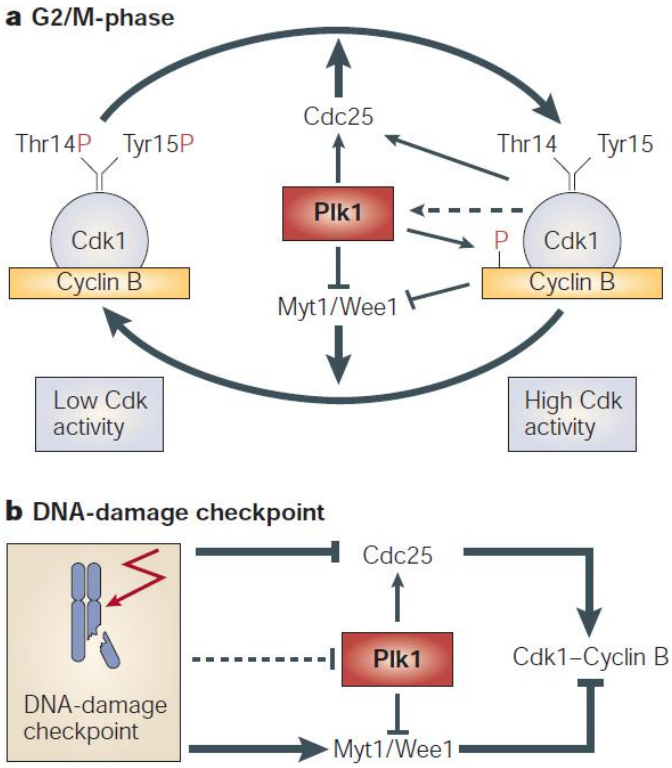

Figure 8. Representation of G2/M phase checkpoint regulation. A complex regulatory network controls the activity of the principal mitotic regulatory kinase, cyclin-dependent kinase-1(Cdk1)8 (see figure, part a). B-type cyclins that are required for Cdk1 activity accumulate during G2 phase.However, thenewly formed Cdk1–cyclin-B complex is maintained in an inactive state, owing to inhibitory phosphorylation of Cdk1at Thr14 and Tyr15 by the Wee1 and membrane-associated Cdk1-inhibitory kinase (Myt1) kinases. Activation of the Cdk1–cyclin-B complex occurs when the activity of the dual specificity phosphatase Cdc25 overcomes the effect of the opposing kinases Wee1/Myt1,which

results in the dephosphorylation of Cdk1.Not depicted in the figure,Cdk1 is also subject to an activating phosphorylation in its T-loop, which is brought about by Cdk-activating kinase (Cak; a complex of Cdk7, cyclin H and Mat1).Once activated,Cdk1 triggers a positive-feedback loop by phosphorylating Cdc25 and Wee1/Myt1, thereby causing their further activation and inhibition, respectively.Plks also affect both Cdc25 and Myt1(and presumably Wee1), but whether they function as trigger kinases for the activation of Cdk1, or merely in the context of a positive-feedback loop might depend on the developmental context (see main text). PLK1 also phosphorylates Homo sapiens cyclin B1 on Ser133 (REFS 48,60), but the consequences of this phosphorylation are not yet known. Conversely,Cdk1–cyclin-B might contribute to Plk1 activation, most likely through indirect mechanisms (dashed arrow). DNA damage or failure to complete DNA replication result in the activation of DNA-damage checkpoints (see figure, part b). (*Barr FA et al., 2004*)

Cell division must be finely regulated in order to distribute complete and accurate copies of the genome to daughter cells. Genomic instability occurs when cells enter to mitosis with chromosomes partially replicated or damaged by a double-strand DNA break (DSB). If unrepaired, such damages can lead to cell death or give rise to deleterious mutations able to develop in neoplastic transformation. In order to maintain genomic stability, cells have develop a complex network of signaling pathways – collectively known as the DNA damage response (DDR) – that enable DNA damage or DNA replication stress to be resolved with transient cell cycle arrest (*Jackson & Bartek, 2010; Ciccia & Elledge, 2011*). Several studies have demonstrated that DDR proteins are activated in early tumorigenesis, thereby limiting tumor development in its early stages by acting as a barrier for proliferation of malignant cells (*Bartkova et al., 2005; Gorgoulis et al., 2005*). Deficiency in DDR mechanisms have been shown to be contributing factors in tumor development (*Negrini et al., 2010*). In fact, many malignant tumor show functional loss or deregulation of important proteins involved in DDR, such as p53 or the BRCA1/2 genes, which encode for two proteins involved in double-strand DNA break repair. Such mutations allow pre-cancerous cells to breach the proliferation barrier posed by the DDR, thereby promoting malignant transformation.

Among the many different types of DNA damage, the DNA double strand breaks (DSBs) are one of the most deleterious; evidences have suggested that a single DSB may be sufficient to induce cell death and misrepaired DSBs can results in loss of genetic information or chromosomal rearrangement which potentially lead to cancer development (Bennett et al., 1993). The cellular responses to DNA damage and replication-fork stalling are controlled by ATM (ataxia

telangiectasia mutated), ATR (ATM and Rad3-related) and DNA-PKs (DNA-dependent protein kinases) (Figure 9). ATM and ATR are members of the PIKK (phosphoinositide-3-like-kinase kinase) family of serine/threonine protein kinases, which also comprises mTOR (mammalian target of rapamycin) and SMG1 (suppressor of morphogenesis in genitalia). ATM begins the checkpoint response to DSBs. The recruitment of ATM to the DSB sites is mediated by the MRN protein complex, which consists of Mre11 (a nuclease), Rad50 (a dimeric scaffolding protein with ATPase activity), and Nbs1 (an adaptor protein) subunits. Once localized at DNA ends, ATM phosphorylates proteins involved in cell-cycle checkpoints, DNA repair and chromatin structure, as the histone variant H2AX on Serine 139 (γH2AX). This phosphorylation triggers a cascade which assembles DDR components at the breakage site (*Paull et al., 2000; Scully and Xie, 2013*) thus promoting DNA repair. ATM also plays a critical role in the activation of the G1/S checkpoint, which prevents cell with damaged DNA to entry into S-phase. In response to DNA damage, ATM directly phosphorylates the tumor suppressor protein p53 on serine 15 (*Kastan et al., 2000*). The checkpoint kinase 2 (CHK2) is an ATM downstream target which also phosphorylate p53, stabilizing it and preventing its Mdm2-mediated ubiquitinylation and degradation. Upon activation, p53 acts as a transcription factor and drives the expression of proteins involved in the cell cycle checkpoints, as p21, and in the process of apoptosis. Further, CHK2 phosphorylation induces the ubiquitinylation and the degradation of the S-phase-promoting phosphatase Cdc25A (*Falck et al., 2001*).

Similarly to ATM, ATR is a protein involved in DDR. ATR is activated by single strand DNA structures which may arise in case of stalled replication fork. During DNA replication, DNA lesion or limiting supplies of deoxynucleotide triphosphates (dNTPs) may cause replicative DNA polymerases to slow down or stall. Nevertheless, the replicative helicase continue to unwind the DNA ahead the replication fork, leading to the generation of long stretches of single strand DNA (ssDNA). This ssDNA is bound by RPA, which elicits a checkpoint response by ATR/ATRIP

(*Branzei and Foiani, 2010*). Once activated, ATR downstream promotes DNA repair, stabilization and restart of stalled replication forks through CHK1 activation. CHK1 inhibits the firing of replication origins by degrading Cdc25A, thus turning slow the progression of DNA replication and providing time for resolution of the damage (*Xiao et al., 2003*). ATR is also involved in the G2/M checkpoint by preventing the premature entry of cells into mitosis before the DNA replication is completed or in presence of DNA damage. This ATR-dependent G2/M arrest is mediated through two mechanisms: 1- the degradation of Cdc25A and 2- the phosphorylation of Cdc25C phosphatase on serine 216 by CHK1, which create a binding site for 14-3-3 proteins. This binding promotes the Cdc25C exit from the nucleus thus preventing Cdc2 activation necessary for mitotic entry (*Karlsson-Rosenthal & Millar, 2006*).

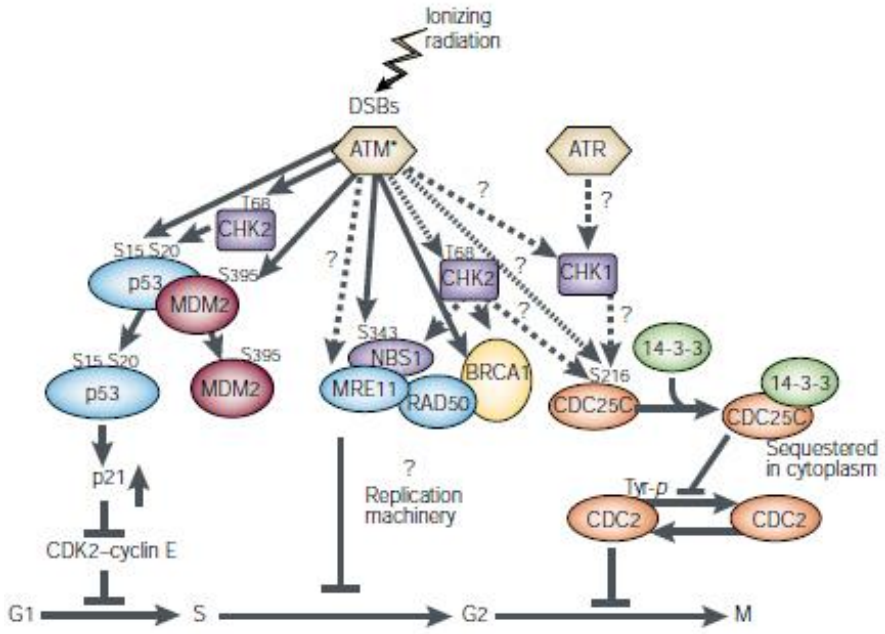

Figure 9. ATM and other molecular signals controlling cell-cycle checkpoints after ionizing radiation. The specific activity of ATM is increased after introduction of DNA doublestrand breaks (DSBs) in DNA through ionizing radiation or other means. G1: Activated ATM (ATM*) directly phosphorylates three proteins involved in controlling p53 functions or levels — p53 (serine 15), CHK2 (threonine 68) and MDM2 (serine 395). The CHK2 kinase is thought to be activated by ATM and it, in turn, phosphorylates p53 on serine 20. This phosphorylation event and the phosphorylation of MDM2 both seem to inhibit binding of MDM2 to p53 and should result in an increase in the level of p53 protein. The increased level of p53 protein transcriptionally induces p21, which inhibits CDK2–cyclin E, and causes arrest in the G1 phase of the cycle. S: Activated ATM also phosphorylates NBS1 (serine 343) and this phosphorylation event is required for the ionizing radiation-induced S-phase arrest. NBS1 exists in a complex with MRE11, RAD50 and BRCA1. The potential role of these proteins in the S-phase arrest remains to be clarified. In addition, CHK2 may also be involved in this pathway after activation by ATM through phosphorylation of BRCA1 or NBS1. G2: Details have not been worked out clarifying the downstream targets of ATM at the G2 checkpoint. CHK2

and CHK1 may possibly be targets for ATM and ATR in the G2–M checkpoint pathway, respectively. CDC25C and 14-3-3 have been implicated in regulation of CDC2 kinase and progression through G2. The dashed arrows and question marks represent possible signalling steps and the solid arrows represent reported hosphorylation events. (*Kastan MB and Lim D, 2000*)

During S phase, the DNA replication occurs and DNA catenations between sister chromatids are formed. These catenations physically link sister DNAs and must be resolved in order to allow proper chromosome condensation and segregation. The completion of mitosis with entangled chromosomes results in a gain and loss of whole chromosomes, thus leading to a condition of genomic instability. The G2 phase decatenation checkpoint delays entry into mitosis until catenations are resolved by the highly conserved eukaryotic enzyme topoisomerase II (topoII). The decatenation checkpoint is distinct from the DNA damage checkpoint as topoII disentangle chromosomes by passing one double helix through a transient DBS in another double helix and releasing the break. Mammalian species express two types of topoisomerase: topoIIα and topoIIβ. The two isoforms are encoded by different genes located on different human chromsomes and they can be distinguished by their mass. TopoIIb is non-essential and constitutively expressed, whereas TopoIIa is an essential gene maximally expressed in G2- and mitosis. The classical topoi inhibitors, as etoposide and teniposide, generate many DBSs and trigger the DNA damage checkpoint in G2 phase. In contrast, the catalytic inhibitors as ICRF-193, inhibit topoII before the DBS formation and activate the decatenation checkpoint, but not the DNA damage checkpoint (*Downes et al. 1994*).

In eukaryotes, the spindle assembly checkpoint (SAC) is an elegant regulatory system that ensures the fidelity of chromosome segregation in mitosis by delaying the onset of anaphase until each and every chromosome has established a bipolar orientation (*Lew D.J. and Burke D.J., 2003*) (Figure 10). Several proteins, identified for the first time in yeast but highly conserved also in mammalian cells, have been shown to be directly involved in the spindle assembly checkpoint: the Bub proteins

(Bub1p, Bub2p and Bub3p), the Mad proteins (Mad1p, Mad2p and Mad3p), and the Mps1 protein (Mps1p). The SAC targets CDC20, a co-factor of the ubiquitin-ligase APC/C. It negatively regulates the ability of CDC20 to activate the APC/C-mediated polyubiquitylation of *cyclin B* and *securin*, thereby preventing their degradation by 26S proteasome. Securin inhibits separase, a protease required to cleave the cohesin complex that holds sister chromatids together and must be cleaved in order to progress into anaphase. At the same time, the proteolysis of cyclin B inactivates CDK1, which promotes exit from mitosis. By targeting CDC20, the SAC is able to regulate this chain of events, prolonging prometaphase until all chromosomes are correctly attached to the microtubules and have become bi-oriented between separated spindle poles on the metaphase plate, the only condition that ensures accurate segregation at anaphase. Cyclin B and securin begin to be degraded after the last chromosome has aligned, and they become largely depleted before anaphase. It has been demonstrated that the addition of spindle poisons during this process, stops the reaction of proteolysis and the anaphase onset is prevent in a SAC-dependent manner. Furthermore, interference with the kinetochore assembly, impairment of microtubule motor proteins (as dynein or CENP-E) and interference with microtubule dynamics also activate the SAC (Clute P & Pines J, 1999; Rieder, C. L. & Maiato, H., 2004). Recent studies revealed a mitotic checkpoint complex (MCC), which includes MAD2, BUBR1/Mad3, BUB3 and CDC20 itself, as a SAC effector (Sudakin V et al., 2001; Morrow CJ et al., 2005). The MCC binds the APC/C and renders it unable to exert its ubiquitin-ligase activity on securin and cyclin B.

During prometaphase, SAC proteins accumulate at unattached kinetochores and move polewards upon microtubule attachment. It is unclear whether the checkpoint proteins are regulated by tension due to the anchoring of microtubules to kinetochores or by the physical occupancy of kinetochores by microtubules (*Nezi L and Musacchio A, 2009*). MAD2 localizes to unattached kinetochores in prometaphase or in cells treated with nocodazole, a drug able to induce microtubules depolymerization thereby prevent microtubule-kinetochore attachment (*Waters JC et al., 1998*).

MAD2 is removed once the kinetochore is occupied by a microtubule. Therefore, the amount of MAD2 becomes highly reduced at metaphase kinetochores (50-100 fold compared with unattached prometaphase kinetochores). This indicates that MAD2 localization can be interpreted to signify lack of attachment.

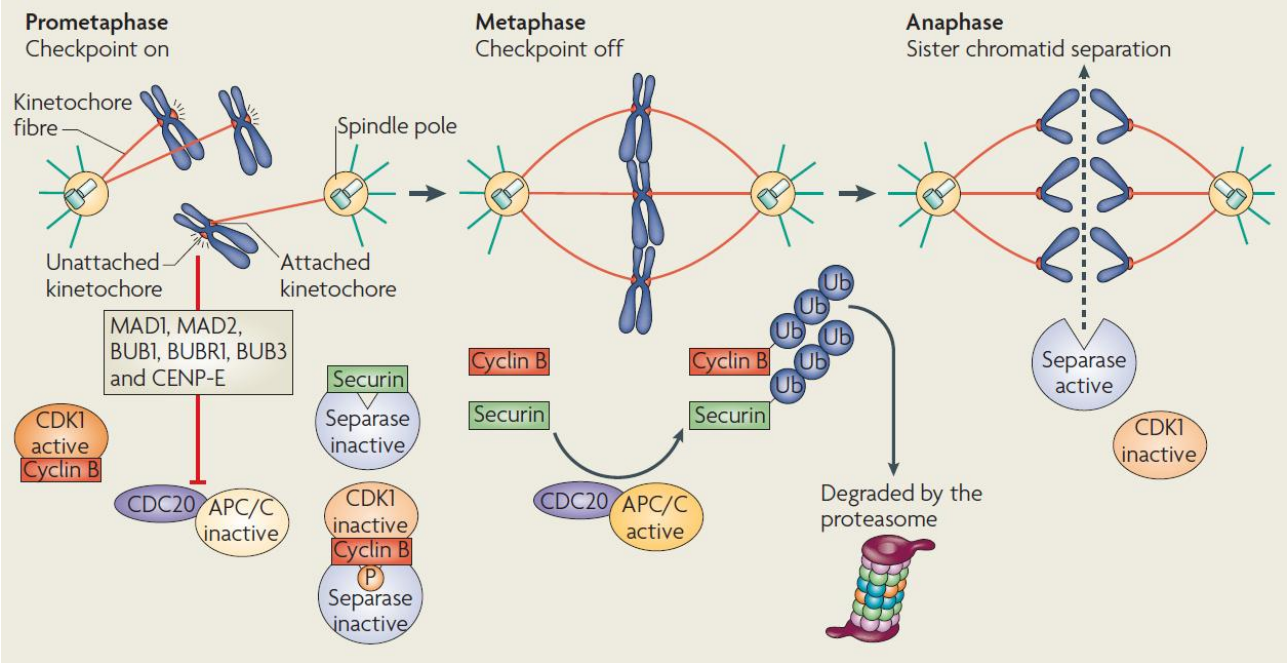

Figure 10. The microtubule-organizing centre of the cell, the centrosome, is duplicated during S phase and separates at thebeginning of mitosis. Microtubules nucleated by the centrosomes overlap to form a bilaterally symmetrical mitotic spindle, with each of the spindle poles organized around a single centrosome. Chromosomes attach to spindle microtubules at specialized proteinaceous structures known as kinetochores, which are assembled on centromeric chromatin early in mitosis (see the figure). To ensure that microtubules pull sister chromatids to opposite sides of the cell, kinetochores of duplicated chromosomes must attach to microtubules emanating from opposite spindle poles, a state known as bi-orientation. Errors in this process lead to the missegregation of chromosomes and the production of aneuploid daughter cells. To guard against chromosome missegregation, cells have evolved a surveillance mechanism called the mitotic checkpoint (also known as the spindle assembly checkpoint), which delays the onset of anaphase until all chromosomes are properly attached and bi-oriented on the microtubule spindle7,8. Core components of the mammalian mitotic checkpoint machinery include MAD1, MAD2, BUB1, BUBR1, BUB3 and centromere protein E (CENP-E). These proteins localize to unattached or malorientated kinetochores, which in turn catalytically generate a diffusible signal90 that inhibits cell division cycle 20 (CDC20)-mediated activation of an E3 ubiquitin ligase, the anaphase promoting complex/cyclosome (APC/C). Separase, the protease that cleaves the cohesins that hold sister chromatids together, is inhibited by at least two mechanisms. The first mechanism involves the binding of the chaperone securin, whereas the second involves the phosphorylation-dependent binding of cyclin B associated with cyclin-dependent kinase 1 (CDK1)91. The binding of CDK1–cyclin B inhibits the activity of both separase and CDK1. Following attachment and alignment of all the chromosomes at metaphase, the checkpoint signal is silenced and the APC/C ubiquitylates and targets securin and cyclin B for proteasome-mediated destruction, thereby initiating anaphase. At the same time, the degradation of cyclin B inactivates CDK1, thereby promoting exit from mitosis. (*Holland AJ and Cleveland DW, 2009*).

The microtubules, from opposite poles, exert pulling forces on the sister chromatids, which exhibit

a complex pattern of movement: some chromosomes move polewards while other chromosomes move away from the spindle poles and others remain relatively motionless. At the end, these different movements result in the migration of chromosomes to the spindle equator and in the entry in a new stage of mitosis, metaphase in which all chromosomes are aligned on the metaphase plate in the middle of the cell. The metaphase-anaphase transition is controlled by the ubiquitin-mediated degradation of several proteins. Sister chromatids have to remain tightly associated by cohesins until anaphase to ensure daughter cells receive only one copy of DNA. At the onset of anaphase, when all kinetochores are attached with the microtubules, Mad2p complex disassociates and releases Cdc20p and APC/CCdc20 becomes active. As previously mentioned, the APC/C is an E3 ubiquitin protein ligase that catalyzes the transfer of ubiquitin to target cell cycle proteins for 26S proteasome degradation. Once activated, APC/CCdc20 targets the ubiquitination and proteasomal degradation of the securin proteins and mitotic cyclin B, triggering chromosome segregation and cytokinetic furrow ingression. Securin is an anaphase inhibitor protein that blocks sister chromatid separation (*Zou H. et al., 1999*). Securin degradation brings to Separase activation. Separase is a cysteine protease, which cleaves the SCC1 (sister chromatid cohesion protein 1) subunit of the cohesion complex, allowing the chromosomes to be pulled by the spindle microtubules towards opposite poles (Anaphase A). Further segregation is achieved by the movement of the spindle poles away from each other (Anaphase B) (*Farr K.A. and Cohen-Fix O., 1999*).

In addition, ubiquitylation and degradation of cyclin B lead to CDK1 inactivation and dephosphorylation of many CDK1 substrates by the counteracting phosphatases, which promote cytokinetic furrow ingression and mitotic exit (*Fededa J.P. and Gerlich D.W., 2012*).

2.4 Regluation of cytokinesis

When each set of chromatids reach the opposite spindle poles, cells enter in telophase. Chromosomes decondense as the nuclear envelope reforms around the two daughter nuclei. The cell is now ready to physically split in two daughter cells in a process called cytokinesis. Cytokinesis is tightly coupled to chromosome segregation, in terms of both its spatial and temporal regulation (*Barr F.A. and Ulrike Gruneberg U., 2007*). Cytokinesis failure results in tetraploid cells with extra centrosomes that are genetically instable owing to perturbed chromosome segregation in subsequent cell divisions. Tetraploid cells derived from experimentally perturbed cytokinesis induce cancer in a mouse model, indicating that understanding the molecular control of cytokinesis may help to elucidate cellular defects underlying carcinogenesis (*Ganem N. J. et al., 2007*).Since anaphase, the CDK1 inactivation leads to a stabilization of microtubules and structural reorganization of the mitotic spindle: astral microtubules grow towards the cell cortex and *the central spindle* is assembled. It is interesting to note that the decline of CDK1 activity at the metaphase-anaphase transition leads to dephosphorylation and subsequent activation of proteins that are critical for the assembly of the central spindle.

The central spindle is composed of antiparallel bundles of microtubules that overlap their plus ends at the central region where microtubule-associated proteins, motor proteins and protein kinases accumulate (*Glotzer M., 2009*). PRC1 (protein required for cytokinesis 1), the tetrameric centralspindlin complex (composed of the kinesin motor protein MKLP1 and the Rho-family GTPase activating protein RhoGAP/MgcRacGAP) and the chromosomal passenger complex (CPC, which includes the kinase aurora B and its co-activator the inner centromere protein, INCENP) are all involved in the central spindle formation; while polo-like kinase 1, PLK1, is required for division plane specification (*Mollinari C. et al., 2002, Brennan I.M. et al., 2007*).

The position of the division plane between the segregated chromosomes seems to be specified by

transmission of a spindle position signal to the cell cortex through a pathway involving the small GTPase RhoA. In numerous cell types, inactivation of RhoA leads to a profound defect in cytokinesis, and in most cases cleavage furrow formation is completely blocked (*Drechsel D.N. et al., 1997*). Both astral and central spindle microtubule organization regulates RhoA localization at the equatorial cortex but the precise mechanisms remain unclear. It is known that PLK1 and centraspindlin activity is critically required for the recruitment of the RhoA guanine-nucleotide exchange factor ECT2 (epithelial cell transforming protein 2) to the central spindle (*Burkard M.E. et al., 2007*). Once activated by ECT2, RhoA induces the formation of a perpendicular *actomyosin contractile ring* at the cleavage furrow site. RhoA promotes actin polymerization through the activation of diaphanous-related formins and myosin II activation by the kinase ROCK, which phosphorylates the myosin regulatory light chain MRLC (*Watanabe S. et al., 2008*). This positive contractile signal is thought to operate alongside relaxation signals transmitted along microtubule asters to the poles of the cell, driving further the net contraction around the equator (*Werner M. and Glotzer M., 2008*).

The force-generating mechanism of actomyosin ring contraction is not understood. Several models have been proposed on the basis of ultrastructural analysis and biophysical considerations. A classical model proposes that bipolar myosin filaments move along actin filaments similarly to the force-generating mechanism in muscle sarcomeres. This tightening ‘purse string’ in turn is believed to provide the contractile force necessary to drive furrow ingression (*Wang Y., 2001*).

Cleavage furrow ingression continues until the actomyosin contractile ring comes into close proximity to the central spindle. At this stage the two daughter cells remains connected only by a narrow intercellular bridge containing dense antiparallel bundles of microtubules at the central spindle and the contactile ring, termed midbody (Figure 11). Midbody microtubules partly derive from bundling of the midspindle during furrow ingression, but also assemble de novo during formation and maintenance of the intercellular bridge. In line with this, the microtubule nucleation

factor γ-tubulin accumulates at the cytoplasmic ends of the midbody microtubule bundles and later in the central midbody region, and injection of anti-γ-tubulin antibody interferes with abscission (*Julian M. et al., 1993*).

Finally, abscission leads to disassembly of microtubules from both lateral sides of the midbody, constriction of cell cortex and irreversible fission of plasma membrane with the creation of two separate cells. Following abscission, the residual midbody structure, known as the midbody derivative, can have different fates depending on the cell type. The midbody derivative is either released to the extracellular medium, degraded by autophagy or persists in the cytoplasm.

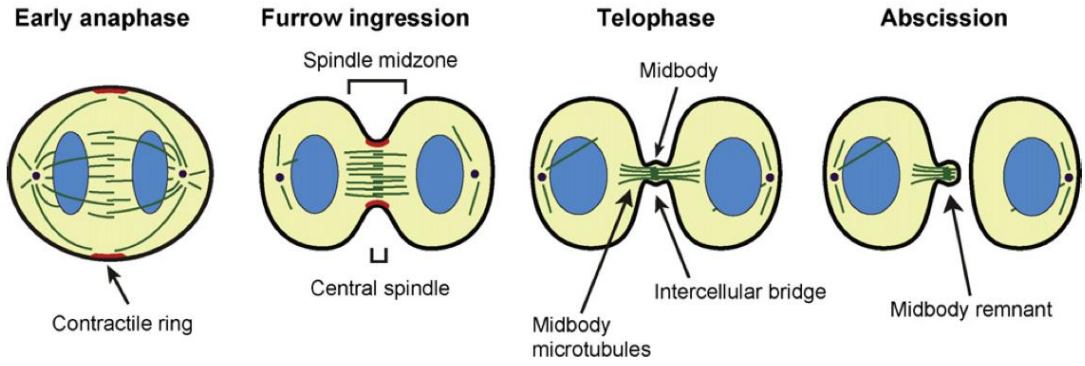

Figure 11. Schematic diagram of the different stages of cytokinesis (microtubules, green; chromatin, blue; plasma membrane, black; contractile actin ring, red; centrosomes, violet). In early anaphase the components of the contractile ring have assembled. Contraction of the actomyosin ring is thought to provide the necessary force for furrow ingression. Once fully ingressed, in late cytokinesis, compression of the central spindle creates an intracellular bridge containing the midbody (from *Guizzetti J. and Gerlich D.W., 2010*).

3. Bipolar spindle assembly and maintenance

During every cell cycle, the genome of a cell must be duplicated and equally segregated into two daughter cells. Chromosome segregation is driven by the *mitotic spindle*, a microtubule-based structure that must form a bipolar configuration in order to equally segregate the genome. The dynamic plus-ends of microtubules, emanating from opposite poles, bind to the kinetochores of the

sister chromatids and a balance of forces drives the alignment of chromosomes (congression) along the metaphase plate, and the subsequently segregation of sister chromatids to the opposite poles of the cell. Defects in mitotic spindle geometry affect the structure bipolar orientation and potentially contribute to chromosome miss-segregation.

3.1 Centrosome dynamics

Centrosome plays critical roles in cell cycle regulation in both mitosis and interphase by providing a central signalling station and controls to trigger the next phases of the cell cycle by integrating, regulating, and amplifying signalling pathways. In animal cells, the centrosome is the primary *microtubule organizing centre* (MTOC) (*Murphy S.M. and Stearns T., 1996*). In nondividing cells, centrosomes are located near the nucleus where they determine cell shape, polarity and proper positioning of the subcellular organelles. In dividing cells, centrosomes duplicate in order to establish bipolar mitotic spindles able to equally segregate the chromosomes between the two daughter cells. The spatial separation of duplicated centrosome determines the length and the orientation of the mitotic spindle. This separation can occur in prophase or after the nuclear envelope breakdown (NEB), in prometaphase. The timing of this process influences the mitotic spindle geometry (*Silkworth WT et al., 2012*).

Centrosome consists of two orthogonal centrioles surrounded by an electron-dense pericentriolar material (PCM). The centriolar cylinders have diameters of about 0.2 μm and they are each composed of nine triplets of short microtubules, arranged to form the wall of the cylinder. The nucleation of new microtubules from the MTOC is mediated by the gamma-tubulin ring complexes (γTURCs), which are surrounded by the PCM. The centrosome is duplicated and separated once each cell cycle and proceeds coordinated with the cell cycle. Centrosomes duplication occurs between the late G1 and the early G2 phase and is characterized by four stages: centriole disengagement; centriole duplication; centriole elongation and centrosome maturation. Centriole

disengagement is essential for limiting centriole duplication to one round per cell cycle and for recruiting PCM (*Wong C and Stearns T, 2003*). Subsequently, the cell contains one centrosome comprised of two structurally and functionally dissimilar centrioles. The mother centriole, which originates from the mother cell, nucleates and organizes microtubules. The daughter centriole, which is replicated from the mother centriole as procentriole, only nucleates microtubules. The synthesis of the daughter centriole takes place in early S phase. The new daughter centrioles that emerge near the proximal ends of mature centrioles then elongate and reach full length by the late G2 or early M phase. In late G2 phase, the PCM increases the γTURCs and its associated proteins in a process called centrosome maturation. This is regulated by Aurora A and Plk1 (*Lane HA and Nigg EA, 1996; Hannak E et al., 2001*). Centrosome maturation begins when Plk1 phosphorylates pericentrin and NEDD1, which targets γTURC to the PCM. Aurora A is then localized to the centrosome and is activated by Plk1. At the G2/M transition, centrosomal cohesion is gradually lost (centrosome disjunction) and centrosomes move toward opposite poles to form a bipolar spindle, a process referred to as *centrosome movement*. This centrosome cycle step is a complex and multi-faced process that remains incompletely understood at the molecular level (*Mardin BR and Shiebel E, 2012*). The kinesin Eg5 is a key regulator of centrosome movement. This motor protein accumulates at centrosomes and astral microtubules, where it generates forces by sliding antiparallel microtubules between centrosome pairs in opposite directions. Although the role of Eg5 in this process has been firmly established, recent studies have demonstrated that additional proteins are also required to generate the necessary forces for centrosome movement (*Tanenbaum ME and Medema RH, 2010, Gayek AS and Ohi R, 2014*).

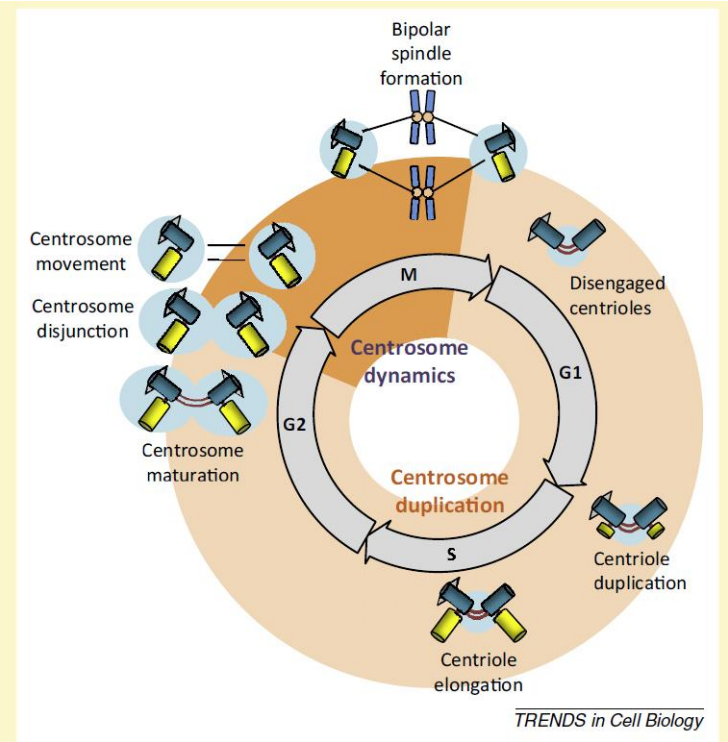

Figure 12. The centrosome cycle. The centrosome cycle is divided into two parts: centrosome duplication, which encompasses centriole disengagement, duplication, elongation, and maturation; and centrosome dynamics, which includes centrosome disjunction and movement. In late mitosis, the daughter centriole disengages from the mother centriole and the two centrioles lose their orthogonal configuration (centriole disengagement). At the G1/S transition, one new daughter centriole is synthesized per mother centriole to form a new centrosome (centriole duplication and elongation). In the late G2 phase, both centrosomes recruit PCM components in order to prepare for mitosis (centrosome maturation). At the G2/M transition, centrosomal cohesion is gradually lost (centrosome disjunction) and centrosomes move toward opposite poles to form a bipolar spindle (centrosome movement). (*Nam H et al, 2014*).

The link between centrosome separation and aneuploidization has been historically overlooked for several reasons. It has been demonstrated that somatic cells can use a spindle-independent pathway for spindle formation in experimental conditions, when centrosomes are removed by laser ablation or microsurgery (*Khodjakov et al., 2000; Hinchcliffe EH et al., 2001*). Further, Drosophila melanogaster lacking centrosomes can accomplish bipolar spindle formation without any evident abnormalities (*Basto R. et al., 2006*). Nevertheless, recent work from several laboratories have demonstrated that proper centrosome dynamics has a critical role in ensuring accurate chromosome segregation; both delayed or accelerated centrosome separation increases rates of spindle geometry defects in metaphase and mitotic errors (*Silkworth WT and Cimini D, 2012; Kaseda K et al. 2012*).

These and other recent studies in cyclin B2 overexpressing cells have demonstrated that accelerated centrosome separation caused abnormal spindle positioning resulting in merotelic attachments, a type of attachment error in which one kinetochore is attached to microtubules originating from both spindle poles (*Nam HJ and van Deursen, 2014*). This type of attachments is potentially dangerous for dividing cells because they are not detectable by the spindle assembly checkpoint thereby resulting in lagging chromosomes if left incorrect. The mechanistic basis for increased merotelic attachment upon accelerated or delayed centrosome separation is still unknown. Modulation of Aurora B kinase activity can be one possible explanation. Aurora B is a member of the chromosome passenger complex (CPC), which also includes the inner centromere protein (INCENP), Borealin and Survivin (*Ruchaud S et al., 2007*). The CPC controls many aspects of mitosis, including the correction of kinetochore-microtubule attachment errors. Aurora B respond to tension generated by the mechanical stretching due to the kinetochore-microtubule attachment: a low stretch in the absence of tension will promote destabilization, whereas a high stretch in the presence of tension will promote stable attachments. Inner centromeric Aurora B is therefore able to destabilize faulty kinetochore-microtubule attachments by phosphorylating its substrates located on outed kinetochores (*Lampson MA and Cheeseman IM, 2011*). The tension generated under asymmetric spindle conditions may silence Aurora B kinase activity by physically dissociating it from its substrates, leaving the erroneous attachment unresolved.

In addition to centrosome separation, also altered centrosome movement, either too slow or too rapid, potentially promotes merotelic attachments and chromosome lagging. It has been demonstrated that defective centrosomal targeting of Eg5 might delay poleward movement resulting in abnormal mitotic spindle and its overexpression promotes chromosomes segregation errors (*Nam H et al, 2014*). In line with this, MEFs that overexpress Eg5 were found to be genomically unstable and were unable to form a proper bipolar spindle in mitosis (*Castillo A et al., 2007*). Although Eg5 is the most obvious target for the alteration of centrosome movement, it has been suggested that

also improper anchoring of the spindle pole at the cell cortex is a source of spindle geometry defects. Cortical anchoring sites are created by specific multi-protein complexes: the G protein Gai accumulates at the anchoring sites and mobilizes LGN, a large scaffold protein. LGN recruits the microtubule binding protein NuMA and the motor complex dynein-dynactin, which provides plus-end directed microtubule-pulling forces (Du Q and Macara IG, 2004).

3.2 Microtubules structure and mitotic spindle assembly

Coordinate with the Nuclear Envelope Breakdown (NEB), there is an increase in the microtubule nucleating capacity of centrosomes. The redial array of microtubules surrounding the centrosomes is referred to as an *aster*; as the disengaged centrosomes move apart, the connected microtubules form an *amphiaster*. This initial stage of mitotic assembly is critical for the establishment of the spindle bipolarity. Aster separation before NEB is driven by forces produced by cytoplasmic dynein/kinesin 5 acting on microtubules emanating from the opposite poles and by nonmuscle myosin II interactions with cortical actin. These force-producing properties of the early-stage spindle are coupled with the dramatic increase in microtubule-nucleating capacity of the duplicated centrosomes.

The microtubules are complex polymers composed by heterodimers of α and β-tubulin, present in all eukaryotic cells and involved in a variety of cellular processes (*Murphy S.M. and Stearns T., 1996*). The tubulin dimers assemble in a head-to-tail manner to form linear polymers called *protofilaments*. Multiple protofilaments, tipically 13, assemble into tubular microtubules structures of 25nm of diameter. The orientation of the heterodimers within the microtubules confers an intrinsic polarity, which is defined by a *minus end* (exposing α-tubulin) and a *plus end* (exposing β-tubulin).

In the mature *mitotic spindle* of animal cells, the microtubules (MTs) are divided in three distinct subclasses in basis of their position, organization and functionality: the astral MTs, the interpolar

MTs and the kinetochore-fibres (K-fibres). *Astral MTs* emanate from the two centrosomes and extend to the cell cortex; they play a major role in centrosome separation during prophase and in spindle positioning (*Rosenblatt J., 2005*). The *interpolar MTs* is the most abundant and dynamic class of MTs: they emanate from the centrosome and extend towards the centre of the spindle where they interact in an antiparallel manner with the interpolar MTs from the opposite spindle pole. Interpolar MTs have multiple functions, including the establishment and maintenance of spindle bipolarity. *K-fibres* are bundles of 20-40 parallel MTs that attach the chromosomes from the kinetochores to the two spindle poles during prometaphase, allowing the following segregation of sister chromatids.

Microtubules are highly dynamic structures, which undergo periods of polymerization (growth) and depolymerization (shrinkage). The co-existing of growing and shrinking microtubules in the same conditions is termed "dynamic instability" (*Mitchison T. and Kirschner M., 1984*). Although microtubules exhibit dynamic instability at both ends, in the mitotic spindle the plus ends are more dynamic than the minus ends, which are often capped at the centrosome (*Walczak C.E. et al., 2010*) (Figure 13). Interpolar MTs and K-fibres exhibit an additional dynamic property, known as microtubule flux, in which there is a net addition of tubulin heterodimers at the plus ends near the kinetochores and a net loss of tubulin subunits at the minus ends near the centrosomes. Thus, the plus-end is the dominant site for tubulin subunits addition and MTs elongation.

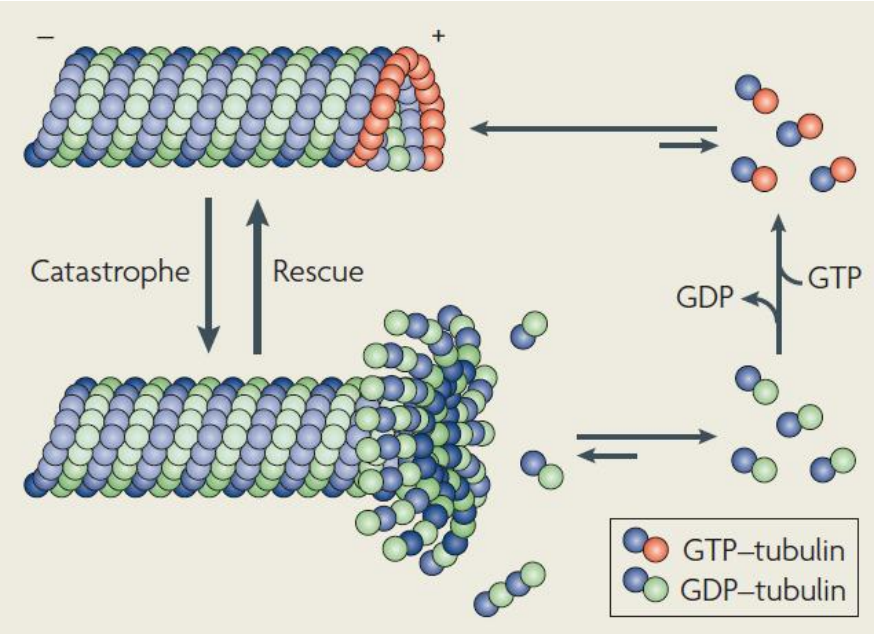

Figure 13. Representation of microtubules dynamics. Microtubules exhibit a specialized non-equilibrium polymerization behaviour, termed dynamic instability, in which polymerizing and rapidly depolymerizing polymers coexist at steady state. The transition from polymerization to depolymerization is referred to as a catastrophe, and the reverse transition is referred to as a rescue. Polymerization triggered GTP hydrolysis on β‑tubulin provides the energy source for this non-equilibrium behaviour; the resulting GDP is locked into the polymer lattice until depolymerization releases the subunit. The energy of GTP hydrolysis is stored as mechanical strain in the GDP–tubulin polymer lattice, resulting in >1,000-fold higher dissociation of GDP–tubulin at a depolymerizing end relative to dissociation of GTP–tubulin at a polymerizing end. A polymerizing microtubule end is thought to persist because of a lag between subunit addition and nucleotide hydrolysis, which results in a stabilizing cap of GTP–tubulin. Loss of this cap, either stochastically or by the action of external factors, triggers release of the stored mechanical strain and a switch to rapid depolymerization. Nucleotide exchange on the released tubulin dimers re-primes these dimers for a new polymerization cycle. Both polymerization and depolymerization generate significant forces and can do productive work in vivo. (*Cheesman IM and Desai A, 2008*).

Microtubules polymerize spontaneously *in vitro* from high concentrations of α/β-tubulin in the presence of GTP and Mg^{2+}. Polymerization occurs in a two-step process that involves a rate-limiting 'nucleation' step followed by rapid elongation. *In vivo*, the polymeration process is assisted and controlled by the centrosomes. The centrosomal protein γ-tubulin is a key factor in microtubule nucleation (*Wiese C. and Zheng Y., 1999; Pereira G. and Schiebel E., 1997; Stearns T. et al., 1991; Zheng Y. et al., 1991*). γ-tubulin is a highly conserved protein in all eukaryotes, and it belongs to two complexes: *the γ-tubulin small complex* (γTuSC), which is composed of two molecules of γ-tubulin associated with the additional proteins GCP2 and GCP3, and *the large γ-tubulin ring complex* (γTuRC) (Fig. 8). This one is composed of multiple copies of γTuSC proteins, which interact laterally each other and with several additional proteins, including GCP4, 5 and 6, GCP-

WD/NEDD1 whose role is less clear (*Luders J. et al., 2006*). γ-tubulin complexes are found in soluble form in the cytoplasm, whereas they are bound to the centrosome or to the spindle polar bodies. Although it has not been tested directly in animal cells, it seems likely that there is dynamic exchange between the centrosomal and cytoplasmic pools of y-tubulin, which allows the centrosome to alter its nucleating capacity in response to intracellular or extracellular signals. For example, the nucleating ability of the centrosome increases at the onset of mitosis, associated with an increased γ-tubulin at the centrosome (*Khodjakov A. and Rieder C.L., 1999*), presumably reflecting the fast recruitment of cytoplasmic γ-tubulin. The mitotic kinases cyclin-dependent kinase 1 (CDK1), polo-like kinase 1 (PLK1) and Aurora A have been shown to be involved in γ-tubulin recruitment to the centrosome (*Blagden S.P. and Glover D.M., 2003*).

3.3 Chromosome attachment to the spindle

Proper chromosome segregation requires the sister chromatids bi-orientation (amphitelic) attachment to the spindle through the kinetochore-microtubule attachment. The bi-orientation is achieved when one kinetochore attaches to the microtubules emanating from one spindle pole and the other kinetochore binds microtubules from the opposite spindle pole. The initial capture of microtubules by kinetochores is a stochastic and asynchronous process. This requires intermediate attachment including the monotelic, in which only one kinetochore binds to spindle microtubules, and the lateral attachment, in which kinetochores bind to the side wall of microtubules. Erroneous k-MTs attachment can form, such as the merotelic attachment, in which the same kinetochore binds to microtubules oriented toward both spindle poles, and the syntelic attachment, in which microtubules emanating from the same spindle pole bind to both kinetochores (*Godek KM et al., 2015*) (Figure 14). These erroneous attachments must be corrected in order to ensure proper chromosome segregation. The mitotic fidelity relies on the dynamic association and dissociation rates of microtubules from kinetochores, because the microtubule forming the erroneous attachment must be released from the kinetochore to enable the formation of a new and correct attachment.

Thus, unstable k-MT attachments, in which microtubules detach frequently, should improve the efficiency of error correction. The combination of these two rates determines the kinetochore-microtubule stability. The connection between k-MT attachments and chromosome segregation fidelity was highlighted through studies of chromosomal instability (CIN) in human cancer cells. CIN is a consequence of a high rate of whole chromosome miss-segregation that leads to continuous changes in chromosome number. Several studies have shown that cells with CIN have hyperstable k-MT attachments relative to chromosomally stable diploid cells, confirming that the efficiency of error correction is reduced (Bakhoum SF et al., 2009; Thompson SL et al., 2011). As aforementioned, the inner centromere Aurora B kinase plays a critical role in the tension-dependent model for regulating k-MT attachment. Tension is generated across the centromere in bi-oriented attachments because sister kinetochores are pulled towards opposite spindle poles. This tension increases the physical distance between the kinetochore and the inner centromere, where resides Aurora B. therefore, as kinetochore substrates are pulled away from Aurora B, they are more subjected to more frequent dephosphorylation by phosphatases located to kinetochores. At the opposite, erroneous k-MT attachment fail to generate the tension and kinetochore substrates are subjected to more phosphorylation because of their close proximity to the Aurora B kinase. However, it has been recently demonstrated that k-MT attachments remain relatively unstable on all chromosomes during prometaphase and that the physical location of Aurora B kinase to inner centromeres is not essential for efficient error correction (*Campbell CS and Desai A, 2013*). This evidence suggests that the regulation of k-MT attachment cannot be explained solely by the tension model. On these bases, a new model based on homeostatic control mechanisms has been recently proposed. This model describes a homeostatic control system that uses cell cycle regulators and feedback networks to precisely adjust k-MT attachments stability. the homeostatic system requires 3 elements: 1- a receptor that monitors and responds to environmental conditions (microtubule-binding proteins of the kinetochore); 2- a core control network that sets the appropriate response based on the input detected by the receptor and engages with effectors to adjust the system (proteins

of the SAC, PLK1, Aurora A and B and cyclin-cyclin-dependent kinases (CDK) complexes; 3- a negative feedback pathway to regulate the core control network (microtubule stabilizers and destabilizers and PP1 and PP2A phosphatases). As cell transits through different phases of mitosis, the core control network integrates the input from multiple sources to stabilizes the k-MTs attachments in order to ensure proper bi-oriented attachments and increase the efficiency of error correction. The combined activities of the core control proteins and phosphatases determines the relative activities of effector proteins such as the k-MT stabilizer BUBR1 and the destabilizer kif2B, which collectively modulate k-MT stability.

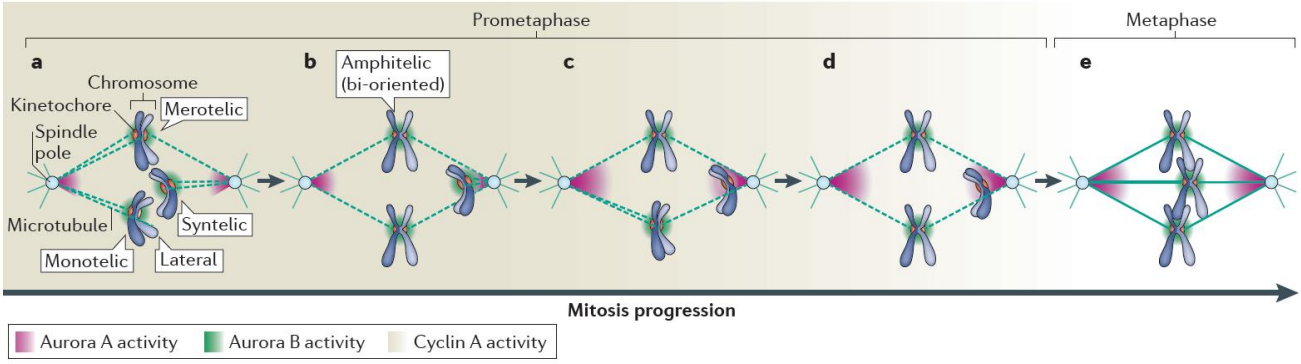

Figure 14. Kinetochore–microtubule attachments during mitosis. Different types of kinetochore–microtubule (k–MT) attachments occur in prometaphase (a-d). These include transient intermediates such as monotelic attachments (in which only one of the sister kinetochores is attached to microtubules from one spindle pole) and lateral attachments (in which kinetochores are bound to the side wall of microtubules). In addition, errors in attachment exist, including syntelic attachments (in which both sister kinetochores are attached to microtubules from the same spindle pole) and merotelic attachments (in which a single kinetochore is attached to microtubules from both spindle poles). As cells progress through mitosis, the erroneous attachments are corrected, leading to end-on, bi-oriented attachments, in which sister kinetochores are attached to microtubules from opposite spindle poles to support faithful chromosome segregation. A core control network regulates the stability of k–MT attachments to promote efficient error correction and ensure faithful chromosome segregation. Note that, for simplicity, only cyclin A, Aurora A kinase and Aurora B kinase — which are key components of the core control network — are shown in the figure. Cyclin A forms a temporal gradient as its abundance declines during prometaphase (a-d), whereas Aurora A and Aurora B kinases form spatial gradients at spindle poles and at centromeres, respectively. Correction of syntely involves the recognition and targeted destabilization of k–MT attachments through the combined activities of Aurora A and Aurora B kinases as chromosomes are pulled towards the spindle poles (a-d). The release of microtubules from kinetochores permits the chromosome to move to the spindle midzone through lateral k–MT attachments to re-establish bi-oriented attachments (c,d). Correction of merotely involves the indiscriminate destabilization of k–MT attachments on aligned chromosomes during prometaphase (a to b, c to d). The high detachment rate of k–MT attachments in prometaphase (dashed lines) that is ensured by cyclin A activity combines with the back-to-back geometry of sister kinetochores to facilitate bi-oriented attachments. In metaphase (e), k–MT attachments switch to more stable attachments (solid lines) as cyclin A levels fall below a critical threshold. (*Godek KM et al., 2015*)

4. Mechanism and Regulation of Cytoplasmic Dynein

4.1 Cytoplasmic dynein structure

As described in the previous chapter, microtubules are dynamic and polar structures, with plus ends usually located near the cell periphery and the minus ends typically embedded within the microtubule organizing centres located at the centrosome. Dyneins are molecular motor proteins that move toward the minus end of the microtubules. In dividing cells, cytoplasmic dynein-1 (hereafter referred to as dynein) and other motor proteins called kinesins, organize the mitotic spindle and play a key role in chromosome segregation. Cytoplasmic dynein-2 and kinesin-2 are used for transport within cilia (intraflagellar transport) and multiple axonemal dyenins (14 in humans) power the movement of cilia. (*Yagi et al., 2009*).

The dynein force-generating subunit lies in the heavy chains, so termed because of their large molecular mass (around 500 kDa) (Figure 15). Each heavy chain contains a motor domain that belongs to the AAA+ superfamily (ATPase associated with various cellular activities), attached to a divergent amino-terminal tail domain. The tail is required for dynein oligomerization and binding dynein's other polypeptide chains, which are implicated in cargo binding. The dynein intermediate chain (DIC) interacts with the dynein regulators dynactin and Nudel/NudE. Dynein's motor self-assembles in a ring of six concatenated AAA+ domains (AAA1-6). The AAA+ ring can be considered as the engine of dynein as it converts the chemical energy from ATP hydrolysis into motion. AAA1 is the principal site of ATP hydrolysis and its activation is necessary for motility. AAA2 lacks the amino acids required for the ATP hydrolysis, whereas the AAA3 and AAA4 domains are able to hydrolyse ATP in cytoplasmic dynein. In fact, mutations that block hydrolysis in AAA3 and AAA4 impair dynein motility. The AAA5 and AAA6 domains do not bind nucleotides but they serve a structural role transmitting conformational changes through the AAA+ ring. Dynein's microtubule domain (MTBD) is located at the end of the coiled-coil stalk that emerges from AAA4. The MTBD is a small a-helix that bind microtubules in the cleft between a-

and b-tubulin subunits. Nucleotide binding at AAA1 domain and microtubule binding at the MTBD are allosterically coordinated by the stalk, where the coiled coil helices slide between different registers. This mechanism is facilitated by an extension of the AAA5 domain called buttress (or strut), which interacts with and modulates the register changes in the stalk. The motor domain comprises also the linker domain. The linker is composed of four a-helical segments and located the N-terminal to dynein's AAA+ ring. It is required for motility and moves in response to the nucleotide state of the AAA1 domain. Following the AAA6 resides the C-terminal domain, which contacts AAA5, AAA6 and AAA1 on the opposite face of the ring relative to the linker.

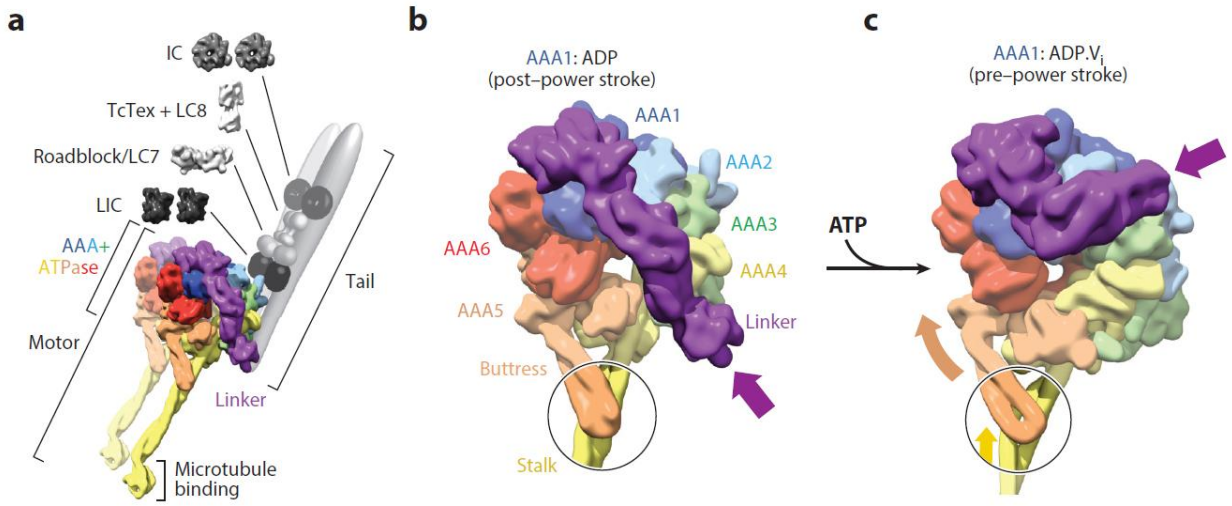

Figure 15. Dynein structure (a) Structure of the cytoplasmic dynein-1 complex. The motor domain contains the AAA+ (ATPases associated with various cellular activities) domains, the microtubule (MT)-binding domain (MTBD), and the linker. The N-terminal tail domain binds the intermediate (IC), light intermediate (LIC), and light (LC) chains. We built the structure of the motor domain by combining entries 3VKG and 4RH7 from the Protein Data Bank (PDB) and displaying the model as a density at a resolution of 10A°. (b) Structure of the dynein motor domain in the post–power stroke state, in which AAA1 is bound to ADP (PDB3VKG). Dynein is colored according to the AAA+ domains. In this state, the linker adopts a traight position across the AAA+ ring; the purple arrow points to the N terminus of the linker, which is connected to the tail domain. The black circle highlights an interaction between the buttress (part of AAA5) and the coiled coil of the stalk (part of AAA4). We rendered the structure as a 10A° density. (c) Structure of the dynein motor domain in the pre–power stroke state, in which AAA1 is bound to ADP.Vi, a transition state analog that mimics the posthydrolysis ADP.Pi state (PDB 4RH7). The bending of the linker domain, which brings its N terminus toward AAA2 (purple arrow), is accompanied by coordinate changes across the ring. These changes include an upward movement of AAA5 and AAA6 (orange arrow) that shifts the registry of the coiled coil in the stalk (yellow arrow inside the circle), lowering the affinity of the MTBD for the MT. We rendered the structure as a 10A° density. (*Cianfrocco MA et al., 2015*)

4.2 Dynein's mechanochemical cycle

Dynein's mechanochemical cycle comprises the conformational changes that can do work and are linked to nucleotide hydrolysis (Figure 16). In the beginning of the cycle, AAA1 is nucleotide free and dynein is tightly bound to the microtubule. The linker lies in the straight, post-power stroke conformation, docked at the AAA5 domain. ATP binding to AAA1 induces rapid dissociation of dynein from the microtubule and it triggers a series of conformational changes: the linker adopts its pre-power stroke conformation; the buttress interacts with the stalk to alter the register of the coiled-coil (low affinity state); the conformation of the MTBD is altered weakening the interaction with the microtubules. Remodelling of the linker extends the search range of the microtubule-binding domain along the microtubule. After hydrolysis of ATP to ADP + Pi (inorganic phosphate), the motor domain engages a new binding site on the microtubule (moving towards the microtubule minus-end). The interaction between the MTBD and the next binding site changes the MTBD's conformation back to the high affinity state leading to another series of conformational changes: the stalk coils alters the register to a high affinity state; the inorganic phosphate (Pi) is released from the AAA1 domain; the linker swings back toward its straight-form. This transition is speculated to represent the powerstroke: the main step in which force (Figure 16) is transmitted to the attached object. Finally, ADP is released from the AAA1 and the cycle restarts.

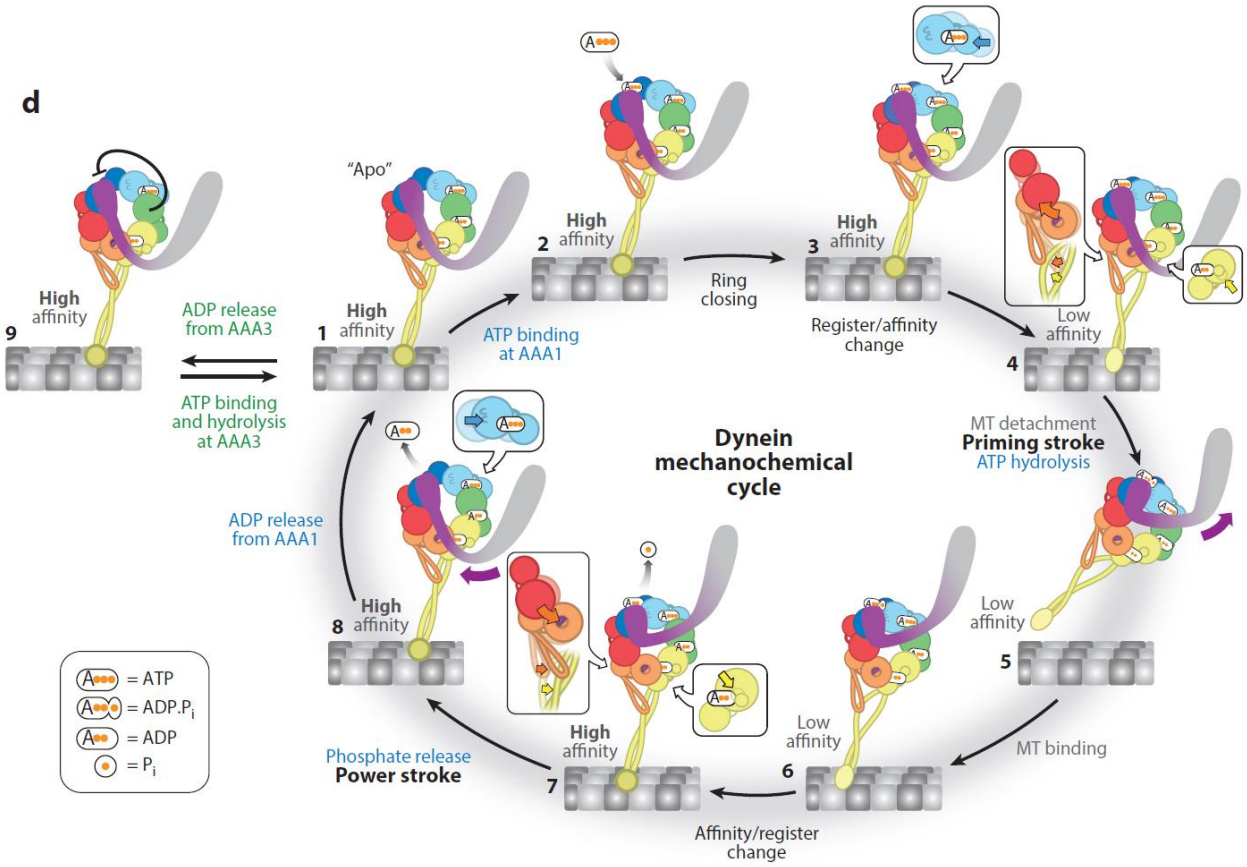

Figure 16. Overview of dynein's mechanochemical cycle. A single dynein head is shown for clarity and is colored according to panel b. For each AAA+ module, the large and small domains are shown as large and small spheres, respectively. Steps 3, 4, 7, and 8 have insets highlighting how nucleotide binding affects the packing of the large and small domains together: Nucleotide binding and unbinding results in tight and loose packing, respectively. (*Cianfrocco MA et al., 2015*)

4.3 Dynactin, regulator of the cytoplasmic dynein

Dynein interacts with several proteins which not belong to the dynein complex, but are critical for adapting the motor to its cellular function. Among the several multifunctional adaptors, dynactin is essential for nearly every cellular function of cytoplasmic dynein. Dynactin helps to target dynein to specific cellular locations, links dynein to cargoes and increases dynein processivity, although a comprehensive model explaining how these activities are integrated has yet to emerge. The dynactin complex has a molecular mass of 1 mDa and comprises 11 different subunits (Figure 17). The central scaffold of dynactin complex is the filamentous actin-related protein (ARP1). ARP1 facilitates the link between dynein and its cargoes interacting with βIIIspectrin, a specialized

isoform found on Golgi membrane and coats the cytoplasmic face of several organelles (*Holleran EA et al., 2001*). The subcomplex at the pointed end of the ARP1 filament contains a second actin-related protein ARP11 and p62, which mediate the interaction of dynactin with cortical actin, and the other adaptor subunits p25 and p27. The dynactin p62 subunit associates with Arp11 and the two smallest dynactin subunits, p25 and p27, to form a heterotetrameric complex that sits at the end of the Arp1 rod opposite to Capz (*Eckley et al.1999*).

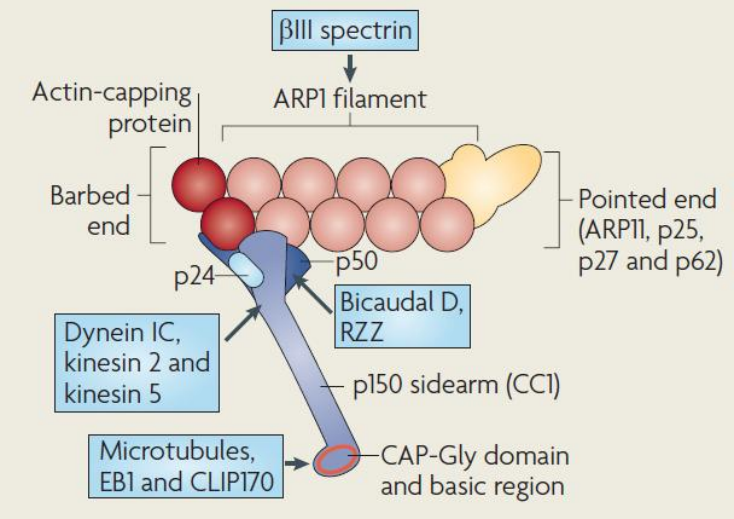

Figure 17. Composition of Dynactin complex. A short (~40 nm) filamentof actin-related protein 1 (ARP1) forms the central scaffold of the dynactin complex and may help to link dynein to cargo through its interaction with spectrin, which coats the cytoplasmic face of several organelles52,143. The subcomplex at the pointed end of the ARP1 filament (yellow) contains ARP11, p62, which might mediate the interaction of dynactin with cortical actin, and two more subunits, p25 and p27 (refs 58,144–148). The barbed end subcomplex is composed of a dimer of p150 (also known as p150Glued, from the Drosophila melanogaster allele), a tetramer of p50 (also known as dynamitin because its overexpression dissociates dynactin into several subcomplexes), the p24 subunit and the actin-capping protein heterodimer (shown in red; dynactin may lack capping protein in some organisms)23,144,145,148,149. p50 interacts with two other dynein adaptors, Bicaudal D and the Rod–ZW10–Zwilch (RZZ) complex105,127,150. The most amino-terminal coiled coil (CC1) of p150 forms the 24 nm sidearm from the ARP1 filament. p150 contains N-terminal microtubule-binding domains, a cytoskeletonassociated protein Gly-rich (CAP-Gly) domain and a basic region (indicated in red) that probably form the globular domain observed at the end of the sidearm144,151. The CAP-Gly domain also binds to the microtubule plus end-associated proteins end binding 1 (eB1; also known as MAPRe1) and CAP-Gly domain-containing linker protein 170 (CLIP170; also known as CLIP1). p150 provides the only documented interaction between dynactin and dynein (through the dynein intermediate chain)4,60,152, and also interacts with kinesin 2 and kinesin 5 (refs 4,5,60,152). The structural arrangement of subunits in the barbed and pointed end subcomplexes have not been resolved148 and are outlined for display purposes only. (*Kardon JR and Vale RD, 2009*).

Extending from dynactin's Arp1 is a projecting arm that contains the three remaining dynactin subunits: p150 (Glued), dynamitin and p24/22. Each dynactin molecule contains four copies of dynamitin and two copies of p150 (Glued) and p24/22. *p150(Glued),* the largest of all the dynactin

subunits, plays an important role in motor binding and the enhancement of dynein motor processivity. P150Glued must be associated with the other subunits to function properly and mutations that prevent p150 from being incorporated into the complex results in non-functional protein (*McGrail et al., 1995*). P150 is predicted to assemble into an elongated dimer that contains two coiled coils. Each of the two globular heads of dynactin arm contains a conserved cytoskeleton associated protein, glycin-rich (CAP-Gly) motif. This motif plays an important role in dynactin function, as it supports dynactin binding to microtubules. In fact, the CAP-Gly motif can bind a shared C-terminal acidic motif in a-tubulin and the plus-end binding protein binding 1 (EB1) and CAP-Gly domain-containing linker protein 170 (CLIP170). Microtubule binding by 150Glued is necessary for its ability to enhance the dynein motor processivity (*Culver-Hanlon TL, 2006*). The Cap-Gly domain may also contribute to microtubule minus-end anchoring at interphase centrosomes (*Quintyne et al., 2002*) and mitotic spindle poles (*Gaglio et al., 1997*). In cultured animal cells and in yeast, dynactin is enriched at centrosomes or spindle pole bodies (Kahana et al., 1998), whereby it proposed to contribute to microtubule anchoring. Dynactin also accumulates at the plus end of microtubules, where it may support microtubule dynamic. Under some circumstances, dynactin associates with cell cortex, regulating the positioning of mitotic spindle apparatus and directed cell movement (*Gonczy et al., 1999; Dujardin et al., 2003*).

4.4 Dynein functions

During mitosis, dynein activity has been shown to be critical for several different processes. This motor protein is remarkably able to fulfill this wide range of functions by the interaction with multiple regulatory proteins that define the time and place where dynein becomes active.

As previously described, one of the earlier steps of mitotic spindle formation is the separation of duplicated centrosomes along the nuclear envelope (NE). This process is mainly driven by Eg5, which pushes the centrosomes apart through antiparallel microtubules sliding. Although in mammalian cells, the most prominent role for dynein in late G2/prophase is tethering the

centrosomes to the nuclear envelope, NE-associated dynein was recently found to contribute to prophase centrosome separation in mammalian cells. In fact, NE-associated dynein can completely take over the role of Eg5 in prophase centrosome separation in cells with reduced Eg5 activity (*Raaijmakers JA et al., 2012*). After the nuclear envelope breakdown (NEB), the mitotic spindle is completed and the microtubules begin to interact with chromosomes at the kinetochores. Dynein is recruited to the outer corona of the kinetochores that have not yet formed stable attachments. Here, a number of different binding partners with their phospho-regulation, allow dynein to be involved in many independent cellular functions, including chromosome congression. Among these functions, dynein is involved in the recruitment of the RZZ complex, which consists of Rod, Zwilch and Zw10 and Spindly, another dynein/dynactin interacting protein. Zw10 plays an essential role in the recruitment of protein involved in the mitotic checkpoint, as Mad1 and Mad2, and Spindly has function in the formation of a stable microtubule/kinetochore attachment. A recent study demonstrated that dynein prevents premature kinetochore-microtubule attachments by bringing peripheral chromosomes closer to Aurora A Kinase, which is involved in microtubule/kinetochore attachment correction, at spindle poles (*Barisic M and Maiato H, 2015*). Once all the microtubule/kinetochore attachments are established correct, the checkpoint needs to be deactivated to allow chromosome segregation. The removal of proteins that are required for SAC activation form attached kinetochores – known as stripping or streaming- is a critical step in this is mediated by dynein activity. Dynein transports certain SAC proteins off kinetochores toward spindle poles along kinetochore-microtubules. Several studies based on ATP depletion assays, which maintained dynein activity but prevented release of its cargo from spindle poles, have demonstrated that several kinetochore components are transported to spindle poles and that inhibition of dynein prevents their removal from attached kinetochores. While it is consensual that Mad1, Mad2 and spindly are dynein cargoes, the data concerning BubR1 and Bub1 transport are mixed (*Howell BJ et al, 2004*; *Famulski JK et al, 2011*). However, a recent study clarified that BubR1 and Bub1 poleward transport is dynein-dependent (*Silva P et al, 2014*).

Dynein is also involved in spindle focusing and mitotic spindle organization. Sliding of the antiparallel overlap is critical for the formation of the bipolar spindle. Although the plus-end directed kinesin-5 motor Eg5 is the key player of this process, dynein generates antagonist forces by sliding antiparallel microtubules inward. Unlike Eg5 that uses two motor domains on each microtubule to generate sliding activity, dynein can walk with one motor domain on each microtubule simultaneously to generate sliding activity (*Tanenbaum et al., 2013*). Alternatively, dynein can split its legs and produce a sliding force by walking on two individual microtubules simultaneously.

Finally, dynein is involved with an evolutionarily conserved ternary complex (nuclear mitotic apparatus protein [NuMA]-LGN-Gα) in spindle positioning. The mitotic apparatus must be placed in the centre of the cell in order to define the position of the future cleavage plane and ensure two daughter cells of equal size. Central positioning of the cleavage plane in symmetrically dividing cells is essential for the generation of two equally sized and correctly positioned cells to maintain tissue organization and integrity (*Morin and Ballaiche, 2011*). On the contrary, positioning the spindle off centre in asymmetrical dividing cells is critical to generate two unequally sized daughter cells with correct distribution of fate determinants, which is essential in stem cell maintenance, cell differentiation and development (*Knoblich et al., 2008*). In both cases, correct spindle positioning relies on dynein mediated pulling forces on microtubules emanating from spindle poles. Regulated spindle positioning requires a nonhomogeneous distribution of dynein at the cell cortex. Indeed, dynein is distributed in distinct crescents at the cell cortex adjacent to the spindle poles (*Busson et al., 1998*). It has been demonstrated that actin-rich retraction fibers (that adhere cells to their substrates) dictate spindle orientation in cells grown on adhesive micropatterns (*Schuster M et al., 2011*), suggesting that also extrinsic signals – in cooperation with intrinsic signalling pathways- regulate dynein localization at the correct zones. As the spindle moves toward the crescent with most dynein molecules, the proximity of spindle poles close to the cell cortex was shown to disrupt

the recruitment of dynein/dynactin complex at the cortical sites close to the pole. Loss of dynein from one side of the cell coincided with enhanced recruitment of dynein at the opposite side of the cell (*Collins et al., 2012*; *Kiyomitsu and Cheeseman, 2012*). This feedback loop causes spindle oscillations that eventually position the spindle apparatus in the centre of the cell.

Material and Methods

Reagents

All reagents were obtained from Sigma Aldrich unless otherwise specified. ATM/ATR inhibitors, NaPP1, BIM-1, EHNA and Ciliobrevin were obtained from Calbiochem. Blu557 was kindly provided by Peter Parker, Protein Phosphorylation Laboratory, The Francis Crick Institute, London, UK.

Cell lines

Cervix adenocarcinoma HeLa cells and colon adenocarcinoma DLD1-(GFP-PKCε-M486A) cells were routinely cultured in DMEM containing 10% FCS, antibiotics (50 U/mL penicillin, 50 µg/mL streptomycin) and were incubated at 37°C and 10% CO_2.

Erythroleukemia HEL cells were routinely cultured in RPMI containing 10% FCS, antibiotics and incubated at 37°C and 5% CO_2.

Normal keratinocytes NCTC2544 were routinely cultured in DMEM containing 10% FCS, antibiotics and MEM Non Essential AminoAcids (Gibco), incubated at 37°C and 5% CO_2.

Normal retina epithelial RPE1-hTERT were routinely cultured in DMEM containing 10% FCS, antibiotics and MEM Non Essential AminoAcids (Gibco), incubated at 37°C and 10% CO_2.

Primary human fibroblasts were cultured in DMEM containing 20% FCS, antibiotics and incubated at 37°C and 5% CO_2. Cells were kindly provided by Professor Bussolati O., Unit of General Pathology, Dept. of Biomedical, Biotechnological and Translational Sciences, University of Parma, Italy.

Cells synchronization and flow cytometry

HEL cells were synchronized in G_1/S border by culturing in growth medium supplemented with 2mM Thymidine for 16 h. Cells were washed and released into growth medium for 6 h and arrested in G_2/M border adding 10µM RO-3306 for 16 h. Cells were then released into growth medium for 90' to obtain the population enriched in metaphase.

To assess the efficiency of synchronization, aliquots of HEL cells blocked in G_1/S and G_2/M phases were permealized with 70% ethanol for 1h at 4°C, washed with PBS and incubated with PBS containing 20 µg/mL propidium iodide (PI) and 100 µg/mL RNAse-A for 15' in dark room temperature before analysis. To validate the protocol of synchronization of HEL cell line, 4 independent experiments were performed. Analysis of samples was performed by FC500 flow cytometer (Beckman Coulter) and the Expo ADC software (Beckman Coulter).

DLD1-(GFP-PKCε-M486A) and HeLa cells were synchronized in metaphase by a sequential block and release with Thymidine and RO-3306. Cells were monitored using the Leica DM IL phase contrast microscope (40X/0.5NA) and cells were collected when 50-60% were in metaphase. DLD1-(GFP-PKCε-M486A) cell line was cultured with Doxocycline (100 ng/mL) overnight to induce expression of GFP-PKCε.

shRNA cell infection

HEL cells were infected and were subsequently cultured in the presence of puromycin (2µg/mL), to select infected, puromycin-resistant cells. Cells were then collected after 5 days of puromycin-selection. For short hairpin RNA (shRNA)-based gene silencing, pLKO.1 lentiviral vector encoding shRNA against human PKCε (NM_005400; shPKCε) were obtained from Open-Biosystem (Thermo Fisher Scientific). As control (shRNA CT), we used the MISSION pLKO.1-puro Non-target shRNA Control Plasmid, not targeting any known genes (Sigma-Aldrich). The shRNA expressing viruses were produced in 293TL cells according to standard protocols.

Pharmacological inhibition of PKCε and dynein activity

DLD1-(GFP-PKCε-M486A) cell line was cultured with Doxocycline (100 ng/mL) 1μM NaPP1 to inhibit PKCε activity, as previously described (*Saurin et al., 2008*). In HeLa, RPE-1, NCTC2544, and human fibroblasts PKCε was inhibited using 500nM Blu557 or 1μM BIM-1. Dynein activity was inhibited using 100μM EHNA or 20μM Ciliobrevin.

Proteolytic digestion and nanoLCMS analysis

All chemicals were purchased from Sigma at the highest grade possible unless otherwise stated. All solvents and nanoLC-MS additives were purchased as LC-MS grade from Fisher Scientific. Proteins were separated using SDS-PAGE and 8 bands from each lane were excised and processed further using the previously described in gel digestion procedure (*Shevchenko A et al., 1996*) adapted for a Janus liquid handling system (Perkin Elmer). 10 μL of gel extracted peptides in 1 % acetonitrile and 1 % formic acid in water were analysed by nano liquid chromatography in tandem with mass spectrometry (nanoLCMS) using an Acquity UPLC (Waters) connected to a LTQ Orbitrap XL Mass Spectrometer (Thermo Scientific). Raw files containing MS spectra were processed using a protein database search, carried out using MaxQuant (version 1.5.2.8) as previously described (*Cox J et al., 2011*), against a UniProt human database. Intensity-based absolute quantification (iBAQ) (*Schwanhausser B et al., 2011*) was utilised for label free quantitation of the reported proteins. Data was then further analysed using Perseus (version 1.4.0.2) (*Cox J and Mann M, 2012*).

Live-cell imaging

For videomiscroscopy experiments, cells were cultured on LabTek chambered coverglass slides (Nunc) in Liebovitz CO_2-independent media (Gibco). All experiments were performed at low light level inverted microscope (Nikon TE2000) imaging system equipped with a lamina-flow heater maintaining a constant temperature of 37±0.01°C, a Plan-Fluor 40X DIC lens and a Xenon lamp for

fluorescence excitation. Images were taken using a high quantum efficiency charge coupled device camera (Andor Ixon) every 3 minutes.

Immunofluorescence microscopy and image analysis

Adherent cells were grown on 13mm glass coverslips and fixed and permeabilized with PHEM buffer (60mM PIPES pH6.8, 25mM HEPES pH7.4, 10mM EGTA pH8, 4mM $MgSO_4$, 4% paraformaldeyhyde and 0.1% Triton X-100) for 20min. HEL samples were fixed in methanol for 5' at -20°C, centrifuged onto 1 µg/mL poly-*l*-lysine-coated 10mm coverslips, permeabilized with 0,5% Triton X-100 for 7min. Cells were then blocked using 3% BSA/PBS and probed using the following primary antibodies, diluted 1:100 unless otherwise specified, in 3% BSA/PBS: mouse anti-Dynein IC (Sigma Aldrich), mouse anti-p150(Glued) (BD Transduction Laboratory), 1:200 mouse anti-Mad2 (Santa Cruz Biotechnology), mouse anti-BubR1 (Novus Biologicals), mouse anti-PLK(F-8) (Santa Cruz Biotechnology), rabbit anti-phosphoAurA (Thr288) (Cell Signaling Technology), rabbit anti-Kif2A (Novus Biologicals), rabbit anti-phosphoCENP-A (S7) (Cell Signaling Technology), 1:300 human anti-centromere (ACA) (Antibodies Inc.15-234-0001), 1:500 mouse anti-αtubulin (Sigma Aldrich), rabbit anti-αtubulin (AbCam), 1:250 rabbit anti-PKCε (Abcam). The secondary antibodies used were obtained from Thermo Fisher Scientific and were all used diluted 1:1000 in 3% BSA/PBS: goat anti-rabbit and goat anti-mouse Alexa Fluor 549, goat anti-rabbit e goat anti-mouse Alexa Fluor 488 and goat anti-human Alexa Fluor 647 (Thermo Fischer). All coverslips were mounted using ProLong Gold with DAPI (Invitrogen).

HeLa and RPE1-hTERT images are acquired using Carl Zeiss LSM 780 confocal microscope equipped with a X63 Plan-APOCHROMAT DIC oil-immersion objective and serial 1uM Z-sections were taken. Image analysis was carried out using Metamorph image analysis software. HEL, DLD1-(GFP-PKCε-M486A), NCTC2544 and human fibroblasts were examined with a Nikon Eclipse 80i (Tokyo, Japan) fluorescent microscope equipped with Nikon Plan color 40X/0.75 and

Nikon Plan Apo VC 100X/1.4 oil immersion objective. Images were obtained using Nikon Camera DS-JMC and images acquisition was performed using Nis element F2.30 (Nikon, Japan). Image analysis was performed using ImageJ software.

In situ Proximity Ligation Assay (PLA)

The DuoLink *in situ* PLA kit (Olink Bioscience) with the DuoLink *in situ* Detection Reagent Orange (Sigma Aldrich) was used to detect PKCε/Dynein interaction according to the manufacturer's protocols. HeLa cells were grown on 8-well CultureSlides (Falcon) overnight and treated with or without Blu557 for 1h. Cells were subsequently fixed and permeabilized with PHEM buffer and blocked with 3% BSA/PBS. The slides were directly used for the assay and primary antibody mix solution containing anti-PKCε (AbCam) and anti-DyneinIC (Sigma Aldrich) diluted in 3% BSA/PBS was added to each sample and incubated in a humidity chamber for 1h at room temperature. Mouse IgG and Rabbit IgG (Santa Cruz) were used as negative controls. The assay was subsequently performed following the manufacturer instructions. The slides were mounted with ProLong Gold with DAPI (Invitrogen). Images were acquired using Carl Zeiss LSM 780 confocal microscope equipped with X63 Plan-APOCHROMAT DIC oil-immersion objective and analyzed and serial 1μm Z-sections were taken using ZEN image analysis software. Z-sections were summed and PKCε/Dynein interaction was quantified counting the number of signals each field counted using Image J.

ATM/ATR inhibition

RPE1-hTERT cells were treated with 1μM ICRF193, 100nM ATM inhibitor and 10mM ATR inhibitor for 24h. Following 23h, cells were incubated with Blu557, BIM-1 and EHNA for 1h. Cells were subsequently fixed and stained for α-tubulin.

Formaldehyde crosslinking

Synchronized cells were scraped, pelleted and incubated using formaldehyde 1% at 4°C for 10min. Following a centrifugation 1800rpm for 3min, the cross-linking reaction was quenched with 1.25M Glycine/PBS, as described by Klockenbush C. and Kast J.

Immunoprecipitation and immunoblotting

For co-immunoprecipitation experiments, HeLa cells were collected in ice cold RIPA buffer (50mM Tris pH 7.4, 150mM NaCl, 1mM EDTA, 1% Nonidet P-40, 0,1% SDS and 0.5% sodium deoxycolate) supplemented with fresh protease inhibitors and 1mM phenylmethylsulfonyl fluoride and incubated for 30min at 4°C. Lysed proteins were immunoprecipitated with Dynabeads Protein G (Invitrogen) for 1h at 4°C after coating with control IgM. Protein complexes were eluted with SDS 2X sample buffer after washing with RIPA buffer. Specifically, 10μg mouse anti-Dynein IC (Sigma Aldrich) and mouse-IgG (Santa Cruz) were used for immunoprecipitation. Proteins were resolved in 10% polyacrylamide gels and analyzed by immunoblotting using specific primary antibodies diluted as described by manufacturer's protocol. Specifically, 1:1000 rabbit anti-PKCε (Merck Millipore), 1:1000 mouse anti-Dynein IC (Sigma Aldrich).

For the endogenous protein expression analysis, the following antibodies were used: 1:1000 Cyclin B1 (Santa Cruz), 1:1000 rabbit anti-PKCε (Merck Millipore), 1:5000 mouse anti-glyceraldehyde-3-phosphate dehydrogenase (GAPDH) (Merck Millipore). Membranes were washed and incubated for 1 hour at room temperature with 1:5000 peroxidase-conjugated anti-rabbit (Thermo Scientific) or 1:2000 peroxidase-conjugated anti-mouse IgG (Thermo Fisher) and resolved by ECL Supersignal West Pico Chemiluminescent Substrate detection system (Thermo Fisher). Protein densitometric analysis was performed by using the ImageJ software system.

Statistical tests

Statistical analyses were performed by using analysis of variance (ANOVA) and Dunnett's test when applicable. The level of statistical significance is represented as follows: n.s.=P>0.05, *=P<0.05,**=P<0.01, ***=P<0.001.

Results

1. PKCε co-localization with γ-tubulin at the centrosome

We used immunofluorescence microscopy to investigate PKCε subcellular localization in the early stages of mitosis. PKCε localization was studied in 3 transformed cell lines – HeLa, DLD1, and HEL – and in 3 non-transformed cell lines – RPE1, NCTC 2544 and human fibroblasts. As represented in figure 1(a-d), PKCε localizes to the centrosomes from G2/M phase to metaphase in all the cell lines. In order to confirm PKCε localization at the centrosome, we used confocal immunofluorescence microscopy to analyse the co-localization of PKCε and γTubulin at the centrosome in HeLa cells. The representative images in Figure 1e show that PKCε localizes to the centrosome in a pattern identical to that of γ-tubulin. The interaction between PKCε and γ-tubulin was confirmed also in HEL cells using co-immunoprecipitation assays in cells enriched in metaphase, using anti-PKCε and anti-γtubulin antibodies. HEL synchronization was obtained by a sequential block with Thymidine, to arrest cells in G1/S phase, and a block with RO-3306 to arrest them in G_2/M. Western blot analysis demonstrated that γ-Tubulin is present in the immunoprecipitate generated by PKCε antibody (IP-PKCε, Figure 1f). Similarly, when γ-Tubulin is pulled down (IP-γTubulin), almost the total amount of PKCε is bound to it, as represented in Figure 1g.

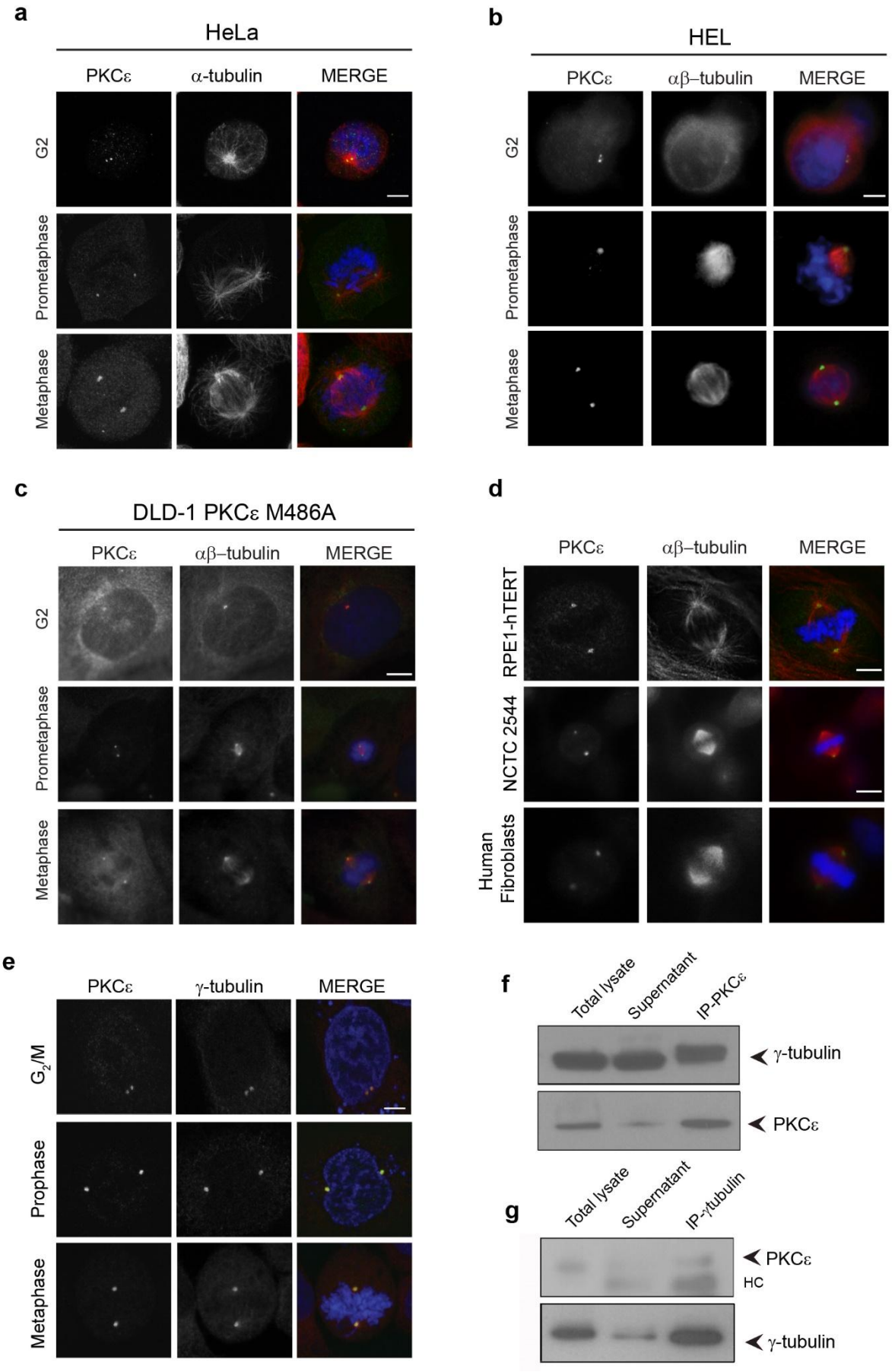
a
HeLa
PKCε
α-tubulin
MERGE
G2
Prometaphase
Metaphase
b
HEL
PKCε
αβ–tubulin
MERGE
G2
Prometaphase
Metaphase
c
DLD-1 PKCε M486A
PKCε
αβ–tubulin
MERGE
G2
Prometaphase
Metaphase
d
PKCε
αβ–tubulin
MERGE
RPE1-hTERT
NCTC 2544
Human Fibroblasts
e
PKCε
γ-tubulin
MERGE
G2/M
Prophase
Metaphase
f
Total lysate
Supernatant
IP-PKCε
γ-tubulin
PKCε
g
Total lysate
Supernatant
IP-γtubulin
PKCε
HC
γ-tubulin

Figure 1 PKCε subcellular localization in G2/M phase, prometaphase and metaphase in transformed cell lines – HeLa cells (**a**), HEL (**b**) and DLD-1 PKCe M486A (**c**). (**a**) Representative confocal images of HeLa cells stained with anti-PKCε (green), anti-αtubulin (red) and DAPI (blue). Scale bar, 5 μm. (**b,c**) Representative images of HEL (**b**;Scale bar, 20 μm) and DLD-1 PKCε M486A (**c**; Scale bar, 20 μm) cells stained with anti-PKCε (green), anti-αbtubulin (red) and DAPI (blue). **PKCε subcellular localization in metaphase in non-transformed cell lines** – RPE-1 hTERT (**d**, *upper panel*; Confocal images; Scale bar, 5μm), NCTC 2544 (**d**, *middle panel*; Scale bar, 10μm) and Human Fibroblasts (d, lower panel). **PKCε co-localization with γ-tubulin at centrosome in HeLa cells in G2/M phase, prophase and metaphase**. Representative images acquired using confocal microscopy of HeLa stained with anti-PKCε antibody (green), anti-gtubulin (red) and DAPI (blue). Scale bar, 5μm. **PKCε co-immunoprecipitates with γtubulin in HEL cells enriched in metaphase.** Immunoprecipitation assays were performed using anti-PKCε and anti-γtubulin. *Immunoprecipitates (IP)*, *Supernatants* and *Total Lysates* were analysed by western blotting. (**f**) IP-PKCε was probed for PKCε, to assess the efficiency of the assay, and for γ-tubulin. (**g**) IP-γtubulin was probed for γtubulin and PKCε. 'HC' labels the heavy chain of the antibody used in the immunoprecipitation.

2. PKCε inhibition affects mitotic spindle morphology in transformed cell lines.

We then sought to explore the physiological relevance of PKCε localization at the centrosome. We inhibited PKCε in several cell lines with different methods. PKCε was inhibited in HeLa cells with a 1 hour treatment with Bisindolylmaleimide 1 (BIM-1), a protein kinase C inhibitor, or Blu577, a structurally unrelated and more selective PKCε inhibitor. In contrast to control cells, in which the microtubules were organized into well-defined radial arrays, Blu577- and BIM-1-treated cells showed an unfocused and disoriented mitotic spindle with misaligned chromosomes (Figure 2a). Strikingly, PKCε inhibition by Blu577 results in a significant higher percentage of cells (52 ± 4 %) which display abnormal mitotic spindle morphology compared to the control (15.66 ± 2.88 % (***P<0.001 vs CT)) (Figure 2b). Interestingly, BIM-1 treatment results in a stronger effect on mitotic spindle organization than Blu577 (72 ± 4.36 % (**P<0.01 *vs* Blu577)). This is likely due to the broader effect of BIM-1, which is able to inhibit not only PKCε but other PKC isoforms including PKCε, which have previously been implicated in microtubule organization and spindle function (*Chen D et al., 2004*). Using a recombinant lentiviral vector to introduce and stably express shRNA that specifically target PKCε (shPKCε) (Figure2 c-e), we observed the effects of PKCε downregulation in HEL cells. Similarly to the phenotype seen in HeLa cells, defects in microtubules organization were observed in mitotic HEL cells infected with shPKCε: microtubules were

unfocused and disorganized and chromosomes resulted spread in the cell (Figure 2c). Finally, we confirmed this finding in the DLD-1 PKCεM486A cell line, using the ATP analog NaPP1 to inhibit the gate-keeper modified kinase (Figure 2f) (*Knight, Z.A and Shokat KM, 2007*). NaPP1 is unable to inhibit any wild-type kinase due to a steric clash with the gatekeeper residue in the ATP binding pocket. Since in DLD1 PKCεM486A cells the gatekeeper residue has been substituted with an alanine, we used NaPP1 to inhibit PKCε activity. Consistently, in all the cell lines tested, we observed an increase in the number of mitotic cells with abnormal spindle geometry following PKCε inhibition (Figure 2g, Table1), suggesting that PKCε may be involved in mitotic spindle organization.

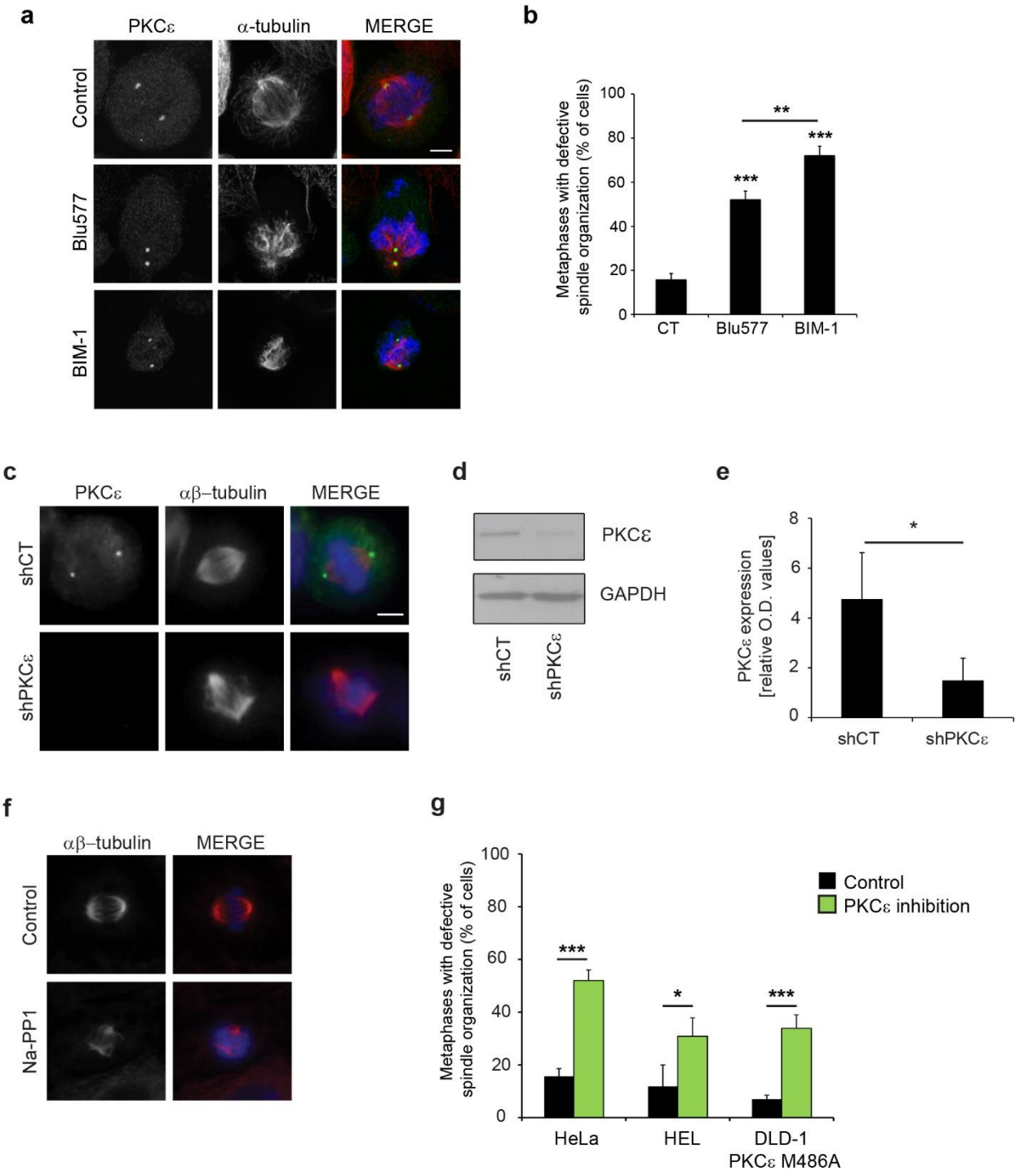

Figure 2 Inhibition of PKCε affects mitotic spindle morphology. (a) Representative images of HeLa cells treated with Blu577 and BIM-1. Cells were stained with anti-PKCε (green), anti-βtubulin (red) and DAPI (blue). Scale bars, 5 μm. (**b**) **The amount of cells with a disrupted mitotic spindle is increased upon treatment with PKCε inhibitors Blu577 and BIM-1.** Quantification of cells in metaphase with a defective mitotic spindle. Chart shows mean of three experiments ± sd, n>100 per condition per experiment. ***P<0.001 vs CT. BIM-1 has stronger effect on mitotic spindle organization (**P<0.01 vs Blu577). (**c**) HEL cells synchronized in metaphase and infected with PKCε-specific shRNA (shPKCε) and untargeted control (shCT), were labeled with anti-PKCε (green) and anti-αβ-tubulin (red). In the upper panel is shown a representative cell infected with shCT, presenting a normal and well-defined microtubule organization. Microtubules in HEL cells infected with shPKCε are disorganized and apparently fragmented, as represented in the lower panel. Scale bar, 20 μm. (**d-e**) Infection of HEL cells with a short hairpin RNA directed against PKCε (shPKCε), results in efficient inhibition of total protein levels. The graph shows the densitometric measurement of western blot

from 4 replicates (means ± sd) *P<0.05. (**f**) Representative images of DLD-1 PKCε M486A cells untreated and treated with NaPP1 to inhibit PKCε. Cells were stained with anti-αβtubulin (red) and DAPI (blue). (**g**) Quantification of the amount of metaphase cells with a defective mitotic spindle (percentage) in all transformed cell lines analysed (HeLa, HEL and DLD-1 PKCε M486A) following the inhibition of PKCε (green charts) compared with control (black charts). ***P<0.001; *P<0.05.

Table 1.

		PKCε inhibition			
	Control	**Blu577**	**BIM-1**	**shRNA**	**NaPP1**
HeLa	15.67± 2.89	52 ± 4***	72 ± 4.36***	-	-
Hel	11.84 ± 8.12	-	-	30.86 ± 6.98*	-
DLD1 PKCεM486A	6.98 ± 1.55	-	-	-	33.99 ± 5.09***

Table 1. Percentages of cells in metaphase with defective mitotic spindle from HeLa, Hel and DLD-1 PKCε M486A cell lines. The inhibition of PKCε has been performed using different methods: HeLa cells were treated with the pharmacological compounds Blu577 and BIM-1; Hel cells were infected with shRNA specific for PKCε; DLD-1 PKCε M486A cells were treated with NaPP1. The table represents the mean of three experiments ± sd, n>100 per condition per experiment. *P<0.05 vs CT; ***P<0.001 vs CT.

We further sought to determine whether the abnormal mitotic spindle morphology caused by PKCε inhibition was restricted to transformed cell models. Normal human keratinocytes (NCTC 2544), primary human fibroblasts and non-transformed RPE1-hTERT cells, were treated with Blu577 or BIM-1 under the same conditions as the HeLa cells. In the primary and non-transformed cell lines, the percentage of cells with spindle defects was significantly lower compared with transformed HeLa cells (Figure 3a); only 6.19 ± 0.68% and 6.46 ± 0.29% RPE1- hTERT cells, respectively treated with Blu577 and BIM-1, respond to PKCε inhibition with an abnormal spindle morphology. To exclude the possibility that PKCε dependency in mitotic spindle organization could be due to differences in the total amount of the protein, we quantified the expression levels of PKCε in the different cell lines used. Western blot analyses demonstrated that PKCε protein levels are

equivalent among all the cell lines (Figure 3b). Brownlow et al. have previously demonstrated a role for PKCε as a regulator of the metaphase catenation response, dependent on escape from the G2 catenation checkpoint (*Brownlow N et al., 2014*). A deficiency in the G2 checkpoint has been reported in many cell lines (*Brownlow N et al., 2014; Damelin M and Bestor TH, 2007*). Since RPE1-hTERT cells have a robust catenation checkpoint, we used an Ataxia Telangiectasia Mutated (ATM)/RAD3-related (ATR) inhibitor in order to weaken this and other G2 checkpoint responses, recapitulating in the RPE cells some of the potential stresses associated with a G2 checkpoint defective, transformed cell line. Immunofluorescence analyses demonstrated that ATM/ATR inhibition, combined with Blu577 or BIM-1 treatment, results in a significant increase in the percentage of metaphase cells with a defective mitotic spindle (Figure 3c,d). These results suggest that the PKCε dependency of mitotic spindle organization is related to the efficiency of G2/M checkpoint(s), defects in which are a hallmark of the transformation status of cells.

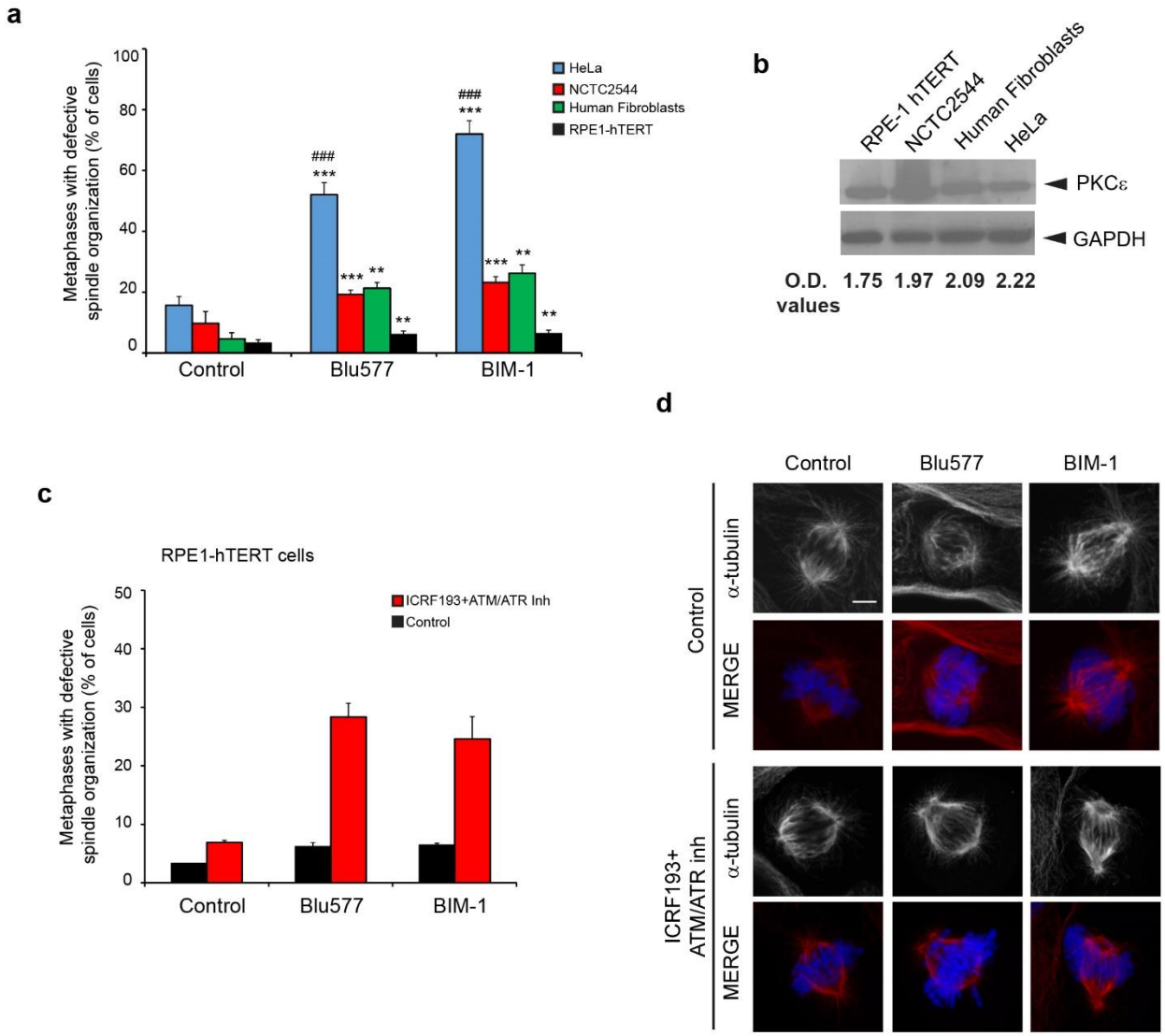

Figure 3 Non-transformed RPE1-hTERT cell line is significantly less responsive to PKCε inhibitors compared with transformed HeLa cells (***P<0.001, **P<0.01 Blu577 and BIM-1 vs Control; ###P<0.001 HeLa vs RPE1-hTERT) **(a).** Chart shows the quantification of the percentage of cells in metaphase presenting defective mitotic spindle in transformed HeLa cells (blue), normal human keratinocytes NCTC2544 (red), primary human fibroblasts (green) and non-transformed RPE1-hTERT cells (black). Mean of three experiments ± sd, n>100 per condition per experiment is represented. (**b**) Detection of PKCε in RPE1-hTERT, NCTC2544, Human Fibroblasts and HeLa cells by western blot. GAPDH was used as loading control. Densitometric values (O.D) of PKCε expression relative to the GAPDH are indicated for each sample. (**c**) PKCε dependency in mitotic spindle organization in RPE1-hTERT cells is increased upon ATM/ATR inhibition. The graph represents the percentage of cells with a disorganized mitotic spindle treated with ICRF193 and ATM/ATR inhibitors (red) compared with control (black). (**d**) Representative images of RPE1 cells with or without ICRF193+ATM/ATR inhibition. PKCε inhibition, combined with ATM/ATR inhibition, results in an increase of the frequency of metaphase cells with defective mitotic spindle (lower panels), compared with the control (upper panels). β-tubulin is represented in red, DAPI in blue.

3. Inhibition of PKCε results in a delayed metaphase entry due to prolonged centrosome migration.

To deeply investigate the effects of PKCε inhibition, we subsequently imaged unsynchronized HeLa cells stably expressing mCherry-H2B and GFP-Tubulin by time-lapse video-microscopy and recorded the time taken from prophase, when the centrosomes are duplicated and the DNA is condensed, to metaphase alignment (Figure 4a). Most control cells (55 ± 7.3%) took less than 10 minutes to reach metaphase alignment. This frequency is dramatically reduced upon treatment with Blu577 or BIM-1 (2.2 ± 2% Blu577, 2.5 ± 1% BIM-1 ($P<0.001$)) (Figure 4b). Consistently, PKCε inhibition causes an increase of the percentage of cells which took from 10 to 20 minutes to reach metaphase (42 ± 7.6% Control *vs* 57.4 ± 3% Blu577 and 58.3% ± 0.5 BIM-1 ($P<0.05$)) or more than 20 minutes (3 ± 0.4% Control *vs* 40.4 ± 1.3% Blu577 and 39.3 ± 1.7% BIM-1 ($P<0.001$)). In accordance with the critical role of PKCε in cytokinesis (*Saurin AT et al., 2009*) the number of cells unable to complete cytokinesis is increased upon PKCε inhibition (Figure 4c). In line with the delay to metaphase entry, we also observed a lag in the timing of centrosome movement toward the opposite poles. We scored the time that centrosome took from their duplication, until they are positioned to the opposite poles assembling the bipolar spindle. Duplicated centrosomes of untreated HeLa cells did not take more than 6 minutes to migrate, whereas upon Blu577 and BIM-1) treatment, centrosomes took more than 10 minutes ((17 ± 5% ($P<0.001$) and 30.5 ± 6.5% ($P<0.001$) minutes, respectively) (Figure 4d).

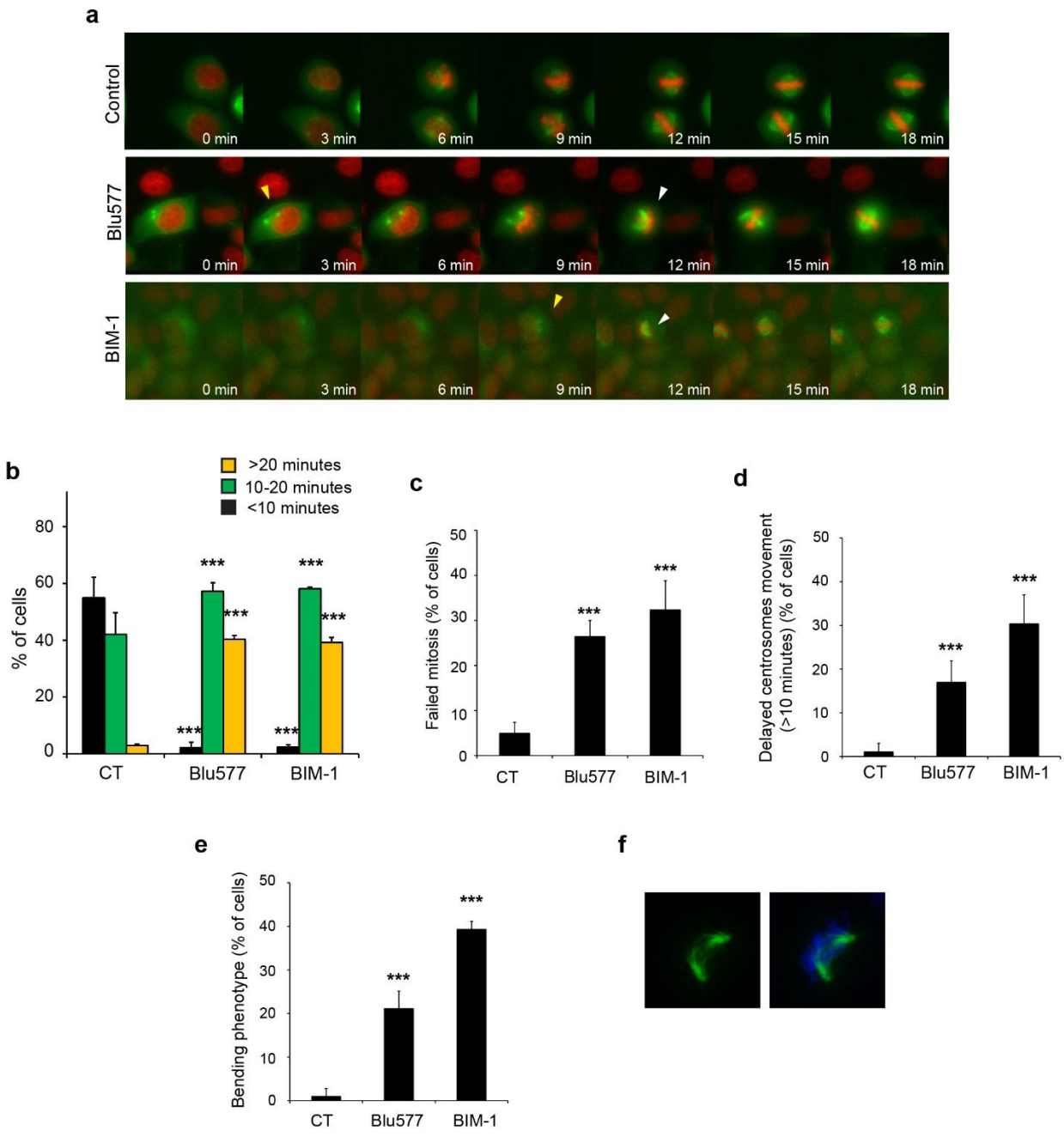

Figure 4 Live-imaging microscopy revealed that PKCε inhibition results in delay of centrosome movement, a "bending" phenotype and thereby in a delay to metaphase entry. (**a**) HeLa cells that stably express mCherry-H2B and GFP-Tubulin were imaged by time-lapse microscopy. Stills taken from time-lapse imaging of HeLa cells upon treatment with Blu577, BIM-1 and Control; time in minutes is marked in white. The yellow arrows indicate the centrosome delay. The white arrows indicate the "bending" phenotype. (**b**) Metaphase is delayed in cells treated with Blu577 and BIM-1. The graph shows time taken in minutes from prophase-to-metaphase, indicating less than 10 minutes (<10) in black, between 10 and 20 minutes (10-20) in green and more than 20 minutes (>20) in yellow. Chart shows the average of three experiments ± sd, n>30 per condition per experiment. ***P<0.001 vs CT. (**c**) Quantification of HeLa cells unable to complete mitosis. Cells stably express mCherry-H2B and GFP-Tubulin were imaged by time-lapse microscopy upon treatment with Blu577 and BIM-1. In line with previous findings, PKCε inhibition increases the number of cells which failed mitosis. Charts show the average of three experiments ± sd, n>30 per condition per experiment. ***P<0.001 *vs* CT. (**d**) PKCε inhibition causes a delay of poleward centrosome movement. The graph represents the percentage of cells which centrosome took more than 10 minutes to move to the opposite poles. Charts show the average of three experiments ± sd, n>30 per condition per experiment. ***P<0.001 vs CT. (**e, f**) PKCε inhibition alters mitotic spindle morphology in a phenotype that we refer to as "bending". The graph represent the

number of cells which displayed the "bending" phenotype. Charts show the average of three experiments ± sd, n>30 per condition per experiment. ***P<0.001 vs CT. (**f**) Representative image of a "bending" phenotype. β-tubulin in green, DAPI in blue.

In addition, we observed in cells treated with PKCε inhibitors an aberrant morphology of the spindle that we refer to as "bending" phenotype (white arrowheads, Figure 4a), observed with increased frequency in cells where PKCε is inhibited, which correlates with the delay in centrosomes movement and consequent mitotic spindle disorganization observed by confocal imaging (Figure 4e, f). The delay of centrosome migration to the opposite side of the cell combined with mitotic spindle disorganization and the delay to metaphase entry when PKCε is inhibited, suggest that PKCε is involved in mitotic progression from prophase to metaphase.

4. Identification of Cytoplasmic Dynein and PKCε as binding partners in G2/M.

We sought then to study how PKCε coordinates the progression of these early mitotic events. First, to investigate the potential PKCε substrate/s involved in this process, we examined the localization of key proteins involved in centrosome disjunction/movement and mitotic spindle nucleation, i.e. Kif2A, Aurora A (phospho-T288) and Plk (Figure 5a). We did not observe any change in the localization of these proteins in cells treated with either Blu577 or BIM-1, providing no evidence of involvement in the PKCε regulation of prometaphase to metaphase progression. We used then tandem mass spectrometry fingerprinting analysis previously performed in order to identify potential PKCε binding partners throughout mitosis. Among the known spindle-associated proteins reported, Dynein Heavy Chain 1 was found to bind PKCε in G2/M and metaphase (Figure 5b). We confirmed the PKCε interaction with Dynein by co-immunoprecipitation of the endogenous proteins in HeLa cells. PKCε physically interacts with Dynein in cells synchronized in metaphase (Figure 5c).

To confirm and determine the subcellular localization of PKCε/Dynein interaction, we used an *in situ* proximity ligation assay (PLA) (*Söderberg, O et al., 2006*). This assay revealed that PKCε interacts with Dynein around the nuclear envelope and chromatin in prophase, and in the mitotic spindle region in prometaphase (Figure 5d). Further, we observed the effects of PKCε inhibition on its interaction with Dynein, performing PLA assays on HeLa cells treated with Blu577 and BIM-1. The number of spots representing the PKCε/Dynein IC in close proximity is reduced in cells treated with PKCε inhibitors, suggesting that the inhibition of PKCε interferes with its interaction with Dynein (Figure 5e, f). No PLA signal was detected in the negative control (Figure 5g). Our findings suggested an involvement of PKCε in mitotic spindle organization and mitotic progression. Since Dynein plays critical roles in centrosome separation and bipolar spindle assembly, we hypothesised that PKCε supports Dynein function and regulates prophase-metaphase progression in these cells.

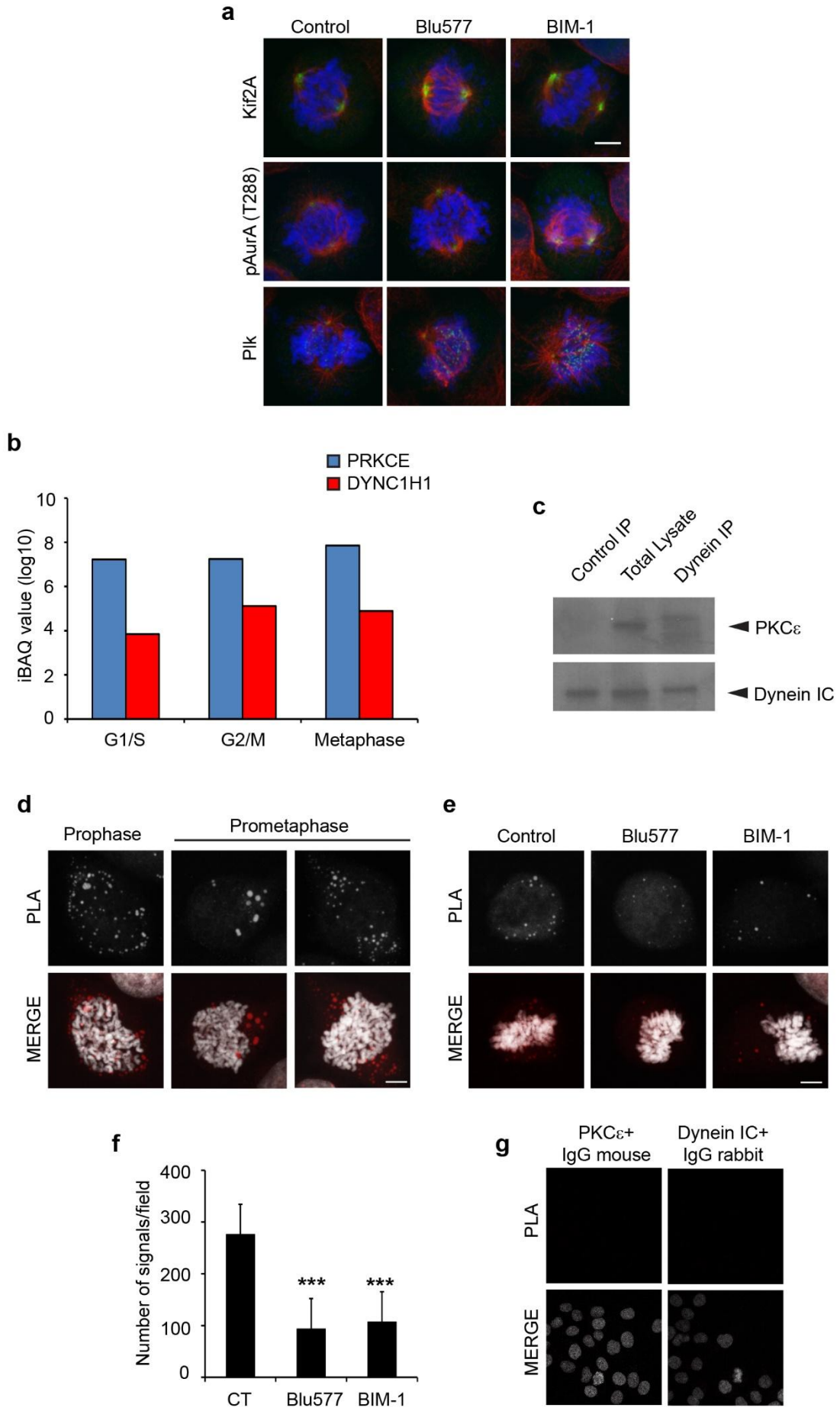
a
Control
Blu577
BIM-1
Kif2A
pAurA (T288)
Plk
b
PRKCE
DYNC1H1
iBAQ value (log10)
10
8
6
4
2
0
G1/S
G2/M
Metaphase
c
Control IP
Total Lysate
Dynein IP
PKCε
Dynein IC
d
Prophase
Prometaphase
PLA
MERGE
e
Control
Blu577
BIM-1
PLA
MERGE
f
Number of signals/field
400
300
200
100
0
***
***
CT
Blu577
BIM-1
g
PKCε+
IgG mouse
Dynein IC+
IgG rabbit
PLA
MERGE

Figure 5 PKCε physically interacts with Dynein in mitotic HeLa cells (a) Confocal images of HELA cells untreated, treated with Blu577 and BIM-1. The inhibition of PKCε does not affect the localization or the fluorescence intensity of Kif2A (green), pAurA (T288) (green) and PLK (green). β-tubulin is represented in red and DAPI in blue. Scale bar, 5 μm. (**b**) Mass spectrometry analysis revealed that PKCε interacts with the Dynein Heavy Chain 1 in G2 phase and metaphase in DLD-1 PKCε M486A cells. Bar graph comparing PRKCE (blue) and DYNC1H1 (red) at G1/S, G2/M and metaphase stages of the cell cycle using log10 transformed intensity based absolute quantification (iBAQ) values. An order of magnitude difference is observed for DYNC1H1 at G1 compared to G2 and metaphase in contrast to PRKCE. (**c**) Co-immunoprecipitation assay was performed using anti-Dynein IC antibody in HeLa cells synchronized in prometaphase/metaphase and cross-linked using 1% formaldehyde. IgG-Mouse used as control, Total lysate and Dynein IP were analysed by western blot and probed for PKCε and for Dynein IC to assess the efficiency of the assay. The image shows that PKCε interacts with Dynein IC in cells enriched in prometaphase/metaphase. (**d**) Detection of PKCε and Dynein IC interaction in HeLa cells using the in situ Proximity Ligation Assay (PLA). The images show a maximum intensity projection of the raw image; PLA signals are shown in red and DNA in grey. PKCε and Dynein IC interact in mitotic HeLa cells. PLA signals are detected in the nucleus and along the nuclear envelope when the cell is in prophase and in the mitotic spindle region in the cells in prometaphase. Scale bars, 5 μm. (**e**) Representative images of PLA assay performed using HeLa cells treated with Blu577 and BIM-1. PKCε inhibition causes a reduction of PKCε/Dynein IC interaction, as indicated by the reduction of the spots. Scale bars, 5 μm. (**f**) Quantification of PKCε/Dynein IC interaction counting the number of signals per field. Chart represents the averages of three independent experiments ± sd. ***P<0.001 vs CT. (**g**) Proximity Ligation Assay (PLA) negative control. Representative images of the control reaction using rabbit anti-PKCε antibody with anti-IgG mouse (left) and mouse anti-Dynein IC antibody with anti-IgG rabbit (right).

5. Dynein ATPase activity inhibition phenocopies inhibition of PKCε.

To investigate whether PKCε regulates Dynein function, I treated HeLa cells with EHNA (Erythro-9-3-(2-hydroxynonyl)adenine), to inhibit Dynein ATPase activity and interfere with Dynein-MT binding (*Yamada M et al, 2015*). One hour inhibition of Dynein activity caused aberrations in mitotic spindle morphology comparable with the spindle defect seen when HeLa cells were treated with Blu577 and BIM-1 (Figure 6a). Cells treated with EHNA showed a defective mitotic spindle when compared with control (84 ± 6% ***P<0.001) (Figure 6b). The aberrant spindle morphology observed upon treatment with EHNA is in line with the important role of Dynein in mitotic spindle orientation and organization. HeLa cells were then imaged by time-lapse microscopy following treatment with EHNA (Figure 4d). As expected, Dynein inhibition resulted in a delay of centrosome movement, thereby delaying mitotic progression. Indeed, prophase to metaphase transition is delayed in most EHNA-treated cells: 61 ± 4 % of cells took 10-20 minutes to transit (***P<0.001) and 33 ± 5% of cells took more than 20 minutes (***P<0.001) to reach metaphase alignment (Figure 6c). Interestingly, the very slow transiting cells (>20min) were unable to properly complete mitosis, indicating that the multiple functions exerted by Dynein throughout

mitosis are essential for the proper completion of cell division. Further, we noted the “bending” of GFP-Tubulin, which was very similar to the phenotype seen with PKCε inhibition (Figure 6e, f).

To confirm that PKCε inhibition is a phenocopy of Dynein inhibition, we filmed HeLa cells upon treatment with a different dynein inhibitor, Ciliobrevin (*Roossien DH et al., 2015*) (Figure 7). Even using a different dynein inhibitor, we observed the same phenotype observed upon EHNA treatment and PKCε inhibition. Collectively, these data indicate that inhibition of Dynein phenocopies PKCε inhibition and suggests that PKCε may regulate Dynein activity in the prophase to metaphase transition.

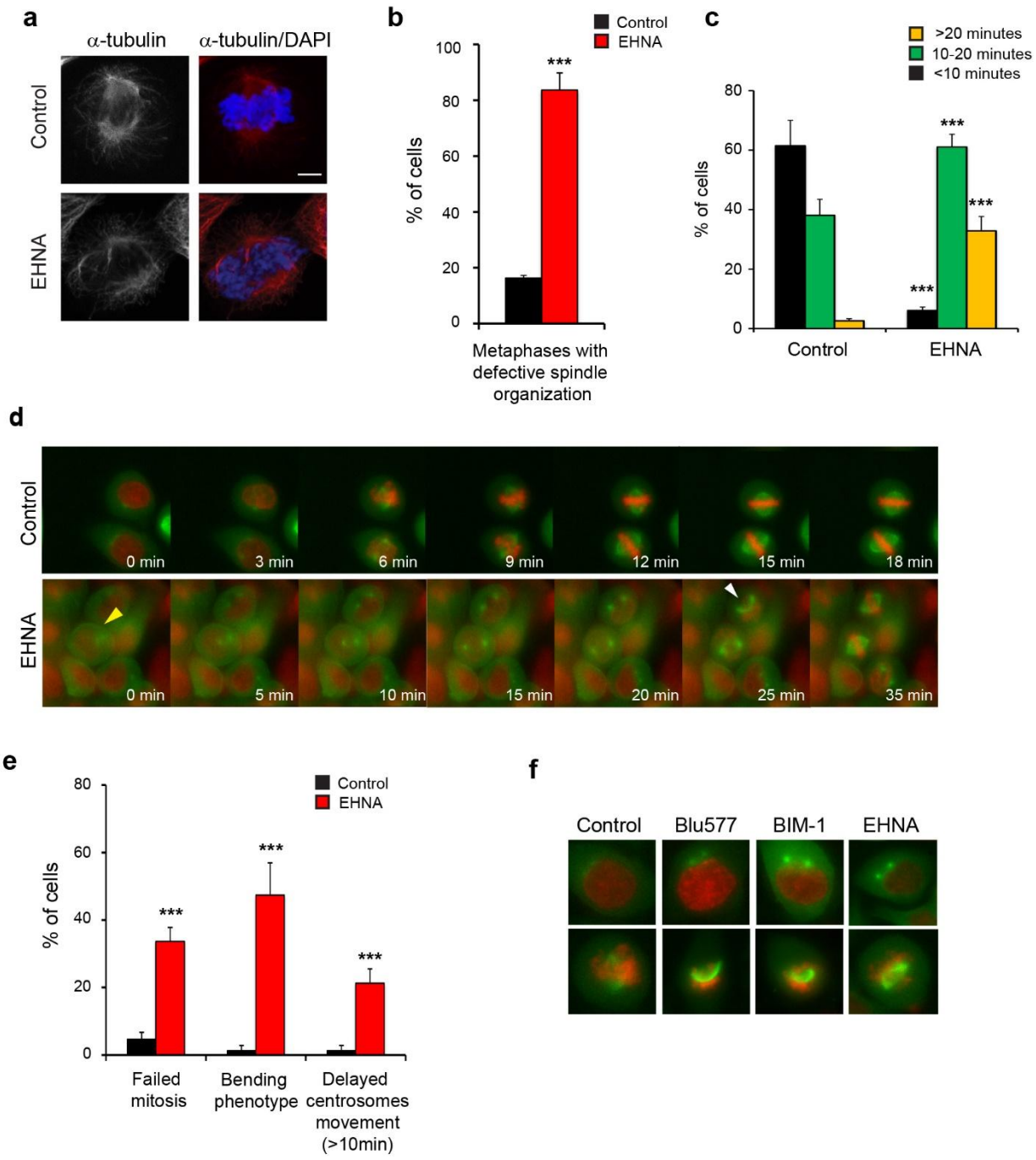

Figure 6 Dynein ATPase activity inhibition phenocopies inhibition of PKCε. (**a**) Confocal images of HeLa cells untreated or treated for 1 hour with EHNA. Mitotic spindle is represented in red (α-tubulin) and DNA in blue (DAPI). Scale bar, 5 μm. (**b**) The amount of mitotic HeLa cells treated with EHNA (red) with a disrupted spindle is significantly higher compared with control (black). Chart shows mean of three experiments ± sd, n>100 per condition per experiment. ***P<0.001 vs CT. (**c-f**) Mitotic events were live-imaged in HeLa cells stably expressing mCherry-H2B (red) and GFP-tubulin (green). (**c**) Dynein inhibition causes a delay to metaphase entry. The graph shows time taken in minutes from prophase to metaphase, indicating less than 10 minutes (<10) in black, between 10 and 20 minutes (10-20) in green and more than 20 minutes (>20) in yellow. Chart shows the average of three experiments ± sd, n>30 per condition per experiment. ***P<0.001 vs CT. (**d**) HeLa cells treated with EHNA show a delay in the centrosomes movement and a "bending" phenotype, equivalent to PKCε inhibition. Stills taken from time-lapse imaging of HeLa cells with or without EHNA treatment; time in minutes is marked in white. Yellow asterisks indicate the centrosome delay, white asterisks indicate the "bending" phenotype. (**e**) The graphs describes that EHNA treatment (red) causes an increase of the percentage of cells unable to complete mitosis, an increase of the number of cells with delayed centrosome movement (> 10 minutes) and with the "bending" phenotype. Charts show the average of three experiments

± sd, n>30 per condition per experiment. ***P<0.001 vs CT. (**f**) Dynein ATPase activity inhibition is a phenocopy of PKCε inhibition. Representative images of the centrosome delay (upper lane) and the "bending" phenotype (lower lane) taken from live imaging of HeLa cells upon EHNA, Blu577 and BIM-1 treatments.

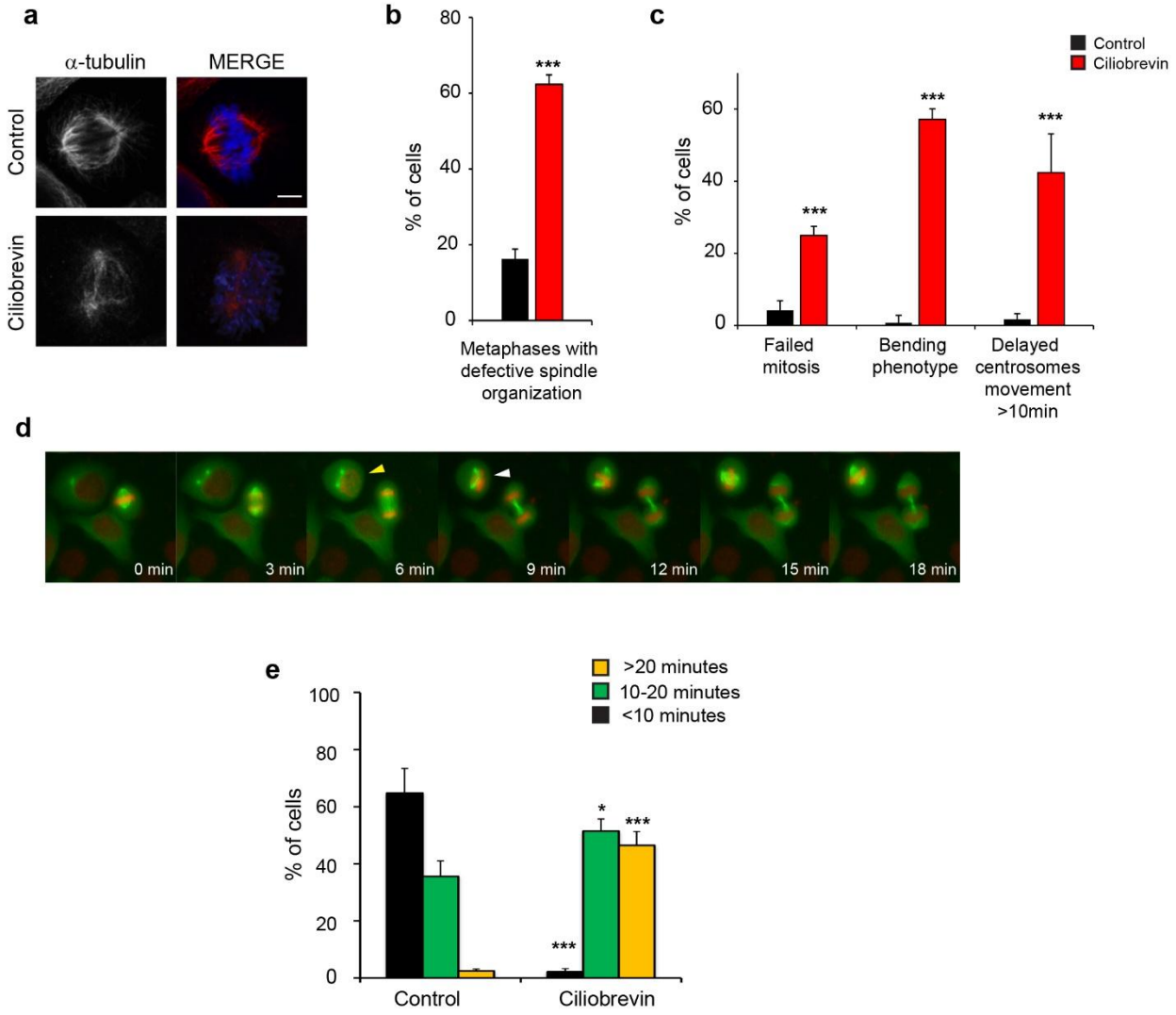

Figure 7 Dynein inhibition using Ciliobrevin is comparable to EHNA treatment and PKCε inhibition. (**a**) Representative images of HeLa cells treated for 1 hour with Ciliobrevin. Scale bar, 5 µm. (**b**) Quantification of Ciliobrevin treated-cells (red) in metaphase with a defective mitotic spindle, compared with control (black). Chart shows mean of three experiments ± sd, n>100 per condition per experiment. ***P<0.001 vs CT. (**c-d**) HeLa cells that stably express mCherry-H2B and GFP-Tubulin were imaged by time-lapse microscopy under Ciliobrevin treatment. The 24.97 ± 2.95% of cells treated with Ciliobrevin (red) were unable to complete mitosis, compared with the control (black). Similarly to EHNA and PKCε inhibitors treatment, we observed in Ciliobrevin-treated cells, an increase of percentage of cells with a "bending" phenotype and the delay of centrosome movement. The red charts represent the percentage of cells treated with Ciliobrevin and in black is represented the control. Chart shows mean of three experiments ± sd, n>100 per condition per experiment. ***P<0.001 vs CT. (**d**) Images taken from the live-imaging microscopy assay. The bending phenotype is indicated with the white arrow and the delay of centrosomes is indicated by the yellow one. (**e**) Ciliobrevin treatment results in a delay to metaphase entry. The graph shows time taken in minutes from prophase to metaphase, indicating less than 10 minutes (<10) in black, between 10 and 20 minutes (10-

20) in green and more than 20 minutes (>20) in yellow. Chart shows the average of three experiments ± sd, n>30 per condition per experiment. ***P<0.001 vs CT.

6. PKCε inhibition delays the silencing of the Spindle Assembly Checkpoint (SAC) by modulating dynein activity.

The bipolar microtubule-kinetochore attachment leads to the silencing of the Spindle Assembly Checkpoint (SAC), a regulatory system that delays the anaphase onset until each chromosomes achieve a bipolar orientation. Silencing of SAC is determined by the streaming poleward of SAC regulators, as Mad2, BubR1 and Bub1, from the kinetochore. Following SAC inactivation, the APC/C complex is activated and cyclinB and securin are degraded leading to anaphase onset. To assess whether PKCε inhibition directly affects dynein function, we monitored BubR1 and Mad2 dynein-mediated streaming in HeLa cells with Blu577 or BIM-1. We therefore scored the number of cells in metaphase alignment, with or without BubR1 and Mad2 at the kinetochores (Figure 8 c). Consistently, we found a great proportion of $BubR1^{+}$ and $Mad2^{+}$ kinetochores in PKCε inhibited cells compared to control (Figure 8a, b), suggesting that dynein-mediated streaming depends on PKCε activity. This is comparable with EHNA treatment which, as expected, caused an increase of the number of cells retaining both dynein cargoes at the kinetochores. This data revealed that PKCε inhibition affects dynein-mediated stripping of BubR1 and Mad2, confirming that PKCε activity regulates dynein function (Figure 8 d, e).

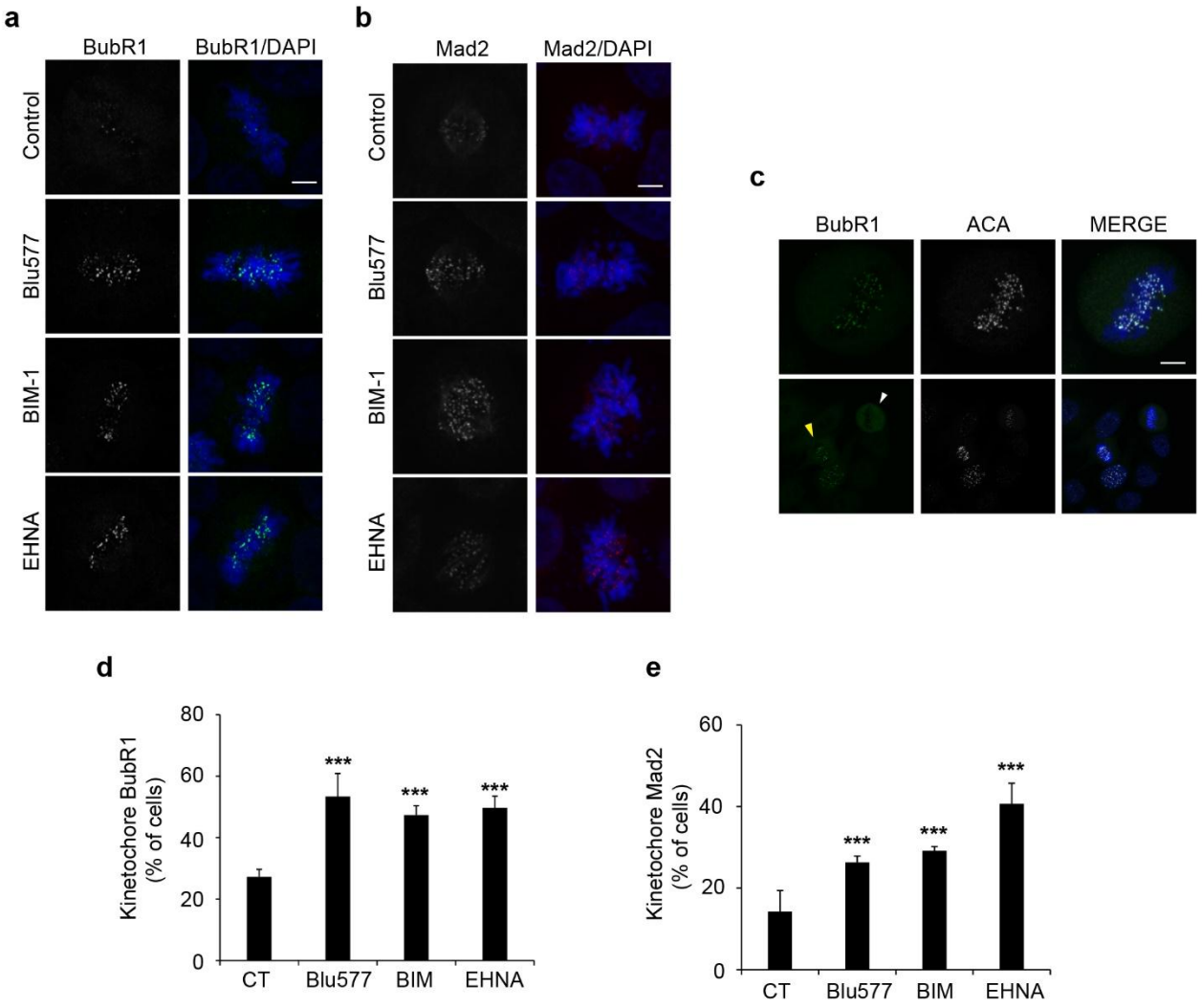

Figure 8 PKCε inhibition affects Dynein cargoes streaming. (**a-d**) Unsynchronized HeLa cells were treated with Blu577, BIM-1 and EHNA for 1 hour and subsequently fixed and stained for BubR1 and Mad2. (**a**) Representative images of BubR1 staining (green) in metaphase cells upon the different treatments. DAPI (blue) represents the aligned chromosomes on the metaphase plate. (**b**) Representative images of metaphase cells labelled for Mad2 (red) with DNA (blue) upon Blu577, BIM-1 and EHNA treatments. (**c**) The double staining with anti-BubR1 or anti-Mad2 and anti-centromere (ACA) antibody was used to score the number of cells in metaphase retaining dynein cargoes (upper lane). In the lower lane are indicated two cells in metaphase, one with BubR1 enriched at the centromeres (yellow arrow) and the other with BubR1 barely detectable at the kinetochores (white). Scale bars, 5 μm. (d-e) Quantification of the amount of HeLa cells in metaphase with BubR1 (**d**) and Mad2 (**e**) retained at the kinetochores. PKCε inhibition using Blu577 and BIM-1 results in a higher percentage of cells which retains both BubR1 and Mad2 at the kinetochores. A similar trend was observed in cells treated with EHNA. Chart shows mean of three experiments ± sd, n>50 per condition per experiment. ***P<0.001 vs CT.

7. Dynein accumulates at kinetochores upon treatment with Blu577 and BIM-1.

Immunofluorescence microscopy studies demonstrated that dynein localizes to kinetochores prior to MTs attachment, where it regulates initial interactions with spindle fibres and coordinates the early aspects of chromosome movement in prometaphase. As chromosomes achieve bipolar attachment, kinetochore dynein staining becomes less prominent and is undetectable once the chromosomes are aligned. Loss of dynein at the kinetochores coincides with an enhanced labelling along the spindle fibres and spindle poles. Since PKCε inhibition results in a prolonged prometaphase, we investigated dynein localization using immunofluorescence in HeLa cells treated for 1hour with Blu577 and BIM-1. Untreated cells in metaphase displayed Dynein labelling on the spindle fibres and at the spindle poles, at the plus end of MTs and at the cortex at one side of the cell (Figure 9a). By contrast, HeLa cells treated with PKCε inhibitors showed a disorganised spindle morphology with chromosomes in a prometaphase-like state and an enrichment of Dynein at the kinetochores and at the plus end of unattached MTs. Indeed, double staining of Dynein and the chromatin-associated protein phospho-CENP-A (Ser7) upon PKCε inhibition confirmed the Dynein localization at the kinetochores (Figure 9b). In an unsynchronized population of HeLa cells, Dynein localization at the kinetochores is detectable in the 2 ± 1 % of cells compared with the significantly higher 37 ± 4 % and the 50 ± 2 % of cells respectively treated with Blu577 and BIM-1 ($P<0.001$) (Figure 9c). This is in line with our previous observation that inhibition of PKCε in an unsynchronized population of cells results in delay of metaphase entry, sustaining the notion that PKCε is required for prophase to metaphase progression. In addition, Dynein localization at the kinetochores can be explained as a perturbation of Dynein streaming from the plus ends of microtubules to the spindle poles, in line with the hypothesis that Dynein activity is dependent on PKCε. We therefore examined Dynein localization in cells treated with EHNA.

As expected, EHNA treatment resulted in a higher percentage of cells with a disorganized mitotic spindle and Dynein enrichment at the kinetochores. This phenotype is similar to the one

seen upon Blu577 and BIM-1 concordant with our observation that Dynein inhibition phenocopies PKCε inhibition (Figure 9d). EHNA treatment revealed also a new localization of PKCε at the kinetochores, as confirmed by the double staining with the centromere antibody ACA (Figure 9e, f). We showed that Dynein interacts with PKCε in prometaphase and the inhibition of Dynein and PKCε results in an accumulation of both proteins at the kinetochores. This suggests that in prometaphase, the PKCε/Dynein complex is trapped at the kinetochores when both the proteins are inhibited. We also examined the localization of p150 (Glued), the largest subunit of Dynactin complex, which links Dynein to cargos and increases its processivity.

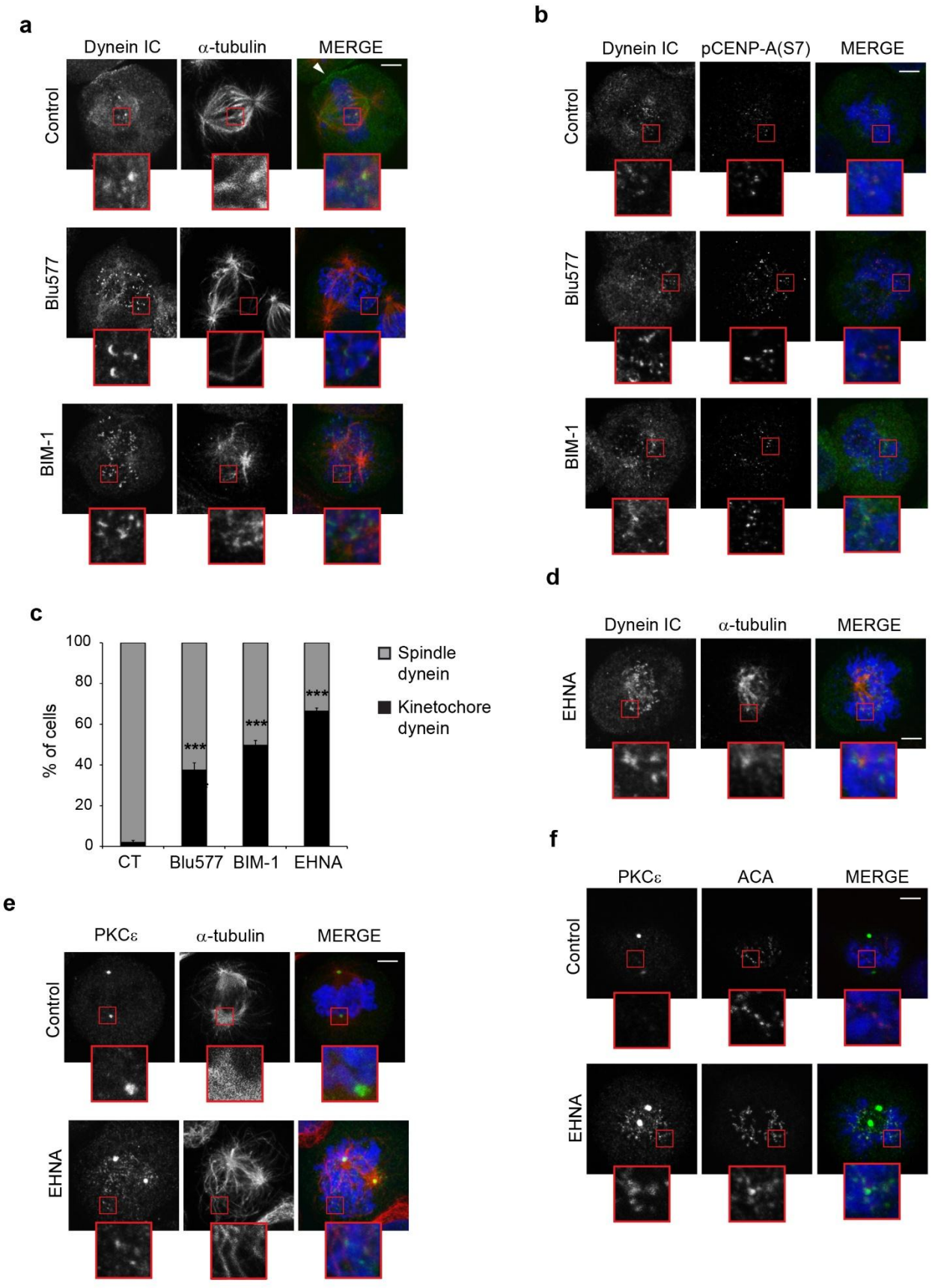

Figure 9 Localization of Dynein IC is dependent on PKCε activity. (**a-b**) Dynein IC is localized at the kinetochores when PKCε is inhibited. The inset panels show a magnification of Dynein IC localization. Scale bars, 5 μm. (**a**)

Confocal images of HeLa cells treated with Blu577 and BIM-1 for 1 hour, fixed and stained with anti-Dynein IC (green), α-tubulin (red) and DAPI (blue). In a control cell in metaphase (upper panel), Dynein IC is localized at the plus end of the microtubules (inset), at the cortex (arrow) and along the microtubules of the mitotic spindle. In HeLa cells treated with the more specific PKCε inhibitor Blu577 (middle panel), the mitotic spindle is disorganised, the chromatids are condensed prophase/prometaphase-like and Dynein is localized at the kinetochores. The same Dynein IC pattern is detectable in HeLa cells treated with BIM-1. (**b**) Representative images of HeLa cells treated with Blu577 and BIM-1 for 1 hour, fixed and stained with anti-Dynein IC (green), pCENP-A(S7) (red) and DAPI (blue). In the control, Dynein IC localizes with pCENP-A(S7) at the plus end of the microtubules (upper panel), whereas it is coupled with the kinetochores when PKCε is inhibited (Blu577, middle panel; BIM-1, lower panel). (**c**) Quantification of mitotic HeLa cells with Dynein IC labelled at the spindle (grey charts) and at the kinetochores (black charts). Chart shows mean of three experiments ± sd, n>100 per condition per experiment. ***P<0.001 vs CT. (**d**) Similarly to PKCε inhibition, dynein is localized ad the kinetochores in cells treated with EHNA. Representative images of Dynein staining in HeLa cells treated with dynein inhibitor EHNA. (**e-f**) PKCε is localized at the kinetochores when Dynein ATPase activity is inhibited. The inset panels show a magnification of PKCε localization. Scale bars, 5 μm. (**e**) PKCε is at the kinetochores in mitotic HeLa cells treated for 1 hour with EHNA. The inset panels show a magnification of PKCε localization. The control (upper lane) displays a bipolar and well defined mitotic spindle (α-tubulin, red), PKCε enrichment at the centrosomes (green; inset) and the chromosomes alignment (blue) at the metaphase plate. The lower lane represents a cell treated with EHNA, which shows a disrupted mitotic spindle (α-tubulin, magenta) and a PKCε localization (green) at the centrosomes and dispersed on the chromatin (blue). (**f**) HeLa cells were stained for PKCε (green) and the centrosomial protein ACA (red), in order to verify the localization of PKCε at the kinetochores following Dynein inhibition. PKCε is enriched at the centrosomes in the control (upper lane) and it is hardly detectable at the metaphase plate (inset). When Dynein activity is inhibited (lower lane), PKCε is detectable both at the centrosomes and at the kinetochores (inset).

As for Dynein, but with a less profound effect, Dynactin localized at the kinetochores to a significantly higher extent in cells treated with PKCε inhibitors indicating that not only Dynein, but the Dynein/Dynactin complex becomes more stably localized at the kinetochores when PKCε is inhibited (Figure 10a, b).

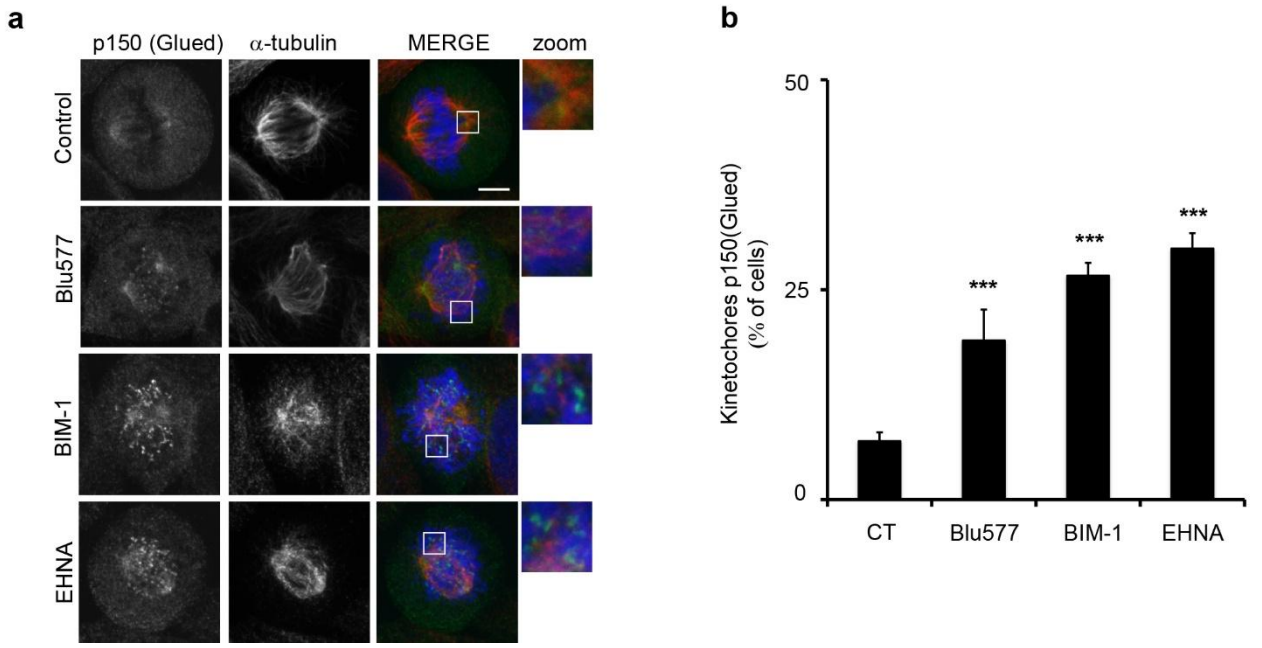

Figure 10 The Dynactin subunit p150 (Glued) is localized at the kinetochores in mitotic cells treated with Blu577 and BIM-1. (**a**) The inset panels show a magnification of p150 (Glued) localization. In the control (upper panel), Dynactin is localized at the mitotic spindle. In HeLa cells treated with PKCε inhibitors (Blu577, middle panel) and BIM-1 (lower panel), the mitotic spindle is disrupted (α-tubulin, red) and Dynactin (green) is located at the kinetochores. DNA is stained with DAPI (blue). (**b**) Quantification of the number of HeLa cells which displays p150 (Glued) at the kinetochores. The amount of cells with the dynactin subunit located at the kinetochores is higher in Blu577-, BIM-1- and EHNA-treated cells. Chart shows mean of three experiments ± sd, n>100 per condition per experiment. ***P<0.001 vs CT.

Discussion

Centrosome movement is a highly orchestrated process critical for bipolar spindle formation and a relationship between centrosome separation and genomic instability is emerging. Recent advances have demonstrated that delayed centrosome separation and movement leads to an increased rate of spindle morphology defects in metaphase and mitotic errors, pointing to a critical role for proper centrosome dynamics in ensuring accurate chromosome segregation (*Silkworth WT and Cimini T, 2012; Lingle WL et al., 2005*). For this reason, the identification of proteins implicated in this process is important in expanding our knowledge of the stepwise process of cellular transformation and neoplasm pathogenesis and in suggesting novel therapeutic targets for cancer.

PKCε is frequently found overexpressed in a wide variety of human cancers and has been implicated in malignant transformation of cells, including invasion and metastasis (*Gorin MA and Pan Q, 2009*). Although it has already been demonstrated that PKCε is involved in several cell cycle processes, such as cytokinesis and mitotic catenation resolution at the metaphase-anaphase transition (*Saurin AT et al., 2008; Saurin AT et al., 2009; Brownlow et al., 2014*), engagement in earlier (pre)mitotic events has not been addressed.

We investigated the effects of PKCε down-regulation in early mitotic events, by using different methods of inhibition in multiple cell models (HeLa human cervical carcinoma, HEL human erythroleukemia and DLD1 human colorectal adenocarcinoma). Consistently, cells in prometaphase from all the cell lines displayed an abnormal mitotic spindle morphology compared with controls, implicating the involvement of PKCε in bipolar spindle assembly. Interestingly, this was not the case in the 'normal' keratinocytes NCTC2544, primary human fibroblasts and the non-transformed retinal pigment epithelium RPE1-hTERT cell lines. The G2/M catenation checkpoint is defective in several cell lines, including HeLa cells, whereas it is functional in 'normal' cells (*Damelin M and Bestor TH, 2007*). Brownlow et al. have previously demonstrated that cells with a leaky G2 catenation checkpoint are dependent on PKCε for catenation resolution in mitosis[23]. In an interesting alignment with this finding, we show that bypassing G2 checkpoints using ATM/ATR inhibitors in RPE1 cells results in a PKC-inhibitor dependent abnormal mitotic spindle morphology in these cells, as observed in HeLa cells, providing evidence that the dependence on PKCε for mitotic spindle assembly is related to the ability of the cell to mount a robust G2 checkpoint response. These findings suggest that PKCε inhibition leads to a delay of metaphase transit in G2-checkpoint stressed cells (typically transformed cells), increasing the risk of failure in MTs/kinetochores attachment and potentially contributing to genomic instability.

Live-cell imaging of asynchronous HeLa cells revealed that PKCε inhibition causes a delay of centrosome migration to the opposite sides of the nucleus. Nevertheless, increasing microtubule nucleation at centrosomes occurs and a mitotic spindle is assembled albeit showing an abnormal morphology, a 'bending' phenotype. This might reflect the dominance of chromosome arm engagement and the kinesin-10 dependent chromosome organization i.e. the polar ejection force (*Gutierrez-Uzquiza A et al., 2015*). The centrosome movement delay and the 'bending' phenotype caused by PKCε inhibition are likely to interfere with the kinetochore capture by the mitotic microtubules, leading to a delay to metaphase entry.

Among the several motor proteins implicated in cell division, cytoplasmic dynein is a microtubule motor complex, which plays key roles in multiple processes, such as centrosome separation and spindle organization. How cytoplasmic dynein is able to fulfill such a wide range of processes in cell division is still unclear, making it challenging to address functions attributed to specific dynein pools. However, it has been demonstrated that the interaction with multiple adaptor proteins is essential to orchestrate the timing and localization of dynein functions (*Zhong A et al., 2016*). Here we demonstrate that PKCε physically and functionally interacts with cytoplasmic dynein from G2/M phase to metaphase. Indeed, the phenotypes observed upon dynein inhibition are comparable with the effects of PKCε inhibition, suggesting that PKCε and dynein are functionally related.

Defects in kinetochore-microtubule (KC-MTs) attachment and the spindle assembly checkpoint (SAC) during cell division are strongly associated with genomic instability. The SAC is active during prometaphase and once the chromosomes are aligned and the mitotic spindle is correctly assembled in metaphase, dynein moves from the kinetochores along the microtubules streaming the proteins involved in the SAC, such as BubR1 and Mad2. It has been demonstrated that BubR1 and Mad2 accumulation at kinetochores indicates lack of KC-MTs attachment (*Waters JC et al., 1998; Skoufias DA et al., 2001*). We show evidence that PKCε inhibition causes the

accumulation of dynein, BubR1 and Mad2 at the kinetochores and it is proposed that this is consequent to the delay in MT end-on engagement of kinetochores. We therefore suggest that the improper kinetochore-microtubule attachment caused by PKCε inhibition compromises the dynein-dependent streaming, delaying alignment and thereby delaying the satisfaction of the SAC.

The interaction of PKCε and dynein (as determined by co-immunoprecipitation and PLA) suggests that PKCε may act as a general regulator of dynein function modifying cargo selection perhaps both in prometaphase (as described here) and at anaphase entry (*Brownlow N et al., 2014*).

Taken together, the presented data demonstrate that PKCε modulates prophase-to-metaphase progression in G2 checkpoint compromised cells, by regulating centrosome migration and mitotic spindle organization via dynein interaction. These findings, and those reported previously, establish PKCε as a key regulator of cell cycle progression where there are DNA-associated stresses encountered. In conclusion, the close relationship between PKCε dependency for mitotic spindle organization and the non-functionality of G2 checkpoint(s), (a hallmark of transformed cells), is a strong prescription for PKCε as a therapeutic target in cancer.

References

Akita Y. Protein Kinase C-ε (PKC-ε): Its Unique Structure and function. J Biochem. 2002; 132: 847-852

Aziz M.H., Manoharan H.T. And Verma A.K. Protein kinase C epsilon which sensitizes skin to sun's UV radiation-induced cutaneous damage and development of squamouse cell carcinomas, associates with Stat3. Cancer Res, 2007; 67: 1385-94

Bae K.M., Wang H., Jiang G., Chen M.G., Lu L. And Xiao L. Protein kinase C epsilon is overexpressed in primary human non-small cell lung cancers and functionally required for proliferation of non-small cell lung cancer cells in a p21/Cip1-dependent manner. Cancer Res, 2007; 67: 6053-63

Baines C.P., Zhang J., Wang G.W., Zheng Y.T., Xi J.X., Cardwell E.M., Bolli R. And Ping P. Mitochondrial PKCepsilon and MAPK form signaling modules in the murine heart: enhanced mitochondria] PKCepsilon-MAPK interactions an differential MAPK activation in PKC-epsilon-induced cardioprotection. Circ. Reg. 2002; 90: 390-397

Bakhoum SF, Genovese G, Compton DA. Deviant kinetochore microtubule dynamics underlie chromosomal instability. Curr Biol. 2009 Dec 1;19(22):1937-42.

Barisic M, Maiato H. Dynein prevents erroneous kinetochore-microtubule attachments in mitosis. Cell Cycle. 2015;14(21):3356-61.

Barr FA, Gruneberg U. Cytokinesis: placing and making the final cut. Cell. 2007 Nov 30;131(5):847-60.

Barr FA, Silljé HH, Nigg EA. Polo-like kinases and the orchestration of cell division. Nat Rev Mol Cell Biol. 2004 Jun;5(6):429-40.

Bartkova J, Horejsí Z, Koed K, Krämer A, Tort F, Zieger K, Guldberg P, Sehested M, Nesland JM, Lukas C, Ørntoft T, Lukas J, Bartek J. DNA damage response as a candidate anti-cancer barrier in early human tumorigenesis. Nature. 2005 Apr 14;434(7035):864-70.

Basto R, Lau J, Vinogradova T, Gardiol A, Woods CG, Khodjakov A, Raff JW. Flies without centrioles. Cell. 2006 Jun 30;125(7):1375-86.

Basu A., Lu D., Sun B., Moor A.N., Akkaraju G.R. And Huang J. Proteolytic activation of protein kinase C-epsilon by caspase-mediated processing and transduction of anti-apoptotic signals. J Biol. Chem. 2002; 277: 41850-41856

Bell R.M. And Bums D.J. Lipid activation of protein kinase C. J Biol Chem 1991; 266: 4661-4664

Bennett CB, Lewis AL, Baldwin KK, Resnick MA. Lethality induced by a single site-specific double-strand break in a dispensable yeast plasmid. Proc Natl Acad Sci U S A. 1993 Jun 15;90(12):5613-7.

Besson A., Wilson T.L. And Yong V.W. The anchoring protein RACK1 links protein kinase Cepsilon to integrin beta chains. Requirements for adhesion and motility. J Biol Chem 2002; 277(24): 22073-22084

Besson A., Wilson T.L. And Yong V.W. The anchoring protein RACK1 links protein kinase Cepsilon to integrin beta chains. Requirements for adhesion and motility. J Biol. Chem. 2002; 277: 22073-22084

Bingham JB, Schroer TA. Self-regulated polymerization of the actin-related protein Arp1. Curr Biol. 1999 Feb 25;9(4):223-6.

Blagden SP, Glover DM. Polar expeditions--provisioning the centrosome for mitosis. Nat Cell Biol. 2003 Jun;5(6):505-11.

Branzei D, Foiani M. Maintaining genome stability at the replication fork. Nat Rev Mol Cell Biol. 2010 Mar;11(3):208-19.

Brehm A., Miska E.A., Mccance D.J., Reid J.L., Bannister A.J. And Kouzarides T. Retinoblastoma protein recruits histone deacetylase to repress transcription. Nature 1998; 391: 597–601

Brennan IM, Peters U, Kapoor TM, Straight AF. Polo-like kinase controls vertebrate spindle elongation and cytokinesis. PLoS One. 2007 May 2;2(5):e409.

Bridges D. And Moorhead G.B. 14-3-3 proteins: a number of functions for a numbered protein. Sci STKE 2005; 296: 1-5

Brownlow, N., Pike, T., Zicha, D., Collinson, L., Parker, P.J. Mitotic catenation is monitored and resolved by a PKCε-regulated pathway. Nat Commun. 5, 5685 (2014)

Burkard ME, Randall CL, Larochelle S, Zhang C, Shokat KM, Fisher RP, Jallepalli PV. Chemical genetics reveals the requirement for Polo-like kinase 1 activity in positioning RhoA and triggering cytokinesis in human cells. Proc Natl Acad Sci U S A. 2007 Mar 13;104(11):4383-8.

Busson S, Dujardin D, Moreau A, Dompierre J, De Mey JR. Dynein and dynactin are localized to astral microtubules and at cortical sites in mitotic epithelial cells. Curr Biol. 1998

Bynagari-Settipalli Y.S. et al. Negatively Protein Kinase C Isoform ε Regulates ADP- Induced Calcium Mobilization and Thromboxane Generation in Platelets. Arteriosclerosis, Thrombosis, and Vascular Biology. 2012; 32: 1211-1219.

Cameron A.J., Parker P.J. Protein kinase C - a family of protein kinases, allosteric effectors or both? Adv Enzyme Regul. 2010; 50(1):169-77.

Campbell CS, Desai A. Tension sensing by Aurora B kinase is independent of survivin-based centromere localization. Nature. 2013 May 2;497(7447):118-21.

Carubbi C, Masselli E, Martini S, Galli D, Aversa F, Mirandola P, Italiano JE Jr, Gobbi G, Vitale M. Human thrombopoiesis depends on Protein kinase Cδ/protein kinase Cε functional couple. Haematologica. 2016; 101(7):812-20.

Castagna M., Takai Y., Kaibuchi K., Sano K., Kikkawa U. And Nishizuka Y. Direct activation of calcium-activated, phospholipid- dependent protein kinase by tumor-promoting phorbol esters. J Biol Chem, 1982; 257: 7847-51.

Castillo A, Justice MJ. The kinesin related motor protein, Eg5, is essential for maintenance of pre-implantation embryogenesis. Biochem Biophys Res Commun. 2007 Jun 8;357(3):694-9.

Cenni V., Doppler H., Sonnenburg E.D., Maraldi N.,Newton A.C. And Toker A. Regulation of novel protein kinase C epsilon by phosphorylation. Biochem J. 2002; 363: 537–545

Cesare P., Dekker L.V., Sardini A., Parker P.J. And Mcnaughton P.A Specific involvement of PKC-epsilon in sensiti zation of the neuronal response to painful heat. Neuron 1999; 23: 617-624

Cheeseman IM, Desai A. Molecular architecture of the kinetochore-microtubule interface. Nat Rev Mol Cell Biol. 2008 Jan;9(1):33-46.

Chen, D., Purohit, A., Halilovic, E., Doxsey, S.J., Newton, A.C. Centrosomal anchoring of protein kinase C betaII by pericentrin controls microtubule organization, spindle function, and cytokinesis. J Biol Chem. 279, 4829-39 (2004)

Chen Z., Indjeian V.B., Mcmanus M., Wang L. And Dynlacht B.D. CP110, a cell cycle-dependent CDK substrate, regulates centrosome duplication in human cells. Dev. Cell 2002; 3: 339–350

Cianfrocco MA, DeSantis ME, Leschziner AE, Reck-Peterson SL. Mechanism and regulation of cytoplasmic dynein. Annu Rev Cell Dev Biol. 2015;31:83-108.

Ciccia A, Elledge SJ. The DNA damage response: making it safe to play with knives. Mol Cell. 2010 Oct 22;40(2):179-204.

Clute P, Pines J. Temporal and spatial control of cyclin B1 destruction in metaphase. Nat Cell Biol. 1999 Jun;1(2):82-7.

Collins ES, Balchand SK, Faraci JL, Wadsworth P, Lee WL. Cell cycle-regulated cortical dynein/dynactin promotes symmetric cell division by differential pole motion in anaphase. Mol Biol Cell. 2012 Sep;23(17):3380-90.

Corbalan-Garcia S., Guerrero-Valero M., Marin.Vincente C. And Gomez-Fernandez J.C. The C2 domains of classical/conventional PKCs are specific PtdIns (4,5) P (2)-sensing domains. Biochem Soc Trans 2007; 35: 1046– 1048

Cox, J. et al. Andromeda: A peptide search engine integrated into the MaxQuant environment. J Proteome Res. 10,1794–805 (2011)

Cox, J., Mann, M. 1D and 2D annotation enrichment: a statistical method integrating quantitative proteomics with complementary high-throughput data. BMC Bioinformatics. 13, S12. (2012)

Culver-Hanlon TL, Lex SA, Stephens AD, Quintyne NJ, King SJ. A microtubule-binding domain in dynactin increases dynein processivity by skating along microtubules. Nat Cell Biol. 2006 Mar;8(3):264-70.

Damelin, M., Bestor, T.H. The decatenation checkpoint. Br J Cancer. 96, 201-5 (2007)

Dekker L.V. And Parker Pj. Protein kinase C a question of specificity. Trends Biochemical Science. 1994; 19(2): 73-7

Di Marcantonio D, Galli D, Carubbi C, Gobbi G, Queirolo V, Martini S, Merighi S, Vaccarezza M, Maffulli N, Sykes SM, Vitale M, Mirandola P. PKCε as a novel promoter of skeletal muscle differentiation and regeneration. Exp Cell Res. 2015; 339(1):10-9.

Ding L., Wang H., Lang W. And Xiao L. Protein kinase C epsilon promotes survival of lung cancer cells by suppressing apoptosis through dysregulation of mitochondrial caspase pathway. J Biol Chem. 2002; 277(38): 35305-35313

Dorn G.W. And Mochly-Rosen D. Intracellular transport mechanisms of signal transducers. Annu. Rev. Physiol. 2002; 64: 407-429

Downes CS, Clarke DJ, Mullinger AM, Giménez-Abián JF, Creighton AM, JohnsonRT. A topoisomerase II-dependent G2 cycle checkpoint in mammalian cells/. Nature.1994 Dec 1;372(6505):467-70.

Drechsel DN, Hyman AA, Hall A, Glotzer M. A requirement for Rho and Cdc42 during cytokinesis in Xenopus embryos. Curr Biol. 1997 Jan 1;7(1):12-23.

Du Q, Macara IG. Mammalian Pins is a conformational switch that links NuMA to heterotrimeric G proteins. Cell. 2004 Nov 12;119(4):503-16.

Dujardin DL, Barnhart LE, Stehman SA, Gomes ER, Gundersen GG, Vallee RB. A role for cytoplasmic dynein and LIS1 in directed cell movement. J Cell Biol. 2003 Dec 22;163(6):1205-11.

Durgan J. et al. The identification and characterization of novel PKC-epsilon phosphorylation sites provide evidence for functional cross-talk within the PKC superfamily. Biochemical Journal. 2008; 411(2): 319-31
Facchinetti V., Ouyang W., Wei H., Soto N., Lazorchak A., Gould C., Lowry C., Newton A.C., Mao Y., Miao R.Q., Sessa W.C., Qin J., Zhang P., Su B. And Jacinto E. The mammalian target of rapamycin complex 2 controls folding and stability of Akt and protein kinase C. EMBO J 2008; 27: 1932-1943

Fagerstrom S., Pahlman S., Gestblom C., Nanberg E. Protein kinase C-epsilon is implicated in neurite outgrowth in differentiating human neuroblastoma cells. Cell Growth Differ. 1996;7(6):775-85.

Falck J, Mailand N, Syljuåsen RG, Bartek J, Lukas J. The ATM-Chk2-Cdc25A checkpoint pathway guards against radioresistant DNA synthesis. Nature. 2001 Apr 12;410(6830):842-7.

Famulski JK, Vos LJ, Rattner JB, Chan GK. Dynein/Dynactin-mediated transport of kinetochore components off kinetochores and onto spindle poles induced bynordihydroguaiaretic acid. PLoS One. 2011 Jan 28;6(1):e16494.

Farr KA, Cohen-Fix O. The metaphase to anaphase transition: a case of productive destruction. Eur J Biochem. 1999 Jul;263(1):14-9.

Fededa JP, Gerlich DW. Molecular control of animal cell cytokinesis. Nat Cell Biol. 2012 May 2;14(5):440-7.

Fujise A. et al. Specificity of the high affinity interaction of protein kinase C with a physiological substrate, myristoylated alanine-rich protein kinase C substrate. The Journal of Biological Chemistry.

1994; 269: 31642-31648.

Gaglio T, Dionne MA, Compton DA. Mitotic spindle poles are organized by structural and motor proteins in addition to centrosomes. J Cell Biol. 1997 Sep 8;138(5):1055-66.

Galli D., Gobbi G., Carubbi C., Di Marcantonio D., Benedetti L., De Angelis M.G., Meschi T., Vaccarezza M., Sampaolesi M., Mirandola P. And Vitale M. The role of PKCe-dependent signaling for cardiac differentiation. Histochem Cell Biol. 2013; 139:3 5-46

Ganem NJ, Storchova Z, Pellman D. Tetraploidy, aneuploidy and cancer. Curr Opin Genet Dev. 2007 Apr;17(2):157-62.
Gayek AS, Ohi R. Kinetochore-microtubule stability governs the metaphase requirement for Eg5. Mol Biol Cell. 2014 Jul 1;25(13):2051-60.

Glotzer M. Cytokinesis: GAP gap. Curr Biol. 2009 Feb 24;19(4):R162-5.

Gobbi G., Di Marcantonio D., Micheloni C., Carubbi C., Galli D., Vaccarezza M., Bucci G., Vitale M. And Mirandola P. Trail Up-Regulation Must be Accompained by Reciprocal PKCε Down-Regulation During Differentiation of Colonic Epithelial Cell: Implications for Colorectal Cancer Cell Differentiation. Journal of Cellular Physiology, 2012; 227: 630-8

Gobbi G., Mirandola P., Carubbi C., Galli D. And Vitale M. Protein Kinase C ε in Hematopoiesis: Conductor or Selector?. Semin Thromb Hemost,2013; 39: 59-65

Gobbi G., Mirandola P., Sponzilli I., Micheloni C., Malinverno C., Cocco L., Vitale M. Timing and expression level of protein kinase C epsilon regulate the megakaryocytic differentiation of human CD34 cells. Stem Cells, 2007; 25(9): 2322–2329

Godek KM, Kabeche L, Compton DA. Regulation of kinetochore-microtubule attachments through homeostatic control during mitosis. Nat Rev Mol Cell Biol. 2015 Jan;16(1):57-64. doi: 10.1038/nrm3916.

Gönczy P, Pichler S, Kirkham M, Hyman AA. Cytoplasmic dynein is required for distinct aspects of MTOC positioning, including centrosome separation, in the one cell stage Caenorhabditis elegans embryo. J Cell Biol. 1999 Oct 4;147(1):135-50.

Gorgoulis VG et al. Activation of the DNA damage checkpoint and genomic instability in human precancerous lesions. Nature. 2005 Apr 14;434(7035):907-13.

Gorin M.A., Pan Q. Protein kinase Cε: an oncogene and emerging tumor biomarker. Molecular Cancer 2009; 8: 9-16

Graness A., Adomeit A., Heinze R., Wetzker R. And Liebmann C. A novel mitogenic signaling pathway of bradykinin in the human colon carcinoma cell line SW-480 involves sequential activation of a Gq/11 protein, phosphatidylinositol 3 kinase beta, and protein kinase C-epsilon. J. Biol. Chem. 1998; 273: 32016-32022

Griner E.M. And Kazanietz M.G. Protein kinase C and other diacylglycerol effectors in cancer. Nat Rev Cancer 2007; 7: 281–294

Hanahan D. And Weinberg R. A. Hallmarks of cancer: the next generation. Cell 2011; 144: 646-74.

Hanahan D. And Weinberg R. A. The hallmarks of cancer. Cell 2000; 100: 57- 70.

Hannak E, Kirkham M, Hyman AA, Oegema K. Aurora-A kinase is required for centrosome maturation in Caenorhabditis elegans. J Cell Biol. 2001 Dec 24;155(7):1109-16.

Harbour J.W. And Dean D.C. The Rb/E2F pathway: expanding roles and emerging paradigms. Genes Dev, 2000; 14: 2393-409

Hinchcliffe EH, Miller FJ, Cham M, Khodjakov A, Sluder G. Requirement of a centrosomal activity for cell cycle progression through G1 into S phase. Science. 2001 Feb 23;291(5508):1547-50.

Hinds P.W., Mittnacht S., Dulic V., Arnold A., Reed S.I. And Weinberg R.A. Regulation of retinoblastoma protein functions by ectopic expression of human cyclins. Cell 1992; 70: 993-1006.

Hirota T. et al. Aurora-A and an interacting activator, the LIM protein Ajuba, are required for mitotic commitment in human cells. Cell 2003; 114: 585–598

Hochegger H., Takeda S. And Hunt T. Cyclin-dependent kinases and cell cycle transitions: does one fit all?. Mol Cell Bio 2008; Vol 9: 910-916

Holland AJ, Cleveland DW. Boveri revisited: chromosomal instability, aneuploidy and tumorigenesis. Nat Rev Mol Cell Biol. 2009 Jul;10(7):478-87.

Holleran EA, Ligon LA, Tokito M, Stankewich MC, Morrow JS, Holzbaur EL. Beta III spectrin binds to the Arp1 subunit of dynactin. J Biol Chem. 2001 Sep 28;276(39):36598-605.

Howell BJ, Moree B, Farrar EM, Stewart S, Fang G, Salmon ED. Spindle checkpoint protein dynamics at kinetochores in living cells. Curr Biol. 2004 Jun 8;14(11):953-64.

Hundle B., Mcmahon T., Dadgar J. And Messing R.O. Overexpression of epsilon-protein kinase C enhances nerve growth factor-induced phosphorylation of mitogen-activated protein kinases and neurite outgrowth. J Biol. Chem. 1995; 270: 30134-30140

Iikeda Y., Olsen G.S., Ziy E., Hansen L.L., Busch A.K., Hansen B.F., Shafrir E. And Mosthaf-Seedorf L. Cellular mechanism of nutritionally induced insulin resistance in Psammomys obesus: overexpression of protein kinase C-epsilon in skeletal muscle precedes the onset of hyperinsulinemia and hyperglycemia. Diabetes 2001; 50: 584-592

Ivasaka J., Vuoriluoto K., Huovinen T., Izawq I., Inagaki M., Parker P.J. PKC-epsilon mediated phosphorylation of vimentin controls integrin recycling and motility. EMBO J. 2005; 24(22): 3834-45

Jackson SP, Bartek J. The DNA-damage response in human biology and disease. Nature. 2009 Oct 22;461(7267):1071-8.

Julian M, Tollon Y, Lajoie-Mazenc I, Moisand A, Mazarguil H, Puget A, Wright M. gamma-Tubulin participates in the formation of the midbody during cytokinesis in mammalian cells. J Cell Sci. 1993 May;105 (Pt 1):145-56.

Kardon JR, Vale RD. Regulators of the cytoplasmic dynein motor. Nat Rev Mol Cell Biol. 2009 Dec;10(12):854-65.

Karlsson-Rosenthal C, Millar JB. Cdc25: mechanisms of checkpoint inhibition and recovery. Trends Cell Biol. 2006 Jun;16(6):285-92.

Kaseda K, McAinsh AD, Cross RA. Dual pathway spindle assembly increases both the speed and the fidelity of mitosis. Biol Open. 2012 Jan 15;1(1):12-8.

Kastan MB, Lim DS. The many substrates and functions of ATM. Nat Rev Mol Cell Biol. 2000 Dec;1(3):179-86.

Khodjakov A, Cole RW, Oakley BR, Rieder CL. Centrosome-independent mitotic spindle formation in vertebrates. Curr Biol. 2000 Jan 27;10(2):59-67.

Khodjakov A, Rieder CL. The sudden recruitment of gamma-tubulin to the centrosome at the onset of mitosis and its dynamic exchange throughout the cell cycle, do not require microtubules. J Cell Biol. 1999 Aug 9;146(3):585-96.

Kikkawq U., Kishimoto A. And Nishizuka Y. The protein kinase C family: Heterogeneity and its implications. Annu Rev Biochem 1989; 58: 31-44

King R.W., Jackson P.K. And Kirschner M.W. Mitosis in transition. Cell 1994; 79: 563-71.

Kinouchi T., Sorimachi H., Maruyama K., Mizuno K., Ohno S., Ishiura S. And Suzuki K. Conventional protein kinase C (PKC)-alpha and novel PKC epsilon, but not -delta crease the secretion of an N-terminal fragment of Alzheimer's disease amyloid precursor protein from PKC cDNA transfected 3Y1 fibroblasts. FEBS Lett. 1995; 364: 203-206

Kiyomitsu T, Cheeseman IM. Chromosome- and spindle-pole-derived signals generate an intrinsic code for spindle position and orientation. Nat Cell Biol. 2012 Feb 12;14(3):311-7.

Klockenbusch, C., Kast, J. Optimization of formaldehyde cross-linking for protein interaction analysis of non-tagged integrin beta1. J Biomed Biotechnol. 2010, 927585 (2010).

Knight, Z.A., Shokat, K.M. Chemical genetics: where genetics and pharmacology meet. Cell 128, 425-430 (2007)

Knoblich JA. Mechanisms of asymmetric stem cell division. Cell. 2008 Feb 22;132(4):583-97.

Kschonsak M, Haering CH. Shaping mitotic chromosomes: From classical concepts to molecular mechanisms. Bioessays. 2015 Jul;37(7):755-66.

Kumagai A, Dunphy WG. Purification and molecular cloning of Plx1, a Cdc25-regulatory kinase from Xenopus egg extracts. Science. 1996; 273(5280):1377-80

Lampson MA, Cheeseman IM. Sensing centromere tension: Aurora B and the regulation of kinetochore function. Trends Cell Biol. 2011 Mar;21(3):133-40.

Lane HA, Nigg EA. Antibody microinjection reveals an essential role for human polo-like kinase 1 (Plk1) in the functional maturation of mitotic centrosomes. J Cell Biol. 1996 Dec;135(6 Pt 2):1701-13.

Larsen E.C., Digennaro J.A., Saito N., Mehtas., Loegering D.J., Mazurkiwicz J.E. And Lennartz M.R. Differen tial requirement for classic and novel PKC isoforms in respira tory burst and phagocytosis in RAW 264.7 cells. J Immunol. 2000; 165: 2809-2817

Lew DJ, Burke DJ. The spindle assembly and spindle position checkpoints. Annu Rev Genet. 2003;37:251-82.

Lüders J, Patel UK, Stearns T. GCP-WD is a gamma-tubulin targeting factor required for centrosomal and chromatin-mediated microtubule nucleation. Nat Cell Biol. 2006 Feb;8(2):137-47.

Mabuchi I, Hamaguchi Y, Fujimoto H, Morii N, Mishima M, Narumiya S. A rho-like protein is involved in the organisation of the contractile ring in dividing sand dollar eggs. Zygote. 1993 Nov;1(4):325-31.

Mardin BR, Schiebel E. Breaking the ties that bind: new advances in centrosome biology. J Cell Biol. 2012 Apr 2;197(1):11-8.

Martinez-Gimeno C., Diaz-Meco M.T., Dominguez I. And Moscat, J. Alterations in levels of different protein kinase C isotypes and their influence on behavior of squamous cell carcinoma of the oral cavity: epsilon PKC, a novel prognositc factor for relapse and survival. Head Neck, 1995; 17: 516-25

Masselli E, Carubbi C, Gobbi G, Mirandola P, Galli D, Martini S, Bonomini S, Crugnola M, Craviotto L, Aversa F, Vitale M. Protein kinase Cε inhibition restores megakaryocytic differentiation of hematopoietic progenitors from primary myelofibrosis patients. Leukemia. 2015; 29(11):2192-201.

Matsushime H., Ewen M.E., Strom D.K., Kato J.Y., Hanks S.K., Roussel M.F. And Sherr C.J. Identification and properties of an atypical catalytic subunit (p34PSK-J3/cdk4) for mammalian D type G1 cyclins. Cell 1992, 71: 323-34.

Mcgowan C.H. Cell Cycle Checkpoint. Encyclopedia of Cancer (Second Edition) Vol 1, 2002; 383-393

McGrail M, Gepner J, Silvanovich A, Ludmann S, Serr M, Hays TS. Regulation of cytoplasmic dynein function in vivo by the Drosophila Glued complex. J Cell Biol. 1995 Oct;131(2):411-25.
Mellor H. And Parker P.J. The extended protein kinase C superfamily. Biochem J. 1998; 332 (Pt 2): 281-92.

Meyerson M. And Harlow E. Identification of G1 kinase activity for cdk6, a novel cyclin D partner. Mol Cell Biol 1994; 14: 2077-2086.

Mischak H., Goodnight J.A., Kolch W., Martiny-Baron G., Schaechtle C., Kazanietz M.G., Blumberg P.M., Pierce J.H. And Mushinski J.F. Overexpression of protein kinase C delta and -epsilon in NIH 3T3 cells induces opposite effects on growth, morphology, anchorage dependence, and tumorigenicity. J Biol. Chem. 1993; 268: 6090-6096

Mitchison T, Kirschner M. Dynamic instability of microtubule growth. Nature. 1984 Nov 15-21;312(5991):237-42.

Mollinari C, Kleman JP, Jiang W, Schoehn G, Hunter T, Margolis RL. PRC1 is a microtubule binding and bundling protein essential to maintain the mitotic spindle midzone. J Cell Biol. 2002 Jun 24;157(7):1175-86.

Morin X, Bellaïche Y. Mitotic spindle orientation in asymmetric and symmetric cell divisions during animal development. Dev Cell. 2011 Jul 19;21(1):102-19.

Moriya S., Kazlauskas A., Akimoto K., Hirai S., Mizuno K., Takenawa T., Fukui Y., Watanabe Y., Ozaki S. And Ohno S. Platelet-derived growth factor activates protein kinase C epsilon through redundant and independent signaling path ways involving phospholipase C gamma or phosphatidylinositol3-kinase. Pros. Natl. Acad. Sci. USA 2006; 93: 151-155

Morrow CJ, Tighe A, Johnson VL, Scott MI, Ditchfield C, Taylor SS. Bub1 and aurora B cooperate to maintain BubR1-mediated inhibition of APC/CCdc20. J Cell Sci. 2005 Aug 15;118(Pt 16):3639-52.

Murphy SM, Stearns T. Cytoskeleton: microtubule nucleation takes shape. Curr Biol. 1996 Jun 1;6(6):642-4.

Murugappan S. et al. Differential role of protein kinase C-delta isoform in agonist-induced dense granule secretion in human platelets. The Journal of Biological Chemistry. 2004; 279: 2360-2367.

Nam HJ, Naylor RM, van Deursen JM. Centrosome dynamics as a source of chromosomal instability. Trends Cell Biol. 2015 Feb;25(2):65-73.

Nam HJ, van Deursen JM. Cyclin B2 and p53 control proper timing of centrosome separation. Nat Cell Biol. 2014 Jun;16(6):538-49.

Negrini S, Gorgoulis VG, Halazonetis TD. Genomic instability--an evolving hallmark of cancer. Nat Rev Mol Cell Biol. 2010 Mar;11(3):220-8

Newton A.C. et al. The substrates and binding partners of protein kinase. Biochem J. 2011; 427(2): 189–196

Newton P.M. And Messing R.O The substrates and binding partners of protein kinase Cε. Biochem J. 2010; 427(2): 189-96

Nezi L, Musacchio A. Sister chromatid tension and the spindle assembly checkpoint. Curr Opin Cell Biol. 2009 Dec;21(6):785-95.

Nigg E.A. And Stearns T. The centrosome cycle: Centriole biogenesis, duplication and inherent asymmetries Nat Cell Biol. 2014; 13(10): 1154–1160

Nigg E.A. Cyclin-dependent protein kinases: key regulators of the eukaryotic cell cycle. Bioessays. 1995; 17(6): 471-80.

Nishizuka Y. Protein kinase C and lipid signaling for sustained cellular responses. FASEB Journal. 1995; 9: 484-496.

Nurse, P. (1975). Genetic control of cell size at cell division in yeast. Nature 256: 547–55l.

Ochoa W.F., Corbalan-Garcia S., Eritja R., Rodriguez-Alfaro J.A., Gomez-Fernandez J.C., Fita I. And Verdaguer N. Additional binding sites for anionic phospholipids and calcium ions in the crystal structures of complexes of the C2 domain of protein kinase calpha. J Mol Biol, 2002; 20: 277-91.

Ohtsubo M., Theodoras A.M., Schumacher J., Roberts J. M. And Pagano M. Human cyclin E, a nuclear protein essential for the G1-to- S phase transition. Mol Cell Biol 1995; 15: 2612-24.

Okuda M., Horn H.F., Tarapore P., Tokuyama Y., Smulian A.G., Chan P.K., Knudsen E.S., Hofmann I. A., Snyder J. D., Bove K. E. And Fukasawa K. Nucleophosmin/B23 is a target of CDK2/cyclin E in centrosome duplication. Cell 2000; 103: 127–140

Ono Y., et al. The structure, expression, and properties of additional members of the protein kinase C family. The Journal of Biological Chemistry. 1988; 263(14): 6927-32

Pagano M., Pepperkok R., Verde F., Ansorge W. And Draetta G. Cyclin A is required at two points in the human cell cycle. EMBO J 1992; 11: 961-71.

Pan Q., Bao L.W., Kleer C.G., Sabel M.S., Griffith K.A., Teknos T.N. And Merajver S. Protein kinase C epsilon is a predictive biomarker of aggressive breast cancer and a validated target for RNA interference anticancer therapy. Cancer Res, 1995; 65: 8366-71

Pan Q., Bao L.W., Teknos T.N. And Merajyer S.D. Targeted disruption of protein kinase C epsilon reduces cell invasion and motility through inactivation of RhoA and RhoC GTPases in head and neck squamous cell carcinoma. Cancer Res 2006; 66(19): 9379-9384

Pardo O.E., Arcaro A., Salerno G., Raguz S. Downward J. And Seckl M.J. Fibroblast growth factor-2 induces translational regulation of Bcl-XL and Bcl-2 via a MEK-dependent pathway: correlation with resistance to etoposide-induced apoptosis. J Biol Chem 2002; 277(14): 12040-12046

Parker P.J. And Murray-Rust J. PKC at a glance. J Cell Sci. 2004; 117(Pt2): 131-2

Paull TT, Rogakou EP, Yamazaki V, Kirchgessner CU, Gellert M, Bonner WM. A critical role for histone H2AX in recruitment of repair factors to nuclear foci after DNA damage. Curr Biol. 2000 Jul 27-Aug 10;10(15):886-95.

Pereira G, Schiebel E. Centrosome-microtubule nucleation. J Cell Sci. 1997 Feb;110 (Pt 3):295-300.

Perletti G.P., Concari P., Brusaferri S., Marras E., Piccinini F. And Tashjian A.H. Jr. Protein kinase C-epsilon is oncogenic in colon epithelial cells by interaction with the Ras signal transduction pathway. Oncogene 1998; 16: 3345-3348

Poon R.Y.C. Cell Cycle Control. Encyclopedia of Cancer (Second Edition) Vol 1, 2002; 393-403

Prekeris R., Mayhew M.W., Cooper J.B. And Terrian D.M. Identification and localization of an actin-binding motif that is unique to the epsilon isoform of protein kinase C and participates in the regulation of synaptic function. J Cell Biol, 1996; 132: 77-90.

Queirolo V, Galli D, Masselli E, Borzì RM, Martini S, Vitale F, Gobbi G, Carubbi C, Mirandola P. PKCε is a regulator of hypertrophic differentiation of chondrocytes in osteoarthritis. Osteoarthritis Cartilage. 2016; 24(8):1451-60.

Quintyne NJ, Schroer TA. Distinct cell cycle-dependent roles for dynactin and dynein at centrosomes. J Cell Biol. 2002 Oct 28;159(2):245-54.

Quittau-Prevostel C., Delaunay N., Collazos A., Vallentin A. And Joubert D. Targeting of PKCalpha and epsilon in the pituitary: a highly regulated mechanism involving a GD(E)E motif of the V3 region. J Cell Sci, 2004; 117: 63-72

Raaijmakers JA, van Heesbeen RG, Meaders JL, Geers EF, Fernandez-Garcia B, Medema RH, Tanenbaum ME. Nuclear envelope-associated dynein drives prophase centrosome separation and enables Eg5-independent bipolar spindle formation. EMBO J. 2012 Nov 5;31(21):4179-90.

Raaijmakers, J.A., Tanenbaum, M.E., Medema, R.H. Systematic dissection of dynein regulators in mitosis. J Cell Biol. 201, 201-15 (2013)

Rieder CL, Maiato H. Stuck in division or passing through: what happens when cells cannot satisfy the spindle assembly checkpoint. Dev Cell. 2004 Nov;7(5):637-51.

Roossien, D.H., Miller, K.E., Gallo, G. Ciliobrevins as tools for studying dynein motor function. Front Cell Neurosci. 9, 252 (2015)

Rosenblatt J. Spindle assembly: asters part their separate ways. Nat Cell Biol. 2005 Mar;7(3):219-22.
Ruchaud S, Carmena M, Earnshaw WC. The chromosomal passenger complex: one for all and all for one. Cell. 2007 Oct 19;131(2):230-1.

Russell, P. and Nurse P. (1987). Negative regulation of mitosis by wee1+ a gene encoding a protein kinase homolog. Cell 49: 559–567.

Saurin A.T., Brownlow N. And Parker P.J. Protein kinase C epsilon in cell division. Cell Cycle 2009; 8(4): 549-555

Saurin A.T., Durgan J., Cameron A.J., Faisal A., Marber M.S. And Parker P.J. The regulated assembly of a PKCepsilon complex controls the completion of cytokinesis. Nat Cell Biol,2008; 10: 891-901

Saurin A.T., Pennington D., Raat N., Latchman D., Owen M. And Marber M. Targeted disruption of the protein kinase C epsilon gene abolishes the infarct size reduction that follows ischaemic preconditioning of isolated buffer-perfused mouse hearts. Cardiovasc Res. 2002; 55: 672

Schuster M, Kilaru S, Fink G, Collemare J, Roger Y, Steinberg G. Kinesin-3 and dynein cooperate in long-range retrograde endosome motility along a nonuniform microtubule array. Mol Biol Cell. 2011

Schwanhausser, B., et al. Global quantification of mammalian gene expression control. Nature. 473, 337–42 (2011)

Scully R, Xie A. Double strand break repair functions of histone H2AX. Mutat Res. 2013 Oct;750(1-2):5-14.

Sharif T.R. And Sharif M. Overexpression of protein kinase C epsilon in astroglial brain tumor derived cell lines and primary tumor samples. Int J Oncol, 1999; 15: 237-43

Shevchenko, A., Wilm, M., Vorm, O., Mann, M. Mass spectrometric sequencing of proteins from silver-stained polyacrylamide gels. Anal Chem. 68, 850–8 (1996)

Shirai Y., Kashiwagi K., Yagi K., Sakai N. And Saito N. Distinct effects of fatty acids on translocation of gamma and epsilon-subspecies of protein kinase C. J Cell Biol. 1998; 143:511-521

Silkworth WT, Cimini D. Transient defects of mitotic spindle geometry and chromosome segregation errors. Cell Div. 2012 Aug 11;7(1):19.

Silkworth WT, Nardi IK, Paul R, Mogilner A, Cimini D. Timing of centrosome separation is important for accurate chromosome segregation. Mol Biol Cell. 2012 Feb;23(3):401-11. doi: 10.1091/mbc.E11-02-0095.

Silva PM, Reis RM, Bolanos-Garcia VM, Florindo C, Tavares ÁA, Bousbaa H. Dynein-dependent transport of spindle assembly checkpoint proteins off kinetochores toward spindle poles. FEBS Lett. 2014 Aug 25;588(17):3265-73.

Skoufias, D.A., Andreassen, P.R., Lacroix, F.B., Wilson, L., Margolis, R.L. Mammalian mad2 and bub1/bubR1 recognize distinct spindle-attachment and kinetochore-tension checkpoints. Proc Natl Acad Sci USA. 98, 4492-7 (2001)

Smits V.A.J. And Medema R.H. Checking out the G2/M transition. Biochimica et Biophysica Acta 2001; 1519(2001): 1-12

Söderberg, O. et al. Direct observation of individual endogenous protein complexes in situ by proximity ligation. Nat Methods. 3, 995-1000 (2006)

Soh J.W. And Weinstein I.B. Roles of specific isoforms of protein kinase C in the transcriptional control of cyclin D1 and related genes. J Biol Chem 2003; 278(36): 34709-34716

Stearns T, Evans L, Kirschner M. Gamma-tubulin is a highly conserved component of the centrosome. Cell. 1991 May 31;65(5):825-36.

Steinberg S.F. Structural Basis of Protein Kinase C isoform Function. Physioll Rev 2008; 88(4): 1341-1378

Sudakin V, Chan GK, Yen TJ. Checkpoint inhibition of the APC/C in HeLa cells is mediated by a complex of BUBR1, BUB3, CDC20, and MAD2. J Cell Biol. 2001 Sep 3;154(5):925-36.

Suryadinata C.R., Sadowski M. And Sarcevic B. Control of Cell Cycle Progression by Phosphorylation of Cyclin-dependent kinase (CDK) substrates. Biosci. Rep. 2010; 30: 243-255

Tachado S.D., Mayhew M.W., Wescott G.G., Foreman T.L. Goodwin C.D., Mcjilton M.A. And Terrian D.M. Regulation of tumor invasion and metastasis in protein kinase C epsilon-transformed NIH3T3 fibroblasts. J Cell Biochem 2002; 85(4): 785-797

Tan S.L. And Parker P.J. Emerging and diverse role of protein kinase C in immune cell signalling. Biochem J. 2003; 376(Pt3): 545-52

Tanenbaum ME, Medema RH. Mechanisms of centrosome separation and bipolar spindle assembly. Dev Cell. 2010 Dec 14;19(6):797-806.

Tanenbaum ME, Vale RD, McKenney RJ. Cytoplasmic dynein crosslinks and slides anti-parallel microtubules using its two motor domains. Elife. 2013 Sep 3;2:e00943.

Thompson SL, Compton DA. Chromosome missegregation in human cells arises through specific types of kinetochore-microtubule attachment errors. Proc Natl Acad Sci U S A. 2011 Nov 1;108(44):17974-8.

Tojima Y., Fujimoto A., Delhase. M., Chen Y., Hatakeyama S., Nakayamak., Kaneko Y., Nimura Y., Motoyama N., Ikeda K., Karin M. And Nakanishi M. NAK is an IkappaB kinase-activating kinase. Nature 2000; 404: 778-782

Toyoshima-Morimoto F., Taniguchi E., Shinya N., Iwamatsu A. And Nishida E. Polo-like kinase 1 phosphorylates cyclin B1 and targets it to the nucleus during prophase. Nature 2001; 410: 215–220

Varga A., Czifra G., Tallai B., Nemeth T., Kovacs I., Kovacs L., Biro T. Tumor grade-dependent alterations in the protein kinase C isoform pattern in urinary bladder carcinomas. Eur Urol,2004; 46: 462-65.

Walczak CE, Cai S, Khodjakov A. Mechanisms of chromosome behaviour during mitosis. Nat Rev Mol Cell Biol. 2010 Feb;11(2):91-102.

Wang YL. The mechanism of cytokinesis: reconsideration and reconciliation. Cell Struct Funct. 2001 Dec;26(6):633-8.

Watanabe S, Ando Y, Yasuda S, Hosoya H, Watanabe N, Ishizaki T, Narumiya S. mDia2 induces the actin scaffold for the contractile ring and stabilizes its position during cytokinesis in NIH 3T3 cells. Mol Biol Cell. 2008 May;19(5):2328-38.

Waters JC, Chen RH, Murray AW, Salmon ED. Localization of Mad2 to kinetochores depends on microtubule attachment, not tension. J Cell Biol. 1998 Jun 1;141(5):1181-91.

Webb B.L.J., Hirst S.J. And Giembycz M.A. Protein Kinase C isoenzymes: a review of their structure, regulation and role in regulating airways smooth muscle tone and mitogenesis. British Journal of Pharmacology 2000; 130: 1433-1452

Werner M, Glotzer M. Control of cortical contractility during cytokinesis. Biochem Soc Trans. 2008 Jun;36(Pt 3):371-7.

Wiese C, Zheng Y. Microtubule nucleation: gamma-tubulin and beyond. J Cell Sci. 2006 Oct 15;119(Pt 20):4143-53.

Wong C, Stearns T. Centrosome number is controlled by a centrosome-intrinsic block to reduplication. Nat Cell Biol. 2003 Jun;5(6):539-44.

Wu D, Thakore CU, Wescott GG, McCubrey JA, Terrian DM. Integrin signaling links protein kinase Cepsilon to the protein kinase B/Akt survival pathway in recurrent prostate cancer cells. Oncogene. 2004; 23:8659–8672.

Wu-Zhangn Ax. et al. Protein Kinase C Pharmacology: Refining the Toolbox. Biochem J. 2013; 452(2): 195–209

Xiao Z, Chen Z, Gunasekera AH, Sowin TJ, Rosenberg SH, Fesik S, Zhang H. Chk1 mediates S and G2 arrests through Cdc25A degradation in response to DNA-damaging agents. J Biol Chem. 2003 Jun 13;278(24):21767-73.

Yagi T. Bioinformatic approaches to dynein heavy chain classification. Methods Cell Biol. 2009;92:1-9.

Yamada, M. et al. LIS1 and NDEL1 coordinate the plus-end-directed transport of cytoplasmic dynein. EMBO J 27, 2471-83. (2008)
Zacheriae W. Progression into and out of mitosis. Current Opinion in Cell Biology 1999; 11: 708–716

Zheng Y, Jung MK, Oakley BR. Gamma-tubulin is present in Drosophila melanogaster and Homo sapiens and is associated with the centrosome. Cell. 1991 May 31;65(5):817-23.

Zhong, A., Tan, F.Q., Yang, W.X. Chromokinesin: Kinesin superfamily regulating cell division through chromosome and spindle. Gene. 589, 43-8 (2016)

II. PKCε promotes human Th17-lymphocytes in vitro polarization

Introduction

1. Psoriasis

Psoriasis is a noncontagious, arytematous-squamose dermatitits characterized by uncontrolled proliferation of keratinocytes, a large increase of mitotic activity and anomalous differentiation. This disease affects both sexes and all races. It is relatively widespread, ranging between the 0 and 11.8% of population, mainly as the result of chronicity and the absence of a cure. In the USA, approximately 2% of the population is affected. High rates of psoriasis have been reported in people of the Faroe Islands, where 2.8% of the population is affected. The prevalence of psoriasis is low in certain ethnic groups, such as the Japanese, and may be totally absent in aboriginal Australians and Indians from South America. In Japan, psoriasis is more frequent in males than females, by a ratio of about two to one. From 6% to 48% of patients affected by psoriasis, resulted affected also by psoriatic arthritis, a chronic inflammatory arthropathy. Nearly two thirds of people with psoriasis have a mild form of the disease, with less than 3% of the skin surface of the body affected, while others have a more extensive involvement of the skin. Psoriasis may begin at any age, from babies to seniors, but it is uncommon under the age of 10. In the field of pediatrics, 10% of psoriasis patients manifest symptoms of the disease before 10, and 2% of patients, before the age of two. It is most likely to appear between the ages of 15 and 20, with a second peak occurring at 55-60 years (*World Health Organization, 2013*). Patients with psoriasis have often a worsened quality of life because of the appearance of their skin: depending on the severity and location of skin lesions, individuals may experience significant physical discomfort. The most validated pattern of transmission is autosomal dominant with low penetrance or with multi-factorial, polygenic inheritance.

The exact etiology of psoriasis is largely unknown. Its genetic basis has long been established through twin studies and family clustering; however they cannot fully explain the

disease pathogenesis. In addition to genetic susceptibility, environmental, as well as trauma, infection, medication, gender and age related factors were also been found to be associated. Several studies indicate that a dysregulated immune system may play a major role in the pathogenesis of psoriasis. Based on histological findings, mouse models and the therapeutic efficacy of TNF-targeted therapies, psoriasis is thought to be a T cell-mediated disease of autoimmune origin (*Chandra A et al., 2015*). The manifestations of psoriasis are not limited to the skin. Comorbidities may complicate moderate to severe psoriasis. In particular, the relative risks of ischemic heart disease, stroke, hypertension, dyslipidemia, diabetes and Crohn's disease are increased in people with psoriasis. The higher rates of hypertension and diabetes may partly explain the increased risk of heart attacks, stroke, and cardiovascular mortality in people with severe psoriasis, reported in large population-based cohort studies.

HIV infection may aggravate psoriasis; in HIV-positive patients psoriasis is more often resistant to treatment and more frequently associated with arthritis.

Currently there is no cure for psoriasis and treatment is directed at decreasing signs and symptoms and modifying the natural progression of the disease. A repertoire of topical and systemic therapies is available for the treatment of psoriasis, such as vitamin D3 analogues, corticosteroids, methotrexate, cyclosporine, systemic retinoids, phototherapy and biologics. Typically, topical agents are used for mild disease, phototherapy for moderate disease and systemic agents for severe disease.

1.2 Psoriasis Evaluation Index (PASI score)

Fredriksson and Pettersson created the *PASI* (*Psoriasis Area and Severity Index*) in 1978. It is the most widely used measure of severity of psoriasis and is a method to evaluate the clinical efficacy of a new treatment for psoriasis. The index combines the assessment of the severity of

lesions and the area affected into a single score in the range 0 (no disease) to 72 (maximal disease) (Louden BA et al.,). PASI consists of two major steps:

1) calculating the BSA (Body Surface Area) covered with lesions

2) assessment of the severity of lesions.

The body is divided into four sections (head H) (10% a person's skin); arms (A) (20%); trunk (T) (30%); legs (L) (40%) and the measurement unit used is the patient's palm. Each of these areas is scored by itself, and then the four scores are combined into the final PASI. For each section, the percentage of area of skin with psoriasis, is estimated and then transformed into a grade from 0 to 6:

grade	0	1	2	3	4	5	6
involved area	0%	<10%	10-29%	30-49%	50-69%	70-89%	90-100%

Table 1. Description of PASI score. The score depends on the percentage of the area of skin altered by the effect of the disease.

Within each area, the severity is estimated by three clinical signs: erythema (redness), induration (thickness) and desquamation (scaling). Severity parameters are measured on a scale of 0 to 4, from none to very severe. The composite PASI score can then be calculated by multiplying the sum of the individual-severity scores for each region by the weighted area-of-involvement score for that respective region (0.1 for head, 0.2 for arms, 0.3 for body and 0.4 for legs), and then summing the four resulting quantities. It is a commonly-used measure of severity in the research as well as the clinical setting. Typically, the PASI would be calculated before, during, and after a treatment period in order to determine how well psoriasis responds to the treatment. A score of more than ten is generally taken to mean that the psoriasis is "moderate-to-severe" and therefore may be suitable for the more powerful forms of treatment. The 50% reduction in the PASI score

(PASI 50) equates to a clinically meaningful improvement in psoriasis and represents a discerning primary endpoint (*Carlin CS et al., 2004*).

1.3 The role of immunity and inflammation in psoriasis

Although the exact etiology of psoriasis is largely unknown, it is now recognized as one of the most common immune-mediated disorders. Cells and molecules, both the innate and adaptive immune system, contribute substantially to pathogenesis of this disease (*Lowes M et al., 2014*). Through the factors mentioned above, T cells, antigen presenting cells (APC's), keratinocytes, Langerhans' cells, macrophages, natural killer cells, an array of Th1 type cytokines, certain growth factors like vascular endothelial growth factor (VEGF), keratinocyte growth factor (KGF), and others, have been indicated as key role players in the pathogenesis of psoriasis. It has been hypothesized that the disease onsets with the activation of T cell by an unknown antigen, which leads to the secretion of an array of cytokines by activated T cells, inflammatory cells, and keratinocytes. The characteristic lesion of psoriasis is due to the hyper-proliferation of the keratinocyte. Langerhans' cells, following the activation and maturation, migrate from skin to lymph nodes presenting the antigen to nodal naïve T cells. Here, T cells are activated by mature Langerhans' cells, differentiate into effector T cells and expand (*Das RP et al 2009*).

Activated T cells migrate from the lymph node to the skin. It has been demonstrated the enhanced expression of adhesion receptors on T cells and Langerhans cells (ICAM-1, E- and P-selectin ligand) and endothelial cells (ICAM-1 and E-selectin) in psoriatic skin. These adhesion molecules facilitate the increased influx of activated T lymphocytes and other immunocomponent cells into the skin, and their extravasation. T cells migration into the epidermis is mediated by the interaction of their α1β1 integrin (VLA-1) with VI collagen of the basal membrane. Once migrated to the skin, T cells release cytokines, responsible for epidermal

and vascular hyperproliferation and pro-inflammatory effects, resulting in the formation of primary plaque psoriasis.

In psoriasis, the main role in the inflammation process is played by lymphocyte Th1, Th2, Th17 and their cytokines (Figure 1). The activity of these cells is modulated by a particular kind of T cells recently described: the T regulatory cells (Treg). These cells are able to inhibit the immunological response and to maintain the cutaneous immunological homeostasis, thus preventing autoimmunity against self-antigens. Although less is described about a Treg involvement in psoriasis, several studies demonstrate that the function of these cells is impaired in this condition and treatments may increase the number and activity of Treg (*Mattozzi C et al., 2013*). T cells also evoke the inflammation through cytokine- and chemokine-mediated interaction with other cells of the skin and epidermis. Three pro-inflammatory cytokines, TNF-α, IL-17 and IFN-γ, seem to play the key role in the development of psoriatic lesions. TNF and IFN-γ induce the synthesis of secondary inflammatory cytokines and chemokines. TNF-α potentially contributes to the recruitment and accumulation of inflammatory cells, in both epidermis and dermis, by inducing the expression of intercellular adhesion molecule-1 (ICAM-1) on the surface of endothelial cells (ECs) and KCs. Interleukin-17, TNF, and IFN-γ synergistically stimulate keratinocytes to synthesize IL-6, IL-7, IL-8, IL-12, IL-15, IL-18, TNF-α, CCL20 (*Nedoszytko B et al., 2014*).

Experimental evidence points to the importance of the cytokine interleukin-17A (IL-17A) in the pathogenesis of psoriasis, which is produced by a subset of T helper cells called Th17 in immunoinflammatory sites in skin. Indeed, levels of IL-17A, IL-17C and IL-17F mRNA are found significantly up-regulated in lesional skin of patients with psoriasis. IL-17A up-regulates the expression of numerous inflammation-related genes in target cells, such as keratinocytes and fibroblasts, leading to an increased production of chemokines, secondary inflammatory cytokines, antimicrobial peptides and other mediators that contribute to clinical disease features. Importantly, IL-17A must be considered within the context of the local microenvironment,

because it acts synergistically or additively with other pro-inflammatory cytokines, including TNF. It has been recently discovered that interleukin-22 (IL-22) is released by Th17 cells and is involved in the pathogenesis and development of psoriasis. IL-22 induces keratinocyte proliferation and epidermal hyperplasia, it inhibits keratinocyte terminal differentiation and it promotes the production of antimicrobial proteins. IL-22 serum levels are correlated with the severity of psoriasis, and IL-22 mRNA is positively expressed in the psoriatic skin lesions, but negatively expressed in the normal controls (*Fujita H, 2013; Hao JQ, 2014*).

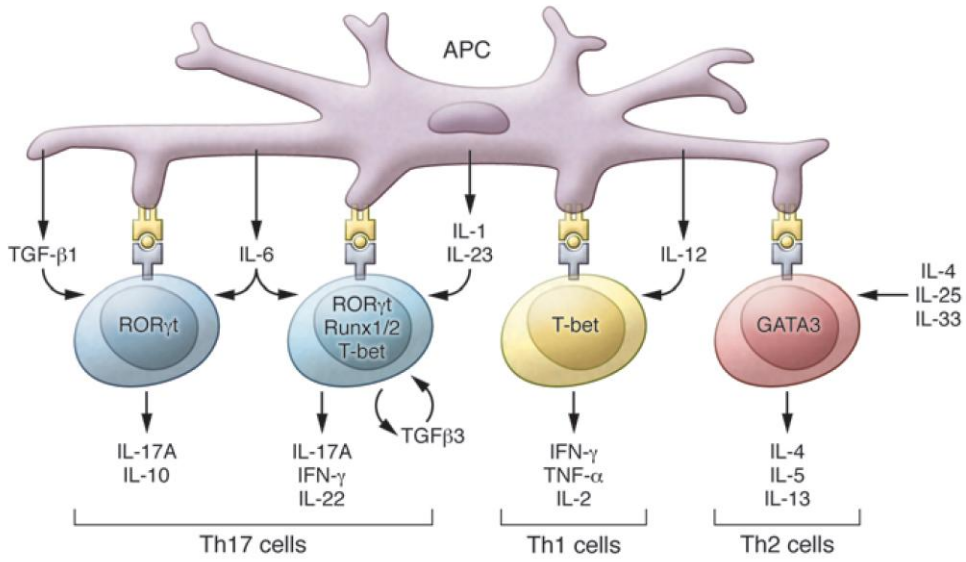

Figure 1. Effector T cell subsets. The subsets of effector Th cells are shown, along with the cytokines that drive their differentiation, lineage-defining transcription factors, and the cytokines they produce. Within the Th17 subset, two distinct subtypes of cells have been described with differing abilities to induce autoimmunity: a pathogenic subtype that produces both IL-17 and IFN-γ and a nonpathogenic subtype that produces IL-17 and IL-10. (*Burkett PR et al, 2015*).

2. Th17/Treg balance in immune-mediated diseases

Regulatory T-cells (Tregs) and T-helper 17 lymphocytes (Th17) cells are subsets of $CD4^+$ T cell, which have emerged as the major players in autoimmunity (Figure 2). Th17 and Treg cells have opposite roles in the development of autoimmune and inflammatory diseases. Th17 cells promote autoimmunity, while Treg cells serve to control it and therefore play a very important role in autoimmune pathogenesis by maintaining self-tolerance and by controlling

expansion and activation of autoreactive $CD4^+$ T effector cells. For this reason, the control of Th17/Treg balance is critical in the development of autoimmune diseases. Furthermore, developmental pathways of Th17 and Treg cells are reciprocally regulated: TGF-β is a common critical factor for Th17 and Treg cells. It is unable to initiate the Th17 differentiation in vitro unless the contribution of pro-inflammatory cytokines, as IL-6 or IL-21. In absence of significant inflammation, TGF-β promotes Treg differentiation that maintains immune tolerance.

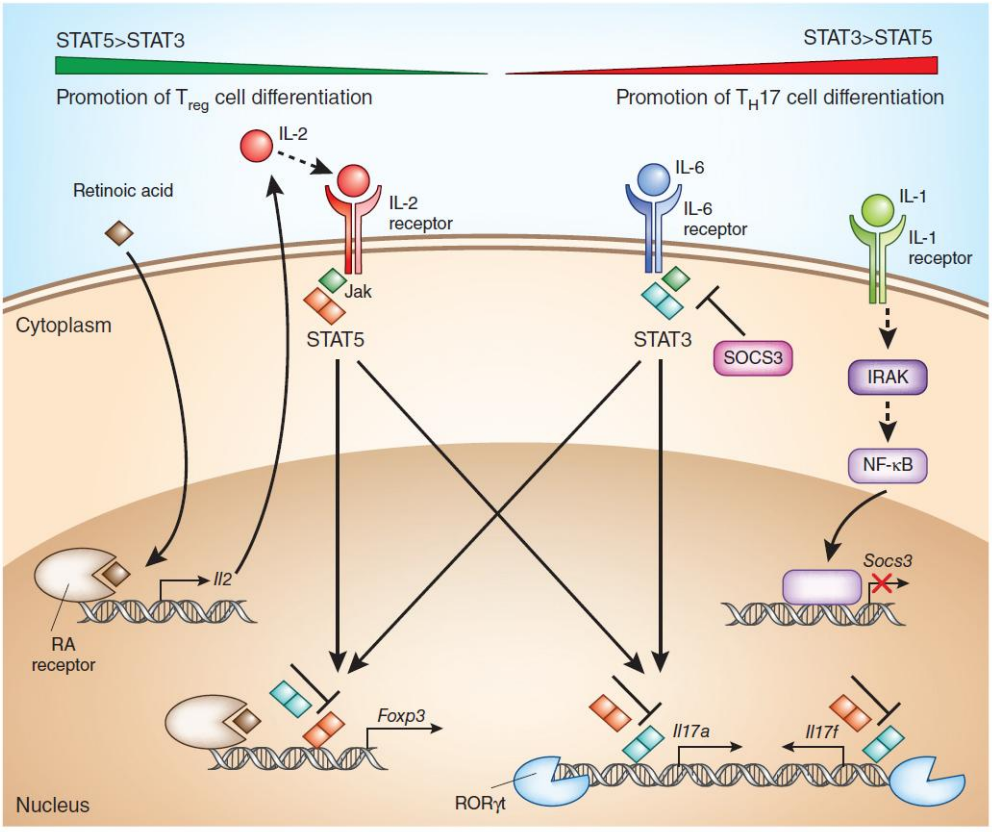

Figure 2. Signaling pathways and transcription factors that regulate the differentiation of TH17 cells and Treg cells. In CD4+ T cells, expression of RORγt leads to differentiation into TH17 cells, whereas expression of *Foxp3* induces differentiation into Treg cells. STAT5, activated by IL-2, leads to expression of *Foxp3* and inhibition of IL-17. Conversely, activation of STAT3 by IL-6 leads to expression of IL-17 in conjunction with RORγt and inhibition of Foxp3 expression. STAT5 and STAT3 antagonize each other by reciprocally binding to similar sites on the *Foxp3* and *Il17a–Il17f* loci. This balance is modified by RA, which induces IL-2 expression and thus greater phosphorylation of STAT5, and by IL-1, which, through NF-κB, inhibits *Socs3* expression and thus enhances the activation of STAT3. (*Villarino AV and Laurence A, 2015*).

Th17 cells with specificity for self-antigens are highly pathogenic and lead to the development of autoimmune and inflammatory diseases, such as rheumatoid arthritis, systemic

lupus erythematosus, multiple sclerosis, psoriasis, inflammatory bowel disease and many others. On the other hand, a reduction in Treg cell numbers and/or loss of Treg function has been observed in many animal models and human autoimmune diseases. It is thought that if Th17/Treg balance is deviated in favor of Th17 cells, the severity of disease could be significantly enhanced. Such contribution justifies developing new therapeutic means to keep an adequate balance between pathogenic Th17 cells and protective Treg cells, for preventing the development and extension of autoimmune and inflammatory diseases (*Noack M and Miosse P, 2014*).

There is currently no clear evidence that a global deficiency in the number of Treg cells is the source of failed regulation in the more common forms of autoimmunity. Instead, the presence of increased numbers of Treg cells in the affected tissues of patients with rheumatoid arthritis, IBD (inflammatory bowel disease) and psoriasis, suggests that the reason for failed regulation in the inflamed tissue may be insufficient or defective Treg cell function due to either cell-intrinsic or cell-extrinsic factors. This hypothesis is supported by the predominance of studies that find an impairment in the suppressive capacity of Treg cells from individuals with autoimmune disease.

Several studies conducted on peripheral blood and the inflamed skin of psoriasis patients, demonstrated an increase of the number of Treg cells (defined by expression of FoxP3) in the peripheral blood, and an increase of the number of $CD4^{+}CD25^{+}FoxP3^{+}$ Treg cells in lesional skin biopsies compared to control or uninvolved skin biopsies (*Buckner JH, 2010*). It also showed that the functional capacity of Treg cells in both the peripheral blood and lesional skin of patients was impaired compared to their ability to suppress both autologous and control effector T cells. In addition, the effector T cells of patients had an enhanced proliferative capacity compared with control cells. The impaired Treg cell-mediated suppression in psoriasis was thought to be due to increased production of IL-6 at the site of inflammation, and potentially due to an increased capacity to respond to IL-6 owing to upregulated receptor expression. Whether autoimmune diseases are characterized by a reduction of the number of Treg, rather than a

dysfunction, is still unclear. Sugiyama et al., have shown a deficiency and a dysfunction of Tregs in the psoriatic plaques: the number of Tregs in peripheral blood of psoriasis patients was normal, but they were dysfunctional (*Sugiyama et al., 2005*). Treg can also show significant plasticity during development and differentiation in the periphery, in response to extrinsic cues. Furthermore, Bovenschen et al. demonstrate that Tregs of patients with severe psoriasis, have an enhanced propensity to differentiate into IL-17A-producing cells on ex vivo stimulation, compared with healthy controls (*Bovenschen HJ et al., 2011*). This enhanced Treg differentiation was linked to unexpectedly high RORγt levels and enhanced loss of FoxP3. IL-23 was identified as the primarily cytokine responsible for this conversion.

3. Th17 and Treg signalling pathways

Th17 cells are characterized by the expression of intracellular RAR-related orphan receptor γt (RORγt) and signal transducer and activator of transcription 3 (Stat3), whereas Treg are characterized by the expression of Foxp3 (Forkhead box P3) and signal transducer and activator of transcription 5 (Stat5) (*Wei L et al., 2008*). Stat3 and Stat5 are members of the Stat protein family. In response to cytokines and growth factors, Stat family members are phosphorylated by the receptor associated kinases, and then form homo- or heterodimers that translocate to the cell nucleus where they act as transcription activators. Stat3 phosphorylation at the Tyrosine 705 site is essential for Stat3 dimerization and nuclear translocation (*Decker T and Kovarik P, 2000*). Stat3 also has a conserved serine 727 residue and its phosphorylation, combined with the Tyrosine 705, is necessary for full activation of Stat3 (*Li and Shaw, 2004*).

Stat3 mediates the expression of a variety of genes in response to cell stimuli, and thus plays a key role in many cellular processes, including control of inflammation and immunity (*Hilmer EJ et al., 2016; Yu H et al., 2009*). Stat3 has recently emerged as an important regulator of the differentiation of Th17 cells, as it upregulates the expression of two Th17-specific orphan

nuclear receptors, RORγ and RORα (Figure 3). IL-21 is a product of Th17 cells and its release is induced in a Stat3-dependent manner. IL-21 also activates Stat3 in Th17 cells via autocrine loop-dependent mechanism, inducing IL-17 production and expression of the transcription factor Rorγt (key transcription factor associated with the Th17 lineage). It is shown that generation of Th17 cells in the conventional manner, is attenuated by blocking IL-21, and its ability to induce Th17 differentiation is abrogated in the absence of Stat3. It is proved that overexpression of Rorγt induces Th17 differentiation, whereas Rorγt-deficient mice lack Th17 cell differentiation. Rorα, another ROR family member, is also involved in the generation of Th17 cells in conjunction with RORγt. All this data argues that IL-21 serves to promote/sustain Th17 lineage commitment, and that Stat3 and Rorγt play a critical role in Th17 differentiation (*Tanaka S et al., 2014; Wei L et al., 2007*).

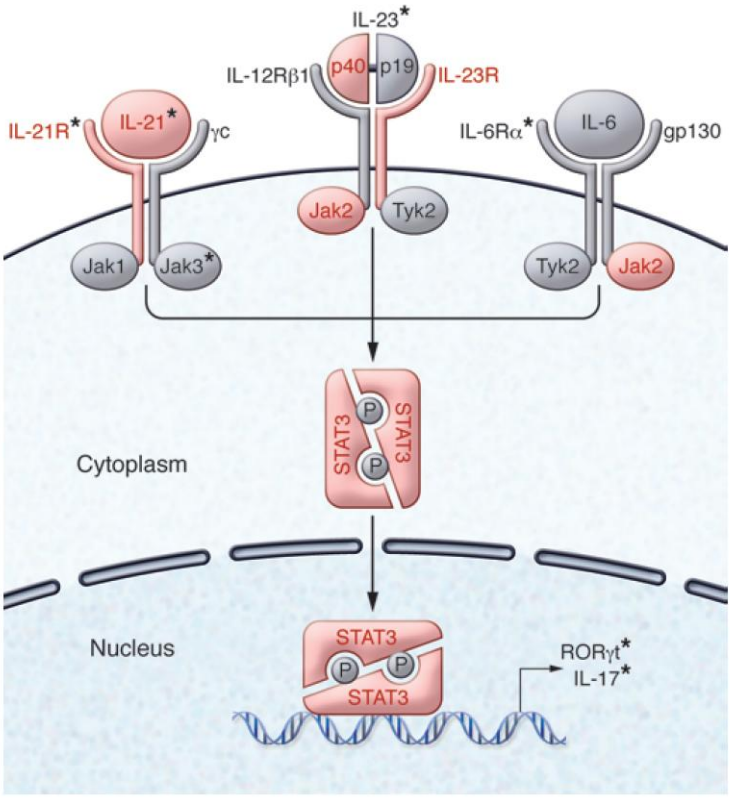

Figure 3. STAT3-dependent cytokines in autoimmunity. Cytokines that activate STAT3, including IL-6, IL-21, and IL-23, play a critical role in promoting Th17 differentiation and have been implicated in human autoimmune disease. The signaling pathways of IL-23, IL-21, and IL-6 are shown. Genes marked in red have SNPs that have been implicated in human autoimmune diseases. Genes marked with an asterisk have targeted therapeutics either approved or in active clinical development for treatment of autoimmune disease (*Burkett PR et al., 2015*).

In diseases characterized by maladaptive immune responses, such as acute coronary syndrome (ACS), lupus and rheumatoid arthritis, the signal transducer and activator of transcription (Stat) activity plays an important role in the differentiation and imbalance of Th17 and Treg cells. In ACS patients, the basal Stat3 phosphorylation level is significantly increased, while the Stat5 phosphorylation level is reduced, compared to healthy controls. This was confirmed by a high number of Th17 and IL-17-producing Treg cells, and by a low number of Treg cells. The pharmaceutical inhibitor TG101348 or the knockdown of Stat3 induce overexpression of Stat5 and, consequently, promote Foxp3 expression and Treg function but reduce Th17 differentiation (*Zheng Y et al., 2015)*. Several studies demonstrated that the modulation of Stat3/Stat5 activity rectifies the imbalance of Th17/Treg cells in patients affected by chronic inflammation or by diseases characterized by maladaptive immune responses (*Zheng Y et al., 2015*; *Ju JH et al., 2012*), suggesting the modulation of Stat3 and Stat5 signaling pathway as novel target molecules for the control of inflammation and autoimmune diseases.

STAT5 proteins regulate multiple genes primarily involved in T cell survival, proliferation, differentiation and homeostasis, either by transcriptional activation or repression through recruitment of negative regulatory cofactors (*Rani A et al., 2016*). Studies in mice demonstrated that Stat5 is essential for normal lymphoid development and functions as it is a critical signal mediator for $CD8^+$ T cell homeostasis (*Kanai T et al., 2014*). Stat5 also is frequently activated many solid cancers as well as in the majority of hematologic malignancies and represents an essential signalling node downstream of the BCR-ABL oncogene. The requirement of Stat5 in BCR-$ABL1^+$ leukemias for transformation and disease maintenance has been well described (*Berger A et al., 2014; Shaller-Shonitz M et al., 2014*). It was reported that BCR-ABL in CML (chronic myeloid leukemia) cells interacts with the IL-3/GM-CSF receptor, which leads to the downstream activation of JAK2 (Stat5 is a direct substrate of JAK2), and that blockage of JAK2-

mediated extrinsic survival signals using JAK2 inhibitors restores sensitivity of CML cells to therapeutic treatment (*Lin H et al., 2014*) .

Stat5 is known to be an important regulator of Treg differentiation, as it is required to bind the Foxp3 promoter and then to induce the full induction of Foxp3 expression (*Elias KM et al., 2008*). It is showed that the defective Foxp3 or Stat5 promotes autoimmunity in both mice and humans. The Jak/Stat5-signalling pathway activated by IL-2, is utilized to maintain Foxp3 expression and the blockage of this pathway completely inhibits the activation of Stat5 and significantly reduces Foxp3 expression in Treg cells (*Josefowicz SZ et al., 2012*).

Generally, diseases characterized by an immune imbalance in Th17 and Treg cells, are characterized by an imbalance in RORγt and Foxp3 expression. Patients with atopic dermatitis showed higher levels of RORγt, IL-17 and also IL-23, both in peripheral circulation and in the skin lesions, as well as reduced levels of Foxp3 and TGF-β mRNA (*Ma L et al., 2013*). The relatively lower level of TGF-β fails to effectively promote Treg cells development and the reduced sensitivity to TGF-β makes it easy for Th17 cells to escape from the immune inhibition of Treg cells. Furthermore, the elevated expression of IL-23 antagonizing the suppressive effect of Foxp3 on RORγt, may lead to the decrease in Treg cells and the increase in Th17 cells, leading to an imbalance of Th17/Treg or Rorγt/Foxp3.

1.5 PKC and autoimmune diseases

Despite several members of the protein kinase C family, including PKCα-, δ-, ε-, η-, θ- and ζ, are expressed at various level in T cells, the θ- isoform is the most studied in T cell response.

PKCθ is a key modulator of T cell receptor (TCR) signaling and is a key regulator of T cell activation and survival (*Altman A et al., 2002*). Beside its critical role in the immune synapse formation (IS), PKCθ is involved in Treg development as it inhibits the differentiation of inducible Tregs (iTregs) from CD4+ T-cells in presence of TGF-1β through the Akt/Foxo1-3A

pathway (*Ma J et al., 2012*). The downregulation or the inhibition of PKCθ reversed the inhibition of Treg differentiation, suggesting its possible involvement in tuning the balance between Treg and Th17 cells characteristic of autoimmune diseases.

Among recent inhibitors of PKCθ, AEB071 (**s**otrastaurin), seems to have achieved an advanced stage of development. It has shown evidence of efficacy in phase II clinical trials in both psoriasis as well as renal transplantation (*Friman et al., 2011*). AEB071 has a strong and specific activity on PKCθ, but also on PKCα, PKCβ, and lesser activity on PKCδ, PKCε, and PKCη, suggesting that AEB071 would inhibit not only T cells, but also a variety of other cells involved in the pathogenesis of autoimmune diseases. AEB071 prevents TCR/CD28-induced T-cell activation and pro-inflammatory cytokine production, but preserves the Treg phenotype. Furthermore, it prevents IL-17A and IFN-γ production by T cells from skin of psoriatic patients (*He X. et al., 2014*). Adverse effects, particularly gastrointestinal disorders, were reported with higher incidence both in psoriatic patients as well as in renal transplantation recipients in phase II clinical trial. Hence, it has been argued whether lower selectivity toward PKC family members would represent an advantage or a disadvantage.

Several studies demonstrated that PKC family members may contribute to the pathogenesis of psoriasis. It has been shown that PKC play a key role in the regulation of proliferation and differentiation of epidermal cells, can induce cutaneous inflammation and that its signalling pathway is altered in psoriatic keratinocytes. It is reported that psoriatic lesions contain elevated levels of 1,2-diacylglycerol, the physiologic activator of protein kinase C, and a PKCζ increase (and an PKCβ-II decrease), compared to normal skin (*Fisher GJ et al., 1993*).

In vivo experiments have demonstrated that also PKCε plays a key role in inflammation, immunity and immune-mediated disorders. In fact, using both knockout mice and PKC peptide modulators, Hucho et al. demonstrated that PKCε inhibition profoundly suppressed the acute and chronic inflammatory pain responses. Infiltration of macrophages and T cells into cardiac grafts,

as well as parenchymal fibrosis, was decreased in animals treated with PKCε inhibitors. (*Hucho TB et al., 2005*). Although among the PKC family members, the θ- and α- isoforms have been well studied in T-cell activation in autoimmunity disorders, Mirandola et al. have demonstrated that PKCε sustains CD4+ T cells from patients with Hashimoto Thyroiditis, an autoimmune pathology characterized by an increase number of Th17 cells in peripheral blood (*Mirandola P et al., 2011*). The specific inhibition of PKCε by siRNA, resulted in a decrease of the proliferating fraction of the cell culture, without affecting cell viability. In contrast, the upregulation of PKCε expression promoted cell proliferation. In absence of PKCε, $CD4^+$ T cells failed to upregulate NF-kB1 and NF-kB2 (which deregulation has been associated with a number of disorders including arthritis, asthma, and inflammatory bowel disease) transcription upon CD3 and CD28 stimulation. As IL-2R chain transcription is under the control of NF-kB, the authors suggested that PKCε upregulation is a critical event for IL-2R chain expression in activated $CD4^+$ T cells.

T cell proliferation is inhibited by several molecule classes such as interleukin, nucleoside, cytokine, with protective function from autoimmune disorders. TGF-1β is a potent regulatory cytokine with pivotal function in the immune system to maintain tolerance via the regulation of lymphocyte proliferation, differentiation, and survival (Sheng J et al., 2015). TGF-1β inhibits the development of immunopathology to self or nonharmful antigens without compromising immune responses to pathogens. Furthermore, Mirandola et al. have demonstrated that the TGF-1β antiproliferative signalling, undetectable when $CD4^+$ T cells are stimulated with CD3 and CD28, is enhanced by the downregulation of PKCε expression levels in CD3/CD28 and in PHA-stimulated cells. To formally prove that PKCε interferes with TGF-1β signalling, PKCε was upregulated in $CD4^+$ T cells stimulated with CD3 alone, inducing a resistance to TGF-1β. In contrast, PKCε silencing in $CD4^+$ T cells potentiated the inhibitory effects of TGF-1β. PKCε is therefore implicated in the $CD4^+$ T cells to both CD3-mediated proliferative stimuli and TGF-1β antiproliferative signals.

In the same study, the authors demonstrated that PKCε expression in $CD4^+$ T cells from HT patients is significantly increased compared to healthy donors, accounting for their enhanced survival, proliferation, and decreased sensitivity to TGF-1β, and that the downregulation of PKCε expression restored their sensitivity to TGF-1β on anti-CD3 stimulation.

Material and methods

Subjects - Patients

Eight patients with Psoriasis (three female and five male) and five healthy donors (three female and two male) were enrolled at the Operative Unit of Dermatology, Department of Surgical Science, University of Parma, after informed consent.

Patients included had a mean age of 47.7 ± 8,7 (41-74) and they were diagnosed with psoriasis vulgaris by clinical features and/or histopathology, with an average PASI score 5.78 ± 1.34 (range 4.4-7.7). Patients were excluded if they had been treated with systemic immune-therapies during the study, and/or within anti-inflammatory drugs the preceding week, and/or within antibiotics the preceding 2 weeks, and/or had other autoimmune disorders, hematologic disease or diabetes, had contraindication for phototherapy, and/or were pregnant or breastfeeding. Patients included had a mean disease duration of 22.1 ± 10.8 (range 7-38) years. Five healthy control donors (HC) with a mean age of 41.8 13.6 (range 27-62) years, without previously diagnosed autoimmune diseases, viral or bacterial infection, or metabolic syndrome were used as control subjects. Blood samples were collected before and after 12-18 narrow-band UVB (NB-UVB) phototherapy treatments. PASI score of 5 patients was assessed before and after phototherapy.

The University of Parma institutional review board (Parma, Italy) approved all the study protocols. All of the patients and controls included in the study gave their written informed consent as laid down in the Declaration of Helsinki.

CD4+ Isolation

Naïve CD4+ T helper cells were isolated from human peripheral blood mononuclear cells (PBMCs) by immunomagnetic negative selection, using the CD4+ T Cell Isolation Kit II (Milteny Biotech, Gladbach, Germany), according to the manufacturer's instructions. Briefly, PBMCs were separated from peripheral blood and buffy coats by Ficoll gradient, then magnetically labeled with a cocktail of biotin-conjugated antibodies against CD8, CD14, CD15, CD16, CD19, CD36, CD56, CD123, TCRγ/δ and CD235a, followed by anti-biotin antibody-coupled magnetic cell sorter (MACS) microbeads. The magnetically labeled cells were then immobilized on a depletion column in the magnetic field of autoMACS apparatus (Milteny Biotech). Purity of CD4+ T cells was assessed by anti-CD4–FITC and anti-CD8–PE staining using flow cytometry. Only samples with a purity exceeding 97% were used.

Cell culture and in vitro Th17 differentiation

Purified CD4+ T helper cells (1-2x106/mL) were seeded on wells pre-coated with anti-CD3 4 µg/ml (BD Pharmingen) and anti-CD28 2,5 µg/ml (BD Pharmingen) with IL-6 (25 ng/ml, Miltenyi Biotec), IL-21 (25 ng/ml, Miltenyi Biotec), IL-23 (20 ng/ml, PeproTech) and IL-1β (10 ng/ml, Miltenyi Biotec) in 10% FBS-enriched RPMI 1640 medium supplemented with penicillin (100 UI/ml)/streptomycin (100 UI/ml) and 1% L-Glutamine for Th17 differentiation for six days. Cells were incubated at 37°C and 5% of CO2. Cytokines were re-added every 2 days to maintain the Th17 polarizing conditions. Aliquots of cultured cells were collected on days 0, 3, 6 of differentiation in order to verify mRNA and proteins levels. At the same point times, 3x105 cells/experimental points were used to assess the Th17 phenotype by flow cytometry.

In some experiments, purified CD4+ T helper cells were cultured in pre-coated plates with anti-CD3 and anti-CD28, as previously described, in 10% FBS-enriched RPMI 1640 medium with

soluble anti-CD28 (1 µg/ml) for 12h in order to maintain T cell activation prior to PKCε modulation experiments and then stimulated with the indicated cytokines.

In order to exclude effects on other PKC isoforms involved in Th17 differentiation and to test shRNA-based gene silencing selectivity for the ε isoform, we used HeLa cell line as a Th17-polarization insensitive cell model. HeLa cells were cultured in 10% FBS-enriched RPMI 1640 medium supplemented with penicillin (100 UI/ml), streptomycin (100 UI/ml) and 1% L-Glutamine. Cells were incubated at 37°C and 10% of CO2.

Immunoblotting

For western blot analysis cells were collected and resuspended in a cells lysis buffer (50 mM Tris-HCl, pH 7.4; 1% Nonidet P-40; 0.25% sodium deoxycholate; 150 mM NaCl; 1 mM EDTA; 1 mM PMSF; 1 mM Na3VO4 ; 1 mM NaF) supplemented with protease inhibitors and protein concentration was determined by bicinchoninic acid protein assay kit (Pierce, Rockford, IL). Twenty-five µg of proteins from each sample were then run on SDS-acrylamide gels, blotted onto nitrocellulose filters and incubated with specific primary antibodies. For the endogenous protein expression analysis, the following antibodies were used: rabbit anti-STAT3 antibody (Cell Signaling, 1:1000 dilution), rabbit anti-pSTAT3 (Tyr705) (Cell Signalling, 1:1000 dilution), rabbit anti-pSTAT3 (Ser727) (Santa Cruz Biotech, 1:1000 dilution), rabbit anti-STAT5 (Cell Signaling, 1:1000 dilution), rabbit anti-PKCε (Millipore, 1:1000 dilution), rabbit anti-PKCθ (Cell Signaling) and mouse anti-PKCδ (BD Transduction Laboratories). Mouse anti-GAPDH (clone 605, Millipore; 1:5000 dilution) was used as housekeeping protein. Immunoblots were incubated with anti-rabbit (Thermo Scientific, 1:5000 dilution) or anti-mouse (Sigma Aldrich, 1:2000 dilution) peroxidase-conjugated secondary Abs. Proteins were revealed by ECL SuperSignal West Pico

Chemiluminescent Substate Detection System (Thermo Scientific) and densitometric analyses were performed using the ImageJ software system.

To obtain absolute quantification of PKCε protein expression levels, a series of dilution of known concentration (5 ng, 2.5 ng, and 1.25 ng) of purified human recombinant PKCε (GenWay Biotech, San Diego, CA) was performed. Hence, PKCε expression levels were determined based on the standard curve.

Immunoprecipitation

On day2 of in vitro Th17 differentiation an immunoprecipitation assay was performed in order to assess PKCε-STAT3 interaction. In brief, a total of 5 x 106 CD4+ T cells per assay were lysed in RIPA buffer, precleared and incubated with anti-PKCε antibody (Abcam, 5 µg per 1 mL of cell lysate) or anti-STAT3 antibody (Cell Signaling, 5 µg per 1 mL of cell lysate) overnight at 4°C. Rabbit anti-human IgG (Sigma Aldrich, 1 µg per 1 mL of cell lysate) was used as negative control. Samples were incubated with Protein A/G PLUS-Agarose beads (Santa Cruz Biotechnology) for 1h at 4°C, washed four times in lysis buffer and resolved by SDS-PAGE.

Flow cytometry

Flow cytometry analysis was performed to assess the purity of CD4+ T cells obtained from PBMC, by labeling cells with anti-CD4 FITC and anti-CD8 PE mABs (Beckman Coulter). To value the expression of cell surface markers of Th17, 3 x 10^5 cells for experimental point were labeled with anti-CD25 PE-Cy7 (eBioscience), anti-CD39 FITC (eBioscience), anti-CD161 PE-Cy5 (Beckton Dickinson). Analysis was performed with a Cytomics FC500 flow cytometer (Beckman Coulter).

Real-time PCR

Total RNA was isolated using RNeasy Mini Kit (Qiagen) according to the manufacturer's instructions. After RNA quantification, 1 µg of total RNA was reverse transcribed with ImProm-II

Reverse Transcription System (Promega). Real-Time qPCR was preformed according to the manufacturer's protocol, using the StepOne Real-Time PCR System (Applied Biosystems) with GoTaq® qPCR Master Mix (Promega) using Syber Green method.

PKCε cDNA was amplified by the sense 5'- CAC CAT CCA GTT TGA GGA GC-3' and antisense 5'- CGA CCC TGA GAG ATC GAT GA-3' primers (Sigma Aldrich). 18S rRNA was used as housekeeping/internal control and was amplified by the sense 5'- ACC GGG TTG GTT TTG ATC TG-3' and antisense 5'- ATC CTG CCA GTA GCA TAT GC-3' primers (Proligo). The mRNA expression levels of specific markers of polarization to Th17 and Treg linages were also analysed: for Th17 cells, RoRγT was amplified by 5'- ACA AGT CGT CTG GGA TCC AC -3' and 5'- AGT TCT GCT GAC GGG TGC A -3' primers (Sigma Aldrich), IL-17 by 5'- TCC ACC TCA CCT TGG AAT CT -3' and 5'- ATG TGG TAG TCC ACG TTC CC-3' primers (Sigma Aldrich), whereas for Treg cells, FoxP3 was amplified by the sense 5'-CAG CGT GGT TTT TCT TCT CG-3' and antisense 5'-GGC ATC GGG TCC TTG TC-3' primers (Sigma Aldrich). cDNA from each sample was run in triplicate for each gene of interest. For comparative quantification, mRNA expression level in each samples was normalized with the relative 18S rRNA mRNA expression and fold increase was calculated by $2^{-(\Delta\Delta Ct)}$.

PKCε up-regulation

PKCε was overexpressed in CD4+ T cells on day 1 of in vitro differentiation. The green fluorescent protein (GFP)-PKCε expression and the control plasmid were kindly provided by Prof. Peter Parker (The Francis Crick Institute, London, UK). The GFP-tagged murine PKCε and the GFP–K522M mutated murine PKCε constructs were cloned in the pCDNA3.1 hygro vector fused with GFP. To maximize transfection efficiency GFP-PKCε plasmids (2μg/transfection) were delivered using the Amaxa Human T Cell Nucleofector Kit (Lonza) according to the manufacturer's protocols (Mirandola P. et al, 2011). Th17 polarizing cytokines were re-added 6h post transfection. Protein and mRNA analyses were performed 48h after transfection, at day 3 of in vitro differentiation.

PKCε down-regulation and inhibition

For shRNA-based gene silencing we used a pLKO.1 lentiviral vector encoding short hairpin RNAs (shRNA) against human PKCε (Open-BIosystem, Thermo Scientific, Waltham, MA) and, as control, a MISSION pLKO.1-puro Non-Target shRNA Control Plasmid, containing an shRNA insert that targets no known genes from any species (Sigma-Aldrich, St. Louis, MO, USA). Cells were infected at Day 1 of in vitro Th17 differentiation, selected according to puromycin-resistance cells and cultured for up to 3 days. Protein and mRNA analyses were performed 48h after the infection.

A short-time PKCε inhibition was performed using 1mM BIM-1 (Cayman Chemical). The compound was added to the culture media on day1 of differentiation. Cells were collected for immunoblotting after 5', 15' or 30' of treatment.

Statistical analysis

Data are presented as mean ± SD and P values were analyzed using Student t-test or one-way ANOVA followed by Dunnett's test for multiple comparisons, when applicable. The relation between PKCε expression levels and PASI score was tested using the linear regression and correlation analysis. ns= no significant; statistically significant values are expressed as *, $p < 0.05$; **, $p < 0.01$; ***, $p < 0.001$.

Results

1. PKCε is overexpressed in CD4+ T cells from patients with psoriasis.

We previously demonstrated that PKCε is overexpressed in CD4+ T cells from patients with Hashimoto Thyroiditis (*Mirandola et al., 2011*). To study PKCε expression in psoriasis, peripheral blood-derived resting CD4+ T cells were isolated from 7 patients before and after NB-UVB treatment and from 7 healthy donors (HD), and the lysates were subsequently analysed using western blot. PKCε concentration (ng/μg of total lysate) was determined and reported with reference to standards of human recombinant PKCε (Figure 1,c). According with our previous findings, CD4+ T cells from psoriasis subjects showed significantly higher levels of PKCε expression (0.71 ± 0.38 ng/μg of total lysate) compared with HD (0.27 ± 0.07 ng/μg of total lysate) and decreased levels after NB-UVB treatment (0.32 ± 0.2 ng/μg of total lysate; **P<0.01 before therapy *vs* HD and after therapy) (Figure 1,a-b). All of the patients completed the NB-UVB course and all of them showed a reduction of the PASI score (1.34 ± 0.64 after therapy *vs* 5.78 ± 1.34 before therapy; ***P<0.001). Interestingly, PKCε expression was positively related with the PASI score both before and after NB-UVB treatment (Figure 1d). These data suggest that PKCε may be implicated in the molecular pathophysiology or the inflammatory response to psoriasis.

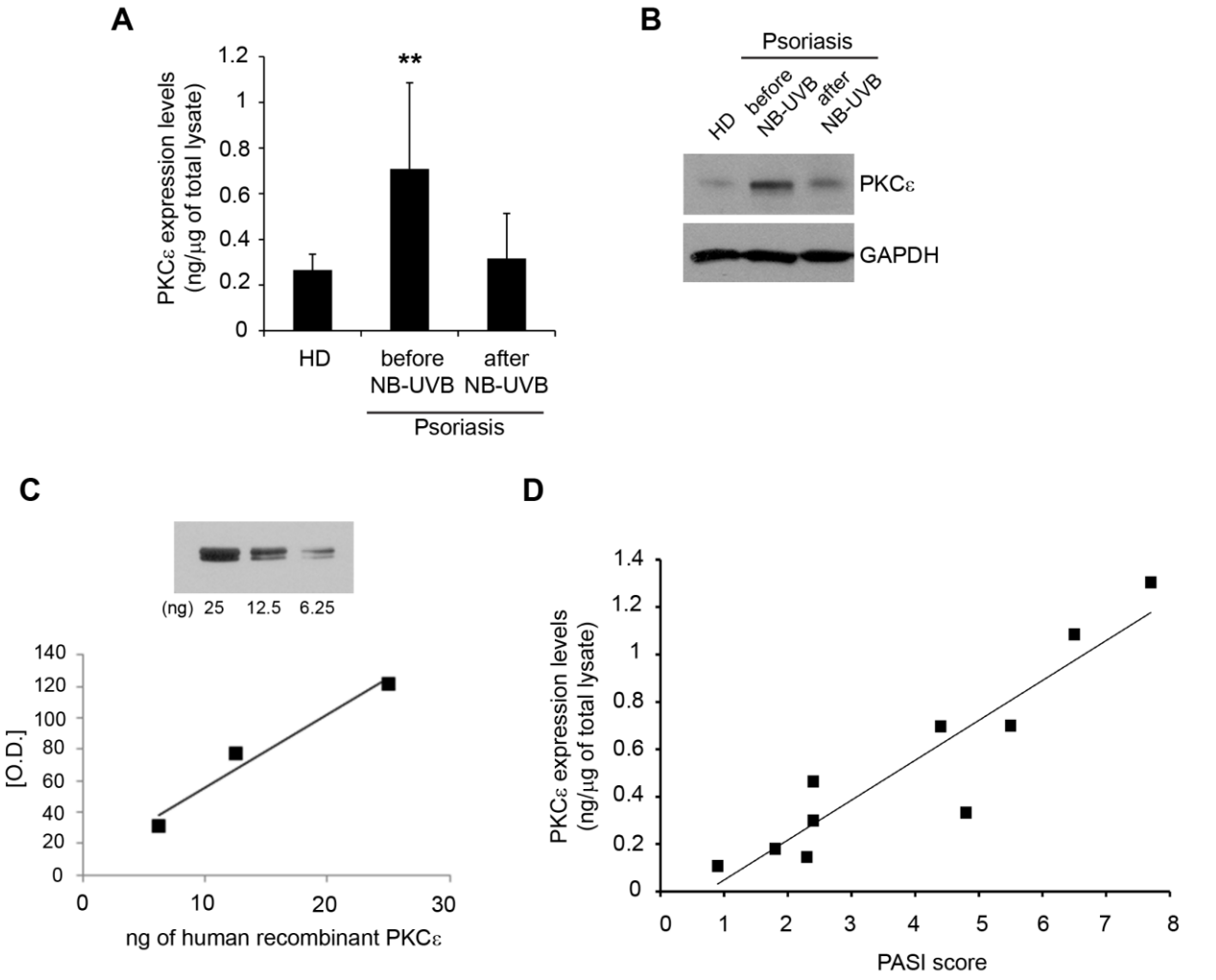

Figura 1 PKCε is overexpressed in patients with psoriasis. (**A**) Quantification of PKCε referred as ng/μg of total lysate detected using western blot in healthy donors (HD), patients with psoriasis before NB-UVB therapy and after NB-UVB therapy. ** P<0.01 (one way ANOVA and Tukey). (**B**) Representation of PKCε expression, detected using western blot, in CD4+ cells from HD, patients with psoriasis before NB-UVB therapy and after NB-UVB therapy. (**C**) Standards of human recombinant PKCε obtained by sequential dilutions 25ng-12.5ng-6.25ng. (**D**) Correlation between PASI score before and after therapy with PKCε expression (ng/μg of total lysate) before and after NB-UVB therapy (R^2=0.85).

2. Th17 and Treg cells contribution in psoriasis.

A number of studies demonstrated that T-cells subset Treg and Th17 cells play a crucial role in the pathogenesis of psoriasis (Deng Y et al., 2016). We used flow cytometry to study the balance between Th17 and Treg cells CD4+ T cells from patients with psoriasis. The ratio of the percentage of circulating CD25+CD161+CD39- (Th17), with the circulating CD25+CD39+CD161- (Treg) cells is reduced after NB-UVB (16.97 ± 6.97% before therapy *vs*

9.76 ± 4.22 after therapy; *P<0.05), indicating that the imbalance of Th17 and Treg cells is restored by the treatment (Figure 2,a). It is well established that Stat3 and Stat5 are upstream regulators of RorγT and FoxP3, which are key transcription factors for Th17 and Treg differentiation, respectively. Accordingly, to better investigate Th17 and Treg signaling pathway in psoriasis, we analyzed Stat3, Stat5, RorγT and FoxP3 expression levels. Western blot and Real-Time PCR demonstrated that the Th17 cells transcription factors Stat3 and RorγT, were significantly reduced after NB-UVB therapy (Figure 2b,c,f), indicating that the treatment result in a downregulation of the Th17 signalling pathway. Conversely, we did not observed any significantly difference in Stat5 and Foxp3 relative expression levels (Figure 2d-f), suggesting that Treg signaling pathway in circulating CD4+ T cells is not affected by NB-UVB therapy.

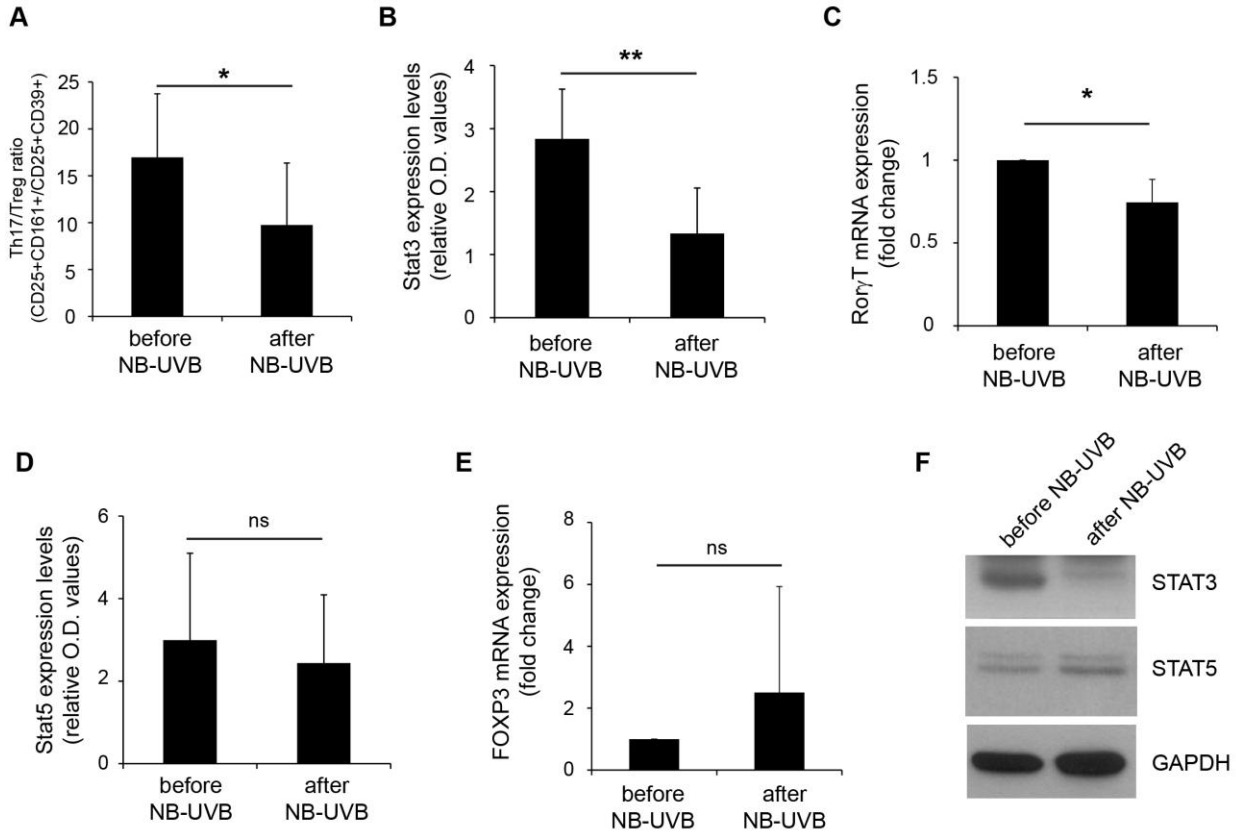

Figura 2. Th17and Treg signalling pathways in CD4+ T cells from patients with psoriasis before and after NB-UVB therapy by western blot and real-time PCR. (A) Ratio of the percentage of cells expressing CD25+CD161+ (Th17) with CD25+CD39+ (Treg) (*P<0.05, t-test). (B-C) Quantification of Stat3 protein levels and RorγT mRNA expression (**P<0.01; *P<0.05. t-test). analysis. (D-E) Quantification of Stat5 protein levels and Foxp3 mRNA expression (ns=non-significant; t-test). (F) Representative image of Stat3, Stat5 and GAPDH detection using western blot.

3. PKCε expression is increased during Th17 in vitro differentiation

To investigate the involvement of PKCε in Th17 differentiation, CD4+ T cells were isolated from healthy donors PBMC, seeded in anti-CD3/CD28-coated wells and kept in culture with IL-6, IL-23, IL1β and IL-21 for 6 days. We studied the expression of molecular factors known to be crucial for Th17 development, as RorγT, IL-17 and Stat3, in order to assess the polarization of the CD4+ T cell population into the Th17 lineage. Real-time PCR analyses show that RorγT and IL-17 mRNA levels were significantly higher at day3 and day6 of in vitro differentiation, compared to day 0 (Figure 3a). We further analysed Stat3 and the Stat3 phosphorylated forms at the Ser727 (pStat3 Ser727) and at the Tyr705 (pStat3 Tyr705) during Th17 differentiation. Under Th17 priming conditions, Stat3 and pStat3-Ser727 expression was significantly increased from day 0 to day 3 and it is maintained until day 6, whereas pStat3 Tyr705 expression levels increased until the last day of culture (Figure 3b,e). In addition, we used flow cytometry to detect the population of cells expressing Th17 antigens (CD25 and CD161) and lacking Treg CD39 marker (Figure 3c). T cells expressing CD25+CD161+CD39- were significantly higher either at day 3 (68.37 ± 2.44%) and day 6 (58.8 ± 3.86%) of culture, compared with day 1 (12.73 ± 1.96%; ***P<0.001 vs day1) (Figure 3d). Finally, we found that the levels of PKCε expression, both the mRNA and the total protein, were significantly increased through the days of culture, supporting that it may be involved in Th17 differentiation (Figure 3f,g).

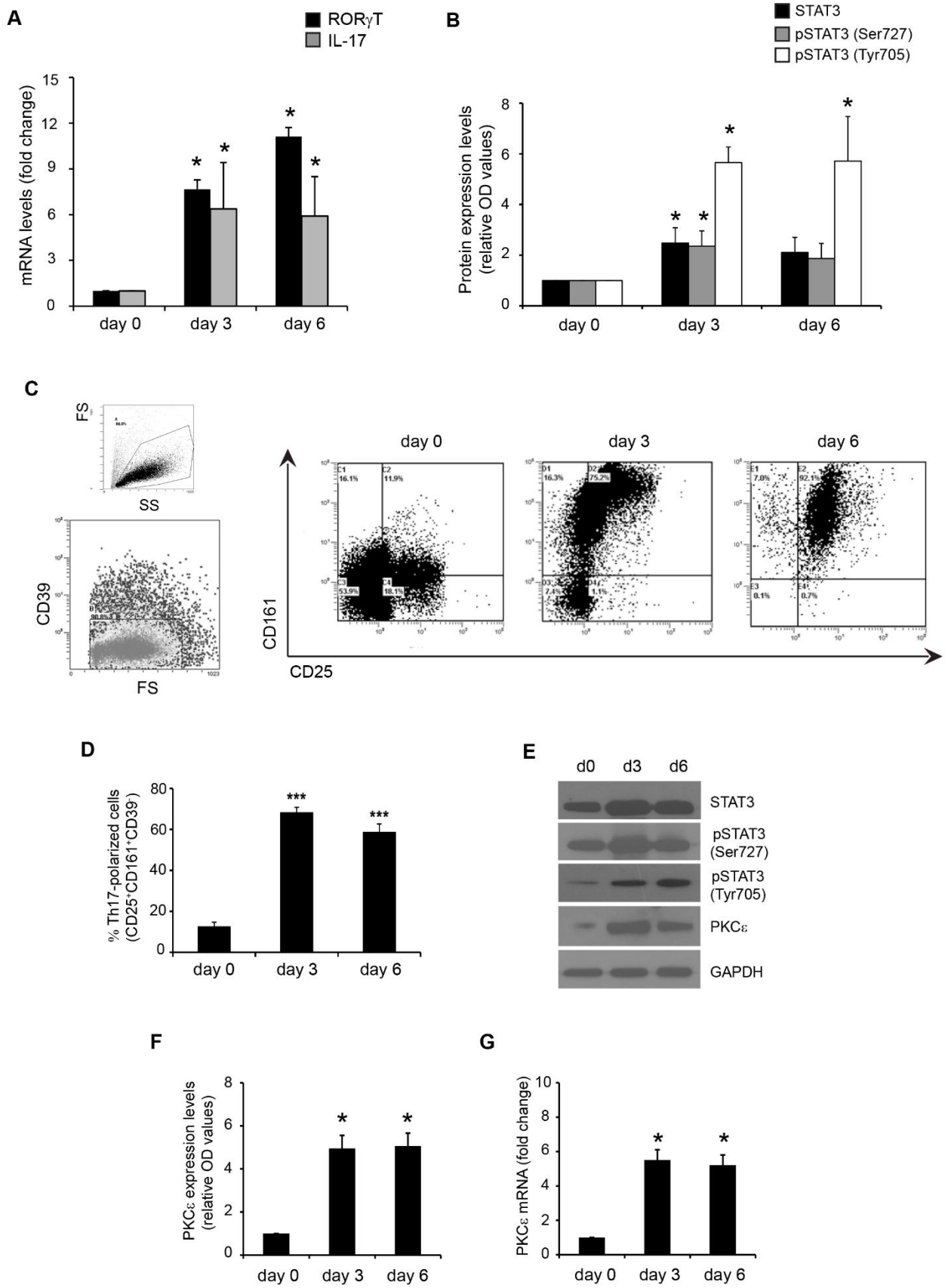

Figura 3. Differentiation of Th17 cells from human naive CD4+ peripheral blood-derived. Specific transcription factors involved in Th17 differentiation were analysed at day0, day3 and day6 of culture. Charts represent the averages of three independent experiments ± standard deviation. (**A**) Quantification of RorγT and IL-17 mRNA expression levels through

the days of culture (*P<0.05, one way ANOVA and Dunnett's vs day0). (**B**) Quantification of Stat3, phospho-Stat3 at Ser727 and phospho-Stat3 at Tyr705 through the days of culture. (*P<0.05, one way ANOVA and Dunnett's vs day0). (**C**) Th17 polarization was assessed in flow cytometry. T cell population was selected referring to the FS and SS parameters (upper panel on the left). Th17 were identified as negative for CD39, a Treg-specific expression marker (lower panel on the left) and positive for CD25 and CD161 through the days of culture (right). (**D**) Quantification of the number of CD39-CD25+CD161+ cells, expressed in percentage (***P<0.001, one way ANOVA and Dunnett's vs day0). (**E, F**) Quantification of PKCε expression protein (**E**) and mRNA (**G**) levels at day0, day3 and day6 of culture. (*P<0.05, one way ANOVA and Dunnett's vs day0).

4. PKCε regulates Th17 in vitro differentiation via Stat3-dependent pathway

Stat3 activation is critical for Th17 differentiation. To demonstrate that PKCε physically interacts with Stat3 during priming Th17 conditions, we performed co-immunoprecipitation assays at the second day of culture. Western blot analysis demonstrated that PKCε is present in the immunoprecipitate generated using anti-Stat3 antibody (Figure 4a). *Vice versa*, Stat3 was detected in the PKCε pull-down (Figure 4b). This result indicates that there is physical interaction between PKCε and Stat3 in CD4+ T cells committed to the Th17 pathway. Hence, we sought to investigate the role of PKCε in Th17 differentiation by modulating its expression. Naïve CD4+ T cells were isolated from healthy controls PMBC and stimulated to Th17 polarization. After 1 day of culture, PKCε was up-regulated by the engineering with a mouse wild type PKCε-GFP fusion protein (PKCε-GFP) or a kinase-inactive fusion protein which harbors a point mutation in the catalytic core of the enzyme (PKCεm-GFP), as previously described (Mirandola P et al., 2011). The transcription factors involved in Th17 signalling pathway were analyzed at day 3 of culture, either by western blot and Real-time PCR. RORγT mRNA levels dramatically increased upon the expression of PKCε-GFP, compared with the inactive PKCεm-GFP, suggesting that the forced expression of PKCε during the first days of differentiation sustained the polarization of CD4+ T cells to a Th17 commitment. As for RORγT, but with a less profound effect, IL-17 mRNA levels were significantly higher in PKCε-GFP T cells (Figure 4c). Stat3 must be phosphorylated at the Ser727 in order to be completely active. As it has been demonstrated that PKCε mediates Stat3 phosphorylation at Ser727

in several cancer cell lines (*Aziz MH et al., 2007*), we sought to investigate whether PKCε sustains Th17 differentiation by regulating the Stat3 signalling pathway. Hence, we studied Stat3 and pStat3 (Ser727) protein levels following PKCε up-regulation. Both the protein levels are higher in PKCε-GFP T-cells than in the inactive PKCεm-GFP, suggesting that PKCε sustained Th17 differentiation via Stat3-dependent pathway (Figure 4d,e). To prove this finding, we used a recombinant lentiviral vector to introduce and stably express shRNA that specifically target PKCε (shPKCε). As control, we used a short hairpin RNA (shCT) that does not target any known gene. In mouse model, PKCθ and PKCδ have been investigated in depth for their role in Th17 differentiation: the expression of both isoforms is significantly modulated during T polarization. To exclude off-target effects of shRNA, we assessed PKCδ and PKCθ expression in T-differentiation unrelated cell, HeLa cells, upon shPKCε infection. Both proteins expression was not affected by PKCε downregulation with shRNA, confirming the specificity of our inhibitory system (Figure 4h). At day 3 of culture, pStat3 (Ser727) expression levels were analysed and we found that PKCε silencing resulted in a significantly reduction of pStat3 (Ser727) expression compared with shControl, proving that PKCε is required for Stat3 complete activation during Th17 differentiation (Figure 4f,g). Finally, we studied the effects of a short-time inhibition of pStat3 (Ser727) expression. At first day of Th17-cytokine stimulation, T cells were treated with Bisindolylmaleimide 1 (BIM-1), a highly selective PKC inhibitor. The compound was added to culture media for 5, 15 and 30 minutes and cells were further analyzed using western blot for pStat3 (Ser727) (Figure 4i,j). Even following 5 minutes of BIM-1 treatment, pStat3 (Ser727) expression levels are significantly decreased, suggesting that 5 minutes of PKCε inhibition are sufficient to impair Stat3 phosphorylation.

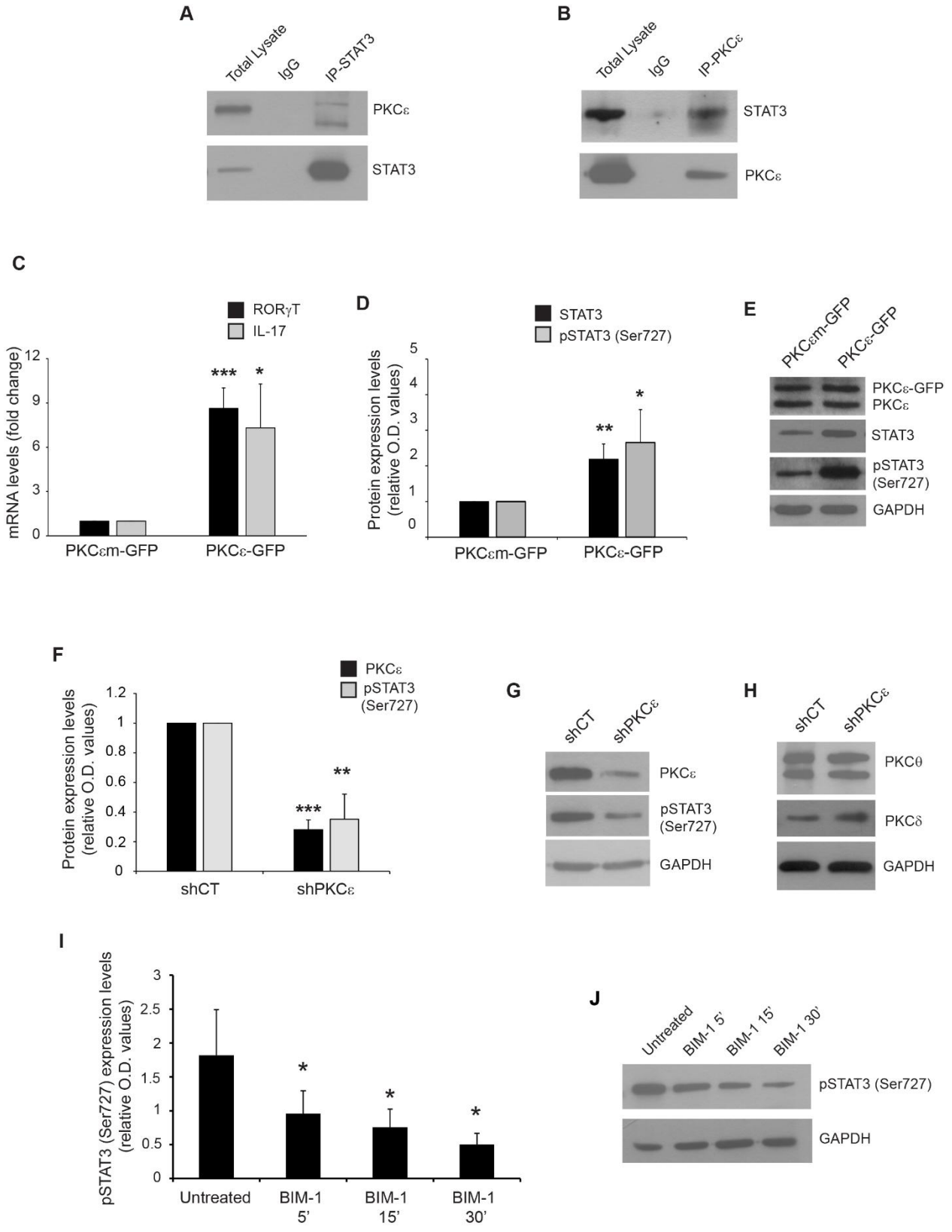

Figura 4 (**A,B**) Immunoprecipitation assays using anti-Stat3 and anti-PKCε. Total lysate, control rabbit IgG and the immunoprecipitated samples (IP-STAT3 or IP-PKCε) were analysed using western blot (**A**) Stat3 immunoprecipitation blotted for Stat3 and PKCε. (**B**) PKCε immunoprecipitation blotted for Stat3 and PKCε. (**C**) Quantification of RorγT and IL-17 mRNA levels at day 3 of culture, upon PKCε up-regulation. (***P<0.001; *P<0.05 t-test) (**D**) Quantification of Stat3 and pStat3 (Ser727) upon PKCε up-regulation (*P<0.05, *P<0.01; t-test). (E) Representative blot of PKCe,

Stat3 and pStat3 (Ser727) and GAPDH detection upon PKCε induction. Exogenous PKCε is indicated as PKCε-GFP (**F**) Quantification of PKCε and pStat3 (Ser727) expression levels upon PKCε downregulation (***P<0.001, **P<0.01. t-test analysis). (**F**) Representation of PKCε and pStat3 (Ser727) detection using western blot analysis. (**H**) Western blot detection of PKCθ and PKCδ in HeLa cells upon PKCε downregulation using specific shRNA. (**I**) Quantification of pStat3 (Ser727) expression levels in CD4+ T cells, at day 1 of differentiation, with or without BIM-1. PKCε inhibitor was added for 5, 15 or 30 minutes. (*P<0.05, one-way ANOVA and Tuckey test vs Control). (**J**) Representative blot of pStat3 (Ser727) detection in CD4+ samples with or without BIM-1 treatment.

Discussion

CD4+ T-lymphocytes, after being activated and differentiated into effector subsets, play an essential role as regulators of the adaptive immune response during infections or inflammatory diseases. Recent studies have identified T helper 17 (Th17) cells and regulatory T (Treg) cells as major players in autoimmune and immune-mediated diseases (*Deng Y et al., 2016; González-Amaro R and Marazuela M, 2016; Kleinewietfeld M and Hafler DA, 2013*). Th17 cells are pro-inflammatory and, when their number is in excess, they contribute to autoimmunity and tissue damage. On the contrary, Treg cells have a suppressor activity important in the establishment and maintenance of self-tolerance. Th17/Treg fine balance has been emerged as a critical point in the development of autoimmune diseases. In fact, if the balance is deviated in favour of Th17 cells, the severity of the diseases is enhanced. For this reason, the identification of proteins implicated in Th17 or Treg signalling pathways could provide novel target molecules for the control of immune-mediated diseases development.

Protein kinase C (PKC) is a family of serine/threonine kinases known to be involved in several pathogenic processes, including T cell activation and proliferation (*Isakov N and Altman A, 2013*). Previously, we and others have shown that PKCε sustains CD4+ T cells proliferation and we found it overexpressed in circulating CD4+ T cells from patients with Hashimoto Thyroiditis, suggesting an involvement of the kinase in the pathogenesis of the disease (*Xue H et al., 2015; Mirandola et al., 2011*). Although in vivo and in vitro experiments have also demonstrated that

PKCε is implicated in inflammation and immunity (*Aksoy E et al., 2004*), its role in the molecular pathogenesis of immune-mediated disorders is not yet clear.

In this study, we quantified PKCε expression in PBMC-derived CD4+ T cells from patients with psoriasis, before and after NB-UVB therapy. Accordingly with our previous study, we found PKCε significantly overexpressed in patients with psoriasis, compared with healthy controls. Furthermore, PKCε expression levels were reduced after NB-UVB therapy, in a pattern of expression similar to the healthy controls. Importantly, PKCε expression levels correlates with the severity of the diseases both before and after the NB-UVB therapy. This result, in addition with our previous findings, points PKCε to a potential clinical relevance, suggesting that PKCε may be implicated in the immune-response or in the pathogenesis of the disease.

Although that psoriasis is an autoimmune disease is still under debate, a body of evidences has demonstrated that psoriasis is an immune-mediated disorder characterized by the contribution of Th17 cells (*Sticherling M, 2016; Fry L et al., 2015*). In circulating CD4+ T cells from our patients, we detected a decrease of Stat3 and RorγT expression levels after NB-UVB therapy, suggesting a decrease of Th17 production follow the treatment. In contrast with Wang X et al., we did not observed a significant increase of Stat5 protein levels and Foxp3 mRNA levels in CD4+ T cells after NB-UVB therapy. This could be explained by the low PASI score of the patients enrolled for this study, compared with the high PASI of the patients studied by Wang et al. However, this result indicates that the factors involved in Treg signalling pathway were not affected by the therapy. In the evaluation of Th17 and Treg contribution in human diseases, the number and the function must be considered. In fact, Prakken et al. have demonstrated that Treg can lose their suppressive function, especially under inflammatory conditions, without changing in number. However, our flow cytometry analysis demonstrated that the ratio of CD4+ cells positive for CD161+ (Th17) and the CD4+ cells positive for CD39+ (Treg), is significantly decreased following NB-UVB therapy, suggesting that the balance in terms of Th17/Treg number of cells is restored after the therapy. This

could demonstrate that psoriasis with a mild score of severity is mainly characterized by an alteration of Th17 cells, instead of Tregs.

Although the discovery of Th17 cells have provided new insight in the pathogenesis of autoimmune and immune-mediated diseases previously attributed to Th1 response, some critical differences regarding the mechanisms of murine and human Th17 differentiation appear to exist. It has been demonstrated that IL-6 and IL-1β are essential factors for human Th17 polarization, whereas the role of TGF-1β is still controversial. However, TGF1 β induces Th17 polarization by the activation of SMAD proteins, whereas IL-6 and IL-1b are known to promote Th17 differentiation via Stat3 pathway. In this study, we primed peripheral CD4+ T cells polarization into Th17 cells using a cocktail of IL-6, IL-1b, IL-21 and IL-23 cytokines, without the addition of TGF1 β. Interestingly, both mRNA and protein expression levels of PKCε increases during Th17 differentiation, indicating a potential implication of the kinase in naïve CD4+ polarization into Th17 cells.

Stat3 must be phosphorylated at Ser727 residue to be completely active. Aziz et al. have demonstrated that PKCε interacts with Stat3 and phosphorylates Stat3Ser727 in several human cancer cells, including skin melanoma, breast, colon and lung. Here we show that PKCε interacts with Stat3 in CD4+ T cells during Th17 differentiation, suggesting that Stat3 activity may be regulated by PKCε in this process. To prove this hypothesis, we studied the effects of PKCε modulation on Stat3 pathway and, consequently, on Th17 differentiation. When we induced PKCε expression on the first day of differentiation, we obtained an increase of both RorγT and IL-17 mRNA expression after 48 hours from the induction. According with the high levels of PKCε found in CD4+ from Hashimoto Thyroiditis and psoriasis, this result indicates that PKCε overexpression leads to an increase of Th17 signalling pathway. This could be due to an up-

regulation of Stat3 signalling pathway, as we found also Stat3 and pStat3 (Ser727) significantly increased following PKCε induction.

In addition, we show that PKCε down-regulation decreases Stat3 phosphorylation levels at Ser727 residue, confirming that PKCε expression is not redundant on the regulation of Th17 differentiation via Stat3 pathway. To assess the effects of PKCε inhibition or down-regulation on Stat3 pathway and Th17 differentiation, we used two different approaches. First, we silenced PKCε using a specific shRNA for 72 hours of Th17 differentiation. CD4+ T cells with downregulated PKCε showed lower levels of pStat3 (Ser727) expression. Second, we used a PKC inhibitor (BIM-1) to evaluate the short-term effects of the inhibition of PKCε function on Stat3 Ser727 phosphorylation, during the first day of differentiation. We showed that 5 minutes of treatment with BIM-1are sufficient to decrease pStat3 (Ser727) expression levels in CD4+ T cells polarized into Th17 cells. Collectively, these results confirm that PKCε is required for Stat3 phosphorylation during Th17 differentiation.

Mechanisms that underlies Th17 differentiation pathway in human are still largely unclear. However, this study demonstrates, for the first time, a role for PKCε in human *in vitro* Th17 differentiation by up-regulating Stat3 signalling pathway. Our research underlines the clinical relevance of PKCε and strongly suggests it could be considered as a potential therapeutic target in Th17-mediated diseases.

References

Aksoy E, Goldman M, Willems F. Protein kinase C epsilon: a new target to control inflammation and immune-mediated disorders. Int J Biochem Cell Biol. 2004 Feb;36(2):183-8.

Altman A, Villalba M. Protein kinase C-theta (PKC theta): a key enzyme in T cell life and death. J Biochem. 2002 Dec;132(6):841-6.

Aziz MH, Manoharan HT, Sand JM, Verma AK. Protein kinase Cepsilon interacts with Stat3 and regulates its activation that is essential for the development of skin cancer. Mol Carcinog. 2007 Aug;46(8):646-53.

Berger A, Hoelbl-Kovacic A, Bourgeais J, Hoefling L, Warsch W, Grundschober E, Uras IZ, Menzl I, Putz EM, Hoermann G, Schuster C, Fajmann S, Leitner E, Kubicek S, Moriggl R, Gouilleux F, Sexl V. PAK-dependent STAT5 serine phosphorylation is required for BCR-ABL-induced leukemogenesis. Leukemia. 2014 Mar;28(3):629-41.

Bovenschen HJ, van de Kerkhof PC, van Erp PE, Woestenenk R, Joosten I, Koenen HJ. Foxp3+ regulatory T cells of psoriasis patients easily differentiate into IL-17A-producing cells and are found in lesional skin. J Invest Dermatol. 2011 Sep;131(9):1853-60.

Buckner JH. Mechanisms of impaired regulation by CD4(+)CD25(+)FOXP3(+) regulatory T cells in human autoimmune diseases. Nat Rev Immunol. 2010 Dec;10(12):849-59.

Burkett PR, Meyer zu Horste G, Kuchroo VK. Pouring fuel on the fire: Th17 cells, the environment, and autoimmunity. J Clin Invest. 2015 Jun;125(6):2211-9.

Carlin CS, Feldman SR, Krueger JG, Menter A, Krueger GG. A 50% reduction in the Psoriasis Area and Severity Index (PASI 50) is a clinically significant endpoint in the assessment of psoriasis. J Am Acad Dermatol. 2004 Jun;50(6):859-66.

Chandra A, Ray A, Senapati S, Chatterjee R. Genetic and epigenetic basis of psoriasis pathogenesis. Mol Immunol. 2015 Apr;64(2):313-23.

Das RP, Jain AK, Ramesh V. Current concepts in the pathogenesis of psoriasis. Indian J Dermatol. 2009;54(1):7-12.

Decker T, Kovarik P. Serine phosphorylation of STATs. Oncogene. 2000 May 15;19(21):2628-37.

Deng Y, Chang C, Lu Q. The Inflammatory Response in Psoriasis: a Comprehensive Review. Clin Rev Allergy Immunol. 2016 Jun;50(3):377-89.

Elias KM, Laurence A, Davidson TS, Stephens G, Kanno Y, Shevach EM, O'Shea JJ. Retinoic acid inhibits Th17 polarization and enhances FoxP3 expression through a Stat-3/Stat-5 independent signaling pathway. Blood. 2008 Feb 1;111(3):1013-20.

Fisher GJ, Tavakkol A, Leach K, Burns D, Basta P, Loomis C, Griffiths CE, Cooper KD, Reynolds NJ, Elder JT, et al. Differential expression of protein kinase C isoenzymes in normal and psoriatic adult human skin: reduced expression of protein kinase C-beta II in psoriasis. J Invest Dermatol. 1993 Oct;101(4):553-9.

Friman S, Arns W, Nashan B, Vincenti F, Banas B, Budde K, Cibrik D, Chan L, Klempnauer J, Mulgaonkar S, Nicholson M, Wahlberg J, Wissing KM, Abrams K, Witte S, Woodle ES. Sotrastaurin, a novel small molecule inhibiting protein-kinase C: randomized phase II study in renal transplant recipients. Am J Transplant. 2011 Jul;11(7):1444-55.

Fry L, Baker BS, Powles AV, Engstrand L. Psoriasis is not an autoimmune disease? Exp Dermatol. 2015 Apr;24(4):241-4.

Fujita H. The role of IL-22 and Th22 cells in human skin diseases. J Dermatol Sci. 2013 Oct;72(1):3-8.
González-Amaro R, Marazuela M. T regulatory (Treg) and T helper 17 (Th17) lymphocytes in thyroid autoimmunity. Endocrine. 2016 Apr;52(1):30-8.

Hao JQ. Targeting interleukin-22 in psoriasis. Inflammation. 2014 Feb;37(1):94-9.

He X, Koenen HJ, Smeets RL, Keijsers R, van Rijssen E, Koerber A, van de Kerkhof PC, Boots AM, Joosten I. Targeting PKC in human T cells using sotrastaurin (AEB071) preserves regulatory T cells and prevents IL-17 production. J Invest Dermatol. 2014 Apr;134(4):975-83.

Hillmer EJ, Zhang H, Li HS, Watowich SS. STAT3 signaling in immunity. Cytokine Growth Factor Rev. 2016 Oct;31:1-15.

Hucho TB, Dina OA, Levine JD. Epac mediates a cAMP-to-PKC signaling in inflammatory pain: an isolectin B4(+) neuron-specific mechanism. J Neurosci. 2005 Jun 29;25(26):6119-26.

Isakov N, Altman A. Regulation of immune system cell functions by protein kinase C. Front Immunol. 2013 Nov 18;4:384.

Josefowicz SZ, Lu LF, Rudensky AY. Regulatory T cells: mechanisms of differentiation and function. Annu Rev Immunol. 2012;30:531-64.

Ju JH, Heo YJ, Cho ML, Jhun JY, Park JS, Lee SY, Oh HJ, Moon SJ, Kwok SK, Park KS, Park SH, Kim HY. Modulation of STAT-3 in rheumatoid synovial T cells suppresses Th17 differentiation and increases the proportion of Treg cells. Arthritis Rheum. 2012 Nov;64(11):3543-52.

Kanai T, Seki S, Jenks JA, Kohli A, Kawli T, Martin DP, Snyder M, Bacchetta R, Nadeau KC. Identification of STAT5A and STAT5B target genes in human T cells. PLoS One. 2014 Jan 30;9(1):e86790.

Kleinewietfeld M, Hafler DA. The plasticity of human Treg and Th17 cells and its role in autoimmunity. Semin Immunol. 2013 Nov 15;25(4):305-12.

Li L, Shaw PE. A STAT3 dimer formed by inter-chain disulphide bridging during oxidative stress. Biochem Biophys Res Commun. 2004 Sep 24;322(3):1005-11.

Lin H, Chen M, Rothe K, Lorenzi MV, Woolfson A, Jiang X. Selective JAK2/ABL dual inhibition therapy effectively eliminates TKI-insensitive CML stem/progenitor cells. Oncotarget. 2014 Sep 30;5(18):8637-50.

Lowes MA, Suárez-Fariñas M, Krueger JG. Immunology of psoriasis. Annu Rev Immunol. 2014;32:227-55.

Ma J, Ding Y, Fang X, Wang R, Sun Z. Protein kinase C-θ inhibits inducible regulatory T cell differentiation via an AKT-Foxo1/3a-dependent pathway. J Immunol. 2012 Jun 1;188(11):5337-47.

Ma L, Xue HB, Guan XH, Shu CM, Wang F, Zhang JH, An RZ. The Imbalance of Th17 cells and CD4(+) CD25(high) Foxp3(+) Treg cells in patients with atopic dermatitis. J Eur Acad Dermatol Venereol. 2014 Aug;28(8):1079-86.

Mattozzi C, Salvi M, D'Epiro S, Giancristoforo S, Macaluso L, Luci C, Lal K, Calvieri S, Richetta AG. Importance of regulatory T cells in the pathogenesis of psoriasis: review of the literature. Dermatology. 2013;227(2):134-45.

Mirandola P, Gobbi G, Masselli E, Micheloni C, Di Marcantonio D, Queirolo V, Chiodera P, Meschi T, Vitale M. Protein kinase Cε regulates proliferation and cell sensitivity to TGF-1β of CD4+ T lymphocytes: implications for Hashimoto thyroiditis. J Immunol. 2011 Nov 1;187(9):4721-32.

Nedoszytko B, Sokołowska-Wojdyło M, Ruckemann-Dziurdzińska K, Roszkiewicz J, Nowicki RJ. Chemokines and cytokines network in the pathogenesis of the inflammatory skin diseases: atopic dermatitis, psoriasis and skin mastocytosis. Postepy Dermatol Alergol. 2014 May;31(2):84-91.

Noack M, Miossec P. Th17 and regulatory T cell balance in autoimmune and inflammatory diseases. Autoimmun Rev. 2014 Jun;13(6):668-77.

Prakken B, Ellen Wehrens, van Wijk F. Editorial: Quality or quantity? Unraveling the role of Treg cells in rheumatoid arthritis. Arthritis Rheum. 2013 Mar;65(3):552-4.

Rani A, Murphy JJ. STAT5 in Cancer and Immunity. J Interferon Cytokine Res. 2016 Apr;36(4):226-37.

Schaller-Schönitz M, Barzan D, Williamson AJ, Griffiths JR, Dallmann I, Battmer K, Ganser A, Whetton AD, Scherr M, Eder M. BCR-ABL affects STAT5A and STAT5B differentially. PLoS One. 2014 May 16;9(5):e97243.

Sheng J, Chen W, Zhu HJ. The immune suppressive function of transforming growth factor-β (TGF-β) in human diseases. Growth Factors. 2015 Apr;33(2):92-101.

Sticherling M. Psoriasis and autoimmunity. Autoimmun Rev. 2016 Dec;15(12):1167-1170.

Sugiyama H, Gyulai R, Toichi E, Garaczi E, Shimada S, Stevens SR, McCormick TS, Cooper KD. Dysfunctional blood and target tissue CD4+CD25high regulatory T cells in psoriasis: mechanism underlying unrestrained pathogenic effector T cell proliferation. J Immunol. 2005 Jan 1;174(1):164-73.

Tanaka S, Suto A, Iwamoto T, Kashiwakuma D, Kagami S, Suzuki K, Takatori H, Tamachi T, Hirose K, Onodera A, Suzuki J, Ohara O, Yamashita M, Nakayama T, Nakajima H. Sox5 and c-Maf cooperatively induce Th17 cell differentiation via RORγt induction as downstream targets of Stat3. J Exp Med. 2014 Aug 25;211(9):1857-74.

Villarino AV, Laurence A. IL-1 watches the watchmen. Nat Immunol. 2015 Mar;16(3):226-7.
Wang X, Wang G, Gong Y, Liu Y, Gu J, Chen W, Shi Y. Disruption of circulating CD4+ T-lymphocyte subpopulations in psoriasis patients is ameliorated by narrow-band UVB therapy. Cell Biochem Biophys. 2015 Jan;71(1):499-507.

Wei L, Laurence A, Elias KM, O'Shea JJ. IL-21 is produced by Th17 cells and drives IL-17 production in a STAT3-dependent manner. J Biol Chem. 2007 Nov 30;282(48):34605-10.

Wei L, Laurence A, O'Shea JJ. New insights into the roles of Stat5a/b and Stat3 in T cell development and differentiation. Semin Cell Dev Biol. 2008 Aug;19(4):394-400.

Xue H, Yu X, Ma L, Song S, Li Y, Zhang L, Yang T, Liu H. The possible role of $CD4^+CD25(high)Foxp3^+/CD4^+IL\text{-}17A^+$ cell imbalance in the autoimmunity of patients with Hashimoto thyroiditis. Endocrine. 2015 Dec;50(3):665-73.

Yu H, Pardoll D, Jove R. STATs in cancer inflammation and immunity: a leading role for STAT3. Nat Rev Cancer. 2009 Nov;9(11):798-809.

Zheng Y, Wang Z, Deng L, Zhang G, Yuan X, Huang L, Xu W, Shen L. Modulation of STAT3 and STAT5 activity rectifies the imbalance of Th17 and Treg cells in patients with acute coronary syndrome. Clin Immunol. 2015 Mar;157(1):65-77.

ATTIVITA' SVOLTE DURANTE IL PERIODO DI DOTTORATO

L'attività di ricerca è stata svolta presso i laboratori di Biologia Molecolare dell'U.O. di Anatomia e Istologia del Dipartimento di Scienze Biomediche, Biotecnologiche e Traslazionali (S.Bi.Bi.T.) dell'Università degli Studi di Parma.
Le principali linee di ricerca, riguardanti il ruolo di PKCε nel ciclo cellulare e nel differenziamento, sono state dettagliate nell'elaborato della Tesi di Dottorato e sono esitate in pubblicazioni attualmente sottomesse a riviste scientifiche internazionali. L'attività di ricerca ha visto inoltre il coinvolgimento in ulteriori progetti, focalizzati su PKCε, attivi nel gruppo di ricerca di cui ho fatto parte durante il periodo di Dottorato, come si evince da parte delle pubblicazioni sotto riportate.

PUBBLICAZIONI

1. Di Marcantonio D, Galli D, Carubbi C, Gobbi G, Queirolo V, Martini S, Merighi S, Vaccarezza M, Maffulli N, Sykes SM, Vitale M, Mirandola P. *PKCε as a novel promoter of skeletal muscle differentiation and regeneration*. Exp Cell Res. 399 (1), 10-9 (2015)

2. Masselli E, Carubbi C, Gobbi G, Mirandola P, Galli D, Martini S, Bonomini S,Crugnola M,Craviotto L, Aversa F, Vitale M. *Protein kinase Cε inhibition restores megakaryocytic differentiation of hematopoietic progenitors from primarymyelofibrosis patients*. Leukemia.29 (11), 2192-201 (2015)

3. Queirolo V, Galli D., Masselli E., Borzì RM, Martini S, Vitale F, Gobbi G, Carubbi C, Mirandola P. *PKCε is a regulator of hypertrophic differentiation of chondrocytes in osteoarthritis*. Osteoarthritis Cartilage. 24, 1451-60 (2016)

4. Carubbi C, Masselli E, Martini S, Galli D, Aversa F, Mirandola P, Italiano JE, Gobbi G, Vitale M. *Human thrombopoiesis depends on Protein kinase Cδ/protein kinase Cε functional couple.* Haematologica. 101, 812-20 (2016)

PUBBLICAZIONI IN SOTTOMISSIONE

1. Martini S, Pike T, Carubbi C, Masselli E, Mirandola P, Gobbi G, Parker PJ and Vitale M. *Protein Kinase Cε regulates mitotic progression by regulating centrosome migration and mitotic spindle assembly in transformed cells.* at Nature Communications
2. Martini S, Pozzi G, Carubbi C, Masselli E, Galli D, Gobbi G, Mirandola P and Vitale M. *PKCε promotes human Th17 in vitro differentiation via Stat3 signalling pathway* at Journal of Autoimmunity.

ABSTRACT A CONVEGNI NAZIONALI ED INTERNAZIONALI CON PUBBLICAZIONE DEGLI ATTI

1. Martini S, Carubbi C, Masselli E, Gildone M, Pozzi G, Grandi D and Vitale M. *Novel role of PKCε in mitotic spindle stability*. 69° Congresso Nazionale SIAI (Società Italiana di Anatomia e Istologia), svolto a Ferrara dal 17 al 19 Settembre 2015.
2. Masselli E, Carubbi C, Gobbi G, Mirandola P, Galli D, Martini S, Pozzi G, Gildone M, Albanese C, Bonomini S, Crugnola M, Craviotto L, Aversa F and Vitale M. *In vitro characteristics of hematopoietic progenitors from primary myelofibrosis patients correlate with IPSS/DIPSS risk category.* 45° Congresso Nazionale SIE (Società Italiana di Ematologia), svolto a Firenze dal 4 al 7 Ottobre 2015.
3. Pigazzani F, Carubbi C, Martini S, Crocamo A, Suma S, Marziliano M, Notarangelo F, Gobbi G, Vitale M and Ardissino D. *Platelet mRNA as a predictive biomarker in acute myocardial infarction.* Eleventh Annual Northwestern Cardiovascular Young Investigators' Forum, svolto a Chicago (USA), dal 15 al 18 Ottobre 2015.
4. Galli D, Martini S, Pozzi G, Masselli E, Carubbi C, Gobbi G, Mirandola P, Vitale M. *PKCε involvement in Th17 in vitro differentiation: implication in psoriasis pathogenesis.* 70° Congresso Nazionale SIAI (Società Italiana di Anatomia e Istologia), svolto a Roma dal 15 al 17 Settembre 2016.
5. Carubbi C, Martini S, Masselli E, Galli D, Pozzi G, Gobbi G, Mirandola P, Vitale M. *Correlation between Protein Kinase Cε expression and thrombotic risk in Primary Myelofibrosis (PMFs).* 70° Congresso Nazionale SIAI (Società Italiana di Anatomia e Istologia), svolto a Roma dal 15 al 17 Settembre 2016.

SEMINARI TENUTI

1. "*Meccanismi molecolari di regolazione della segregazione dei cromosomi: implicazioni nella trasformazione tumorale*"- promosso dalla Rotary Foundation in collaborazione con il Dipartimento di Scienze Biomediche Biotecnologiche e Traslazionali (S.Bi.Bi.T.), tenuto il 17.05.2016 presso l'Aula Canuto della Facoltà di Medicina e Chirurgia dell'Università degli Studi di Parma, a cui hanno partecipato il Magnifico Rettore dell'Università di Parma, del Presidente del Rotary Parma Est, il Direttore Generale dell'AOU e il coordinatore del Dottorato di Ricerca in Medicina Molecolare.

PERIODI SVOLTI ALL'ESTERO

1. Da Ottobre 2015 ad Aprile 2016, al Protein Phosphorylation Laboratory - Francis Crick Institute di Londra (UK).

BORSE DI STUDIO

1. Rotary Foundation District Grant (2015/16)
2. Borsa di Mobilità Internazionale, UNIPR (2015/16)

ATTIVITA' DI TUTORING di studenti iscritti alla laurea triennale in "Biotecnologie", alla laurea magistrale in "Biotecnologie Mediche, Veterinarie e Farmaceutiche" e alla laurea in "Medicina e Chirurgia".

1. "PKCε involvement in mitotic spindle stability", laurea magistrale in "Biotecnologie Mediche, Veterinarie e Farmaceutiche" (Relatori: Prof. Sergio Di Nuzzo e Prof. Prisco Mirandola, A.A. 2013/14);
2. "PKCε expression in peripheral CD4+ T-cells in immune-mediated skin diseases", laurea magistrale in "Biotecnologie Mediche, Veterinarie e Farmaceutiche" (Relatore: Prof. Prof. Prisco Mirandola, A.A. 2013/14);
3. "Espressione della proteina chinasi Cε nei pazienti affetti da psoriasi", laurea in Medicina e Chirurgia (Relatori: Prof. Giuseppe Fabrizi e Prof. Marco Vitale, A.A. 2013/14);
4. "Studio del ciclo cellulare mediante sincronizzazione in vitro", laurea triennale in Biotecnologie (Relatore: Prof.ssa Giuliana Gobbi, A.A. 2013/14);
5. "PKCε, 14-3-3ζ and γ-tubulin complex formation in mitotic spindle stability", laurea magistrale in Biotecnologie Mediche, Veterinarie e Farmaceutiche (Relatore: Prof. Prisco Mirandola, A.A. 2014/15);
6. "PKCε e 14-3-3ζ formano un complesso proteico con γ-tubulina in cellule sincronizzate in metafase", laurea in Biotecnologie (Relatore: Prof.ssa Giuliana Gobbi, A.A. 2014/15);
7. "Analisi dell'espressione di PKCε in piastrine umane mediante citometria a flusso", laurea in Biotecnologie (Relatore: Prof.ssa Cecilia Carubbi, A.A. 2014/15);
8. "Coinvolgimento della Proteina Chinasi C Epsilon (PKCε) nella progressione mitotica", laurea in Biotecnologie (Relatore: Prof.ssa Cecilia Carubbi, A.A. 2015/16).